DURABILITY AND ULTIMATE FLEXURAL LOADING OF SHEAR SPIKE REPAIRED, LARGE–SCALE TIMBER RAILROAD BRIDGE MEMBERS

R. Gutkowski
H. Forsling
Department of Civil Engineering

December 2007

Acknowledgements

This report has been prepared with funds provided by the United States Department of Transportation to the Mountain-Plains Consortium (MPC). The authors would like to acknowledge the support of the Structural Engineering Laboratory at Colorado State University for the use of the test and measurement equipment critical to the collection and evaluation of the data presented in this report.

ABSTRACT

The objective of this research study is to examine the long term effectiveness and durability performance of fiber reinforced polymer (FRP) strengthened full size timber bridge members and to investigate their behavior when ultimately load tested.

The shear spike strengthening approach is aimed at rejuvenating horizontal shear properties by inserting fiberglass pultruded rods through areas of damage. Shear spike fiberglass rods are inserted through pre-drilled holes from the top of the member, perpendicular to the primary bending axis. An epoxy-resin adhesive is incorporated during the process of insertion to bond the shear spikes to the wood. The epoxy adhesive also strengthens the member by filling adjacent cracks and decay voids.

In three preceding investigations, this strengthening method has been proven to restore much of the virgin member stiffness and add horizontal shear resistance in dimension lumber, medium-sized timbers and full-sized bridge timbers, respectively.

For this study, eight full-size railroad bridge timber stringers were intentionally damaged by saw cuts, to mimic deterioration, after which they were strengthened through the process of shear spiking. The stringers were then durability loaded up to 25,000 cycles after which the majority of the sample population was ultimately load tested. The strengthened stringers showed very modest detrimental effects from the repetitive nature of the loading. In subsequent ultimate load testing of the repaired beams, specimens failed predominately in flexure, i.e. failure in the sound wood rather than in the strengthening components. The results found support findings from those previous studies; FRP rods are highly effective in restoring the flexural stiffness and shear strength of deteriorated timber members.

TABLE OF CONTENTS

LIST OF TABLES

LIST OF FIGURES

1. INTRODUCTION

Approximately 101,000 railroad bridges are in service in the United States today. An estimated 35% of them utilize timber as the main construction material (Federal Railroad Administration [26]). Another roughly 40,000 timber vehicular bridges are currently in use the United States (Duwadi and Ritter [24]). The majority of these timber bridges serve secondary rail lines and secondary roads. Clearly timber bridges play an integral role in the nation's transportation infrastructure and are of particular importance to the railroad infrastructure system.

Because of the inherent durability of wood, a considerable number of the timber railroad bridges that were constructed in the early- to mid-20th century are still in service. Although they have typically been rehabilitated and/or rebuilt at intervals, many of them are nearing or have already passed their projected lifetimes due to fatigue and/or decay (Radford et al. [49]). Fatigue describes the phenomenon of progressive and permanent damage of a structural component, or portion thereof, because of long-term repetitive loading at load levels less than the static yield strength of the component. Decay, on the other hand, describes the gradual decomposition process of organic matter, such as wood.

1.1 Fatigue and Aging

If properly protected from the decay, mechanical properties of wood show very little change with time. For example, no strength losses were noticeable from tests of clear wood specimens that had undergone centuries of normal aging conditions (Forest Products Laboratory [27]). However, the nation's rail infrastructure system is expected to carry ever increasing railcar loads traveling at higher speeds. In North America, allowable axle load limits of 66,000 lbs (30,000 kg) were the standard for almost forty years, but with the introduction of double stack train cars in the late 1980s/early 1990s, the allowable axle weight limit was increased to 79,000 lbs (35,700 kg) (Oomen and Sweeney [41]). More recent transportation statistics show the average weight of railcars carrying commodities such as farm products, coal, chemicals, and transportation equipment increased by an average of 5.4% in the decade from 1991 to 2001 (Bureau of Transportation Statistics [14]). Many existing timber bridges are not designed to safely support the increased demands of contemporary railcars; much less the 10% to 20% projected increase in future railcar weights (Oomen and Sweeney [41]).

1.2.1 Preservative Treatments

Pressure treatment with chemical preservatives, such as creosote, can dramatically increase the useful life of wood. Properly selected and preservative-treated structural timbers can provide satisfactory service of over forty years, even under continued harsh environmental exposure. Nonetheless, decay will eventually occur in any timber member that is exposed to the environment, and that decay is still the primary cause of timber bridge replacements (Muchmore [40]).

Wood is treated by utilization of chemical liquid preservatives, such as creosote and creosote solutions, oilborne treatments, or waterborne oxides (Breyer et al. [11]). The preservative is applied to the exterior faces of the member by pressure injection. These chemical preservatives effectively make the treated wood fibers unpalatable to decay causing fungi and other harmful microorganisms. However, the preservative usually does not saturate the complete cross section of the member. The depth of penetration of the preservative varies, depending on application method, wood species, etc, and is known as the "treated zone." Figure 1.1 illustrates a typical cross section of a creosote treated structural timber, clearly depicting the inner untreated zone and the surrounding treated zone.

Figure 1.1 Cross-section of creosote treated, large-size timber.

Since the preservative treatment prevents decay of the surface and near-surface wood fibers, and because splitting and mechanical fasteners provide access for fungi to the inner regions, the decay process in treated timbers starts in the untreated core. Consequently, loss of mechanical properties in treated structural members is usually attributed to a loss of sound wood in the section's interior regions. This loss of sound wood may contribute to a loss of flexural strength and stiffness and a decrease in horizontal shear performance. According to Radford et al. [49], this loss of shear capacity is of particular significance to wood members of relatively low aspect ratio (length to depth), such as bridge stringers, where the flexural stiffness is strongly related to shear performance.

1.2 Background

Because of the aforementioned reasons, in combination with limited maintenance funds, a great need for cost effective timber bridge upgrade methods exist. Considerable research has been conducted with the objective of evaluating and implementing effective and economical structural repair and strengthening programs for timber bridges. *Structural repair* infers a process of reconstruction, i.e. replacement of existing structural components. The *repair* process includes determination and, if possible, removal of causes of distress, removal of damaged and/or deteriorated structural elements, and selection and implementation of appropriate repair components that extend the structure's useful life and/or structural capacity. *Structural strengthening*, on the other hand, infers a process of upgrading the structural capacity of existing elements. Strengthening is performed to either improve a structure's performance under existing loads or to increase a structure's load-carrying capacity (Sitar [58]).

Much of the past research related to upgrading of large-size timber members was focused on repair methods, including replacement of deteriorated members (Uppal and Otter [63]), addition of so-called "helper" stringers along the entire length of a bridge (Uppal et al. [64]), and the installation of additional interior supports along the length of the bridge (Uppal and Otter [63]). However, because of limited availability of the large-size timbers, and since complete replacement is labor intensive, time consuming and costly, much of the research focus has shifted to strengthening methods. Some traditional strengthening methods that have been researched include bonding of steel plates to the outer face(s) of timber members (Peterson [44]), external (Bohannan [9]), and to a lesser degree internal (Lantos [38]) post-tensioning by steel rods, strips or strands, and incorporation if interlaminar aluminum sheets in laminated wood beams (Sliker [59]).

The increased availability and reduced cost of fiber reinforced polymer (FRP) materials in the past few decades has stimulated much research into the use of advanced composites for strengthening of infrastructure components. FRPs have several important advantages over steel when used as a reinforcing material for timber; FRPs are more durable than steel since they are not susceptible to corrosion, are readily bonded to wood, and display high specific strength and stiffness. The specific strength of FRPs can be of the order of 10 to 15 times higher than that of steel. Moreover, FRPs generally have good fatigue strength — about three times that of steel, along with favorable creep characteristics and resistance against abrasion (Gilfillan, Gilbert, and Patrick [30]).

Some of the research utilizing FRPs for strengthening of timber members has been focused on installation of longitudinally-oriented glass-FRP (GFRP) rods near the tension and/or compression face of timbers, bonded to the wood by an epoxy adhesive (Gentile, Svecova, and Rizkalla [29]). Others focused their research on reinforcement of timber member's; tension face by carbon-FRP (CFRP) sheets (Johns and Lacroix [35]), tension and/or compression face(s) by GFRP and CFRP sheets (Gilfillan, Gilbert, and Patrick [30]), sides by CFRP sheets (Triantafillou [62]), and sides and tension face by GFRP sheets (Johns and Lacroix [35]). Moreover, some researchers focused on wrapping (complete encasement) of timber members with GFRP (GangaRao, Sonti, and Supefesky [28]) and carbon fiber (CF) (Buell, T.W. and Saadatmanesh [12]) sheets by method of hand lay-up. Davalos et al. studied the effects of wrapping wood crossties with FRPs by the filament winding process in several studies [19-21]. Common to all above mentioned studies is the use of an adhesive to bond the FRP material to the surface or near surface of the timber member.

FRP strengthening techniques have important drawbacks. Wrapping and composite sheets can only be readily applied to exposed members. For example, in a typical open-deck timber trestle bridge, only the outside of the two outer plies and the bottom face of all plies would be readily accessible for composite wrap or sheet strengthening. Strengthening interior stringers would require removal of adjacent stringers. Externally-applied strengthening components are also exposed to the environment with subsequent degradation of structural performance. Moreover, external application of wraps or sheets is further complicated by the presence of wood preservatives, such as creosote, which tend to degrade the FRP/wood bond performance (Radford et al. [49]).

1.3 Shear Spiking

A strengthening method termed “shear spiking” (also called “Z-spiking”) is not subject to many of the drawbacks associated with conventional FRP repair methods. The process of shear spiking evolved from aerospace-style laminated composites, where the method is used to enhance the interlaminar shear performance of laminated sheets. Shear spiking involves insertion of commercially available, pre-shaped pultruded FRP rods into pre-drilled holes in the deteriorated timber member. This concept makes shear-spiking an attractive option for treated timbers as a method to reconnect sound compressive wood fibers near the top face to the sound tension fibers on the opposite side of a decayed section, thus improving the shear response. The FRP material has high performance, good quality control, relatively low cost, and is compatible with wood. The shear spikes are inserted vertically, through the sound wood of the top (or bottom) face of the decayed member, through the deteriorated wood of the inner core, and then again penetrating the sound wood of the opposite face. An epoxy adhesive is incorporated at the time of insertion ― primarily to improve the load transfer from the wood to the shear spikes. Moreover, the epoxy adhesive fills cracks and decay voids near the shear spike, further enhancing the structural performance of the strengthened member. Since the shear spikes are completely embedded in the timber member, there is little visible repair and environmental exposure is minimized.

Given the relatively low aspect ratio of railroad bridge span timbers, the flexural stiffness is also improved as a consequence of the increased shear performance. The successful use of shear spiking to improve the flexural response and to add horizontal shear capacity to deteriorated timbers has been demonstrated in past research studies (Radford et al. [49], Schilling et al. [55], and Burgers et al. [15]).

1.4 Objective of the Study

The principal objective of the study described herein is to examine the effects of durability loading of shear spike strengthened, full size, timber bridge stringers in a laboratory setting. A secondary objective is to investigate the behavior of shear spike strengthened timber stringers loaded to failure, after completion of the durability loading phase. Successful outcome would be a step toward an ultimate goal of examining the effectiveness of the process of shear spiking on an in-situ timber railroad bridge.

2. STANDARD TIMBER RAILROAD BRIDGES

The vast majority of North American railroad timber bridges can be categorized as either of the “open-deck trestle” type or the “ballast-deck type.” Both systems have short span lengths of 13 to 15 feet (4.0 to 4.6 m), construction using solid sawn timbers, and mechanical fasteners. The timber members used in this study were obtained from an open-deck timber trestle bridge chord.

2.1 Description of an Open-Deck Timber Trestle Bridge

Figures 2.1 and 2.2 show portions of an open-deck timber trestle railroad bridge located just north of downtown Fort Collins, Colorado. Design specifications and procedures for timber railroad bridges are described in the Manual for Railway Engineering by the American Railway Engineering Association (AREA) [3]; construction, maintenance, and inspection procedures are also described. Chapter 7 of the AREA manual describes, in some detail, the main components of an open-deck timber trestle bridge. First, some common railroad industry terminology needs to be explained. The term “ply of stringers” or “ply” is used to describe a lengthwise set of large timber beams used to span the entire length of the bridge. The individual span timbers are termed “stringers.” A “bridge chord,” or simply “chord,” is the term used to describe one half of the bridge, mirrored about its longitudinal centerline. Each railway bridge thus consists of two chords, one under each rail. The terms that will be used exclusively herein are “ply” (“plies”), “stringer(s),” and “chord(s)” to describe these respective components. From Figure 2.3, it can be seen that the bridge is made up of two main components: the substructure and the superstructure.

Figure 2.1 Photograph of part of an open-deck timber trestle bridge, located just north of downtown Fort Collins, CO.

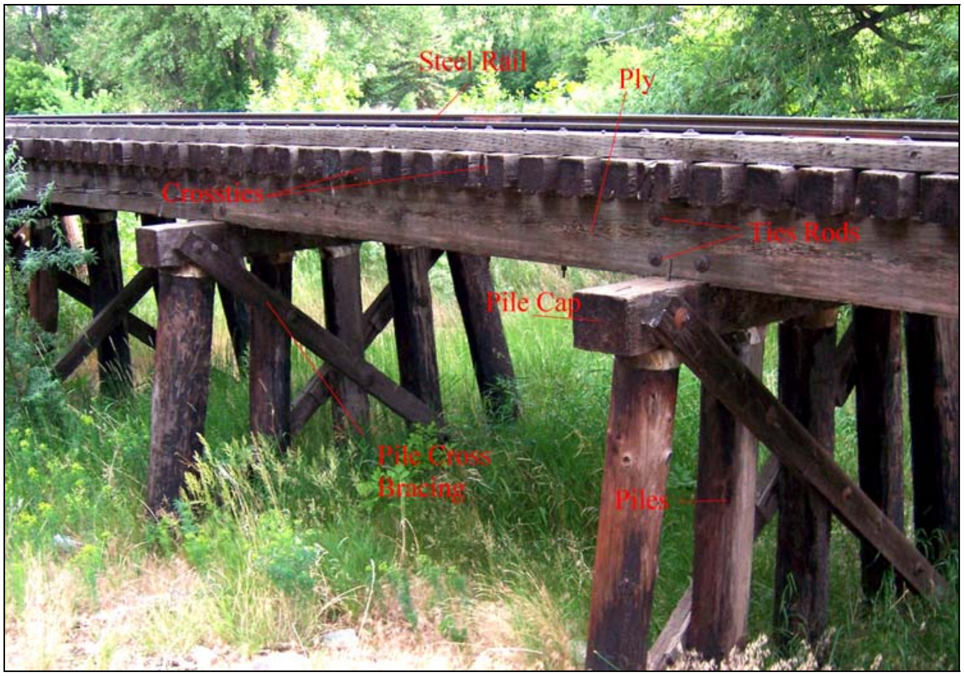

Figure 2.2 Photograph of part of an open-deck timber trestle bridge, located just north of downtown Fort Collins, CO.

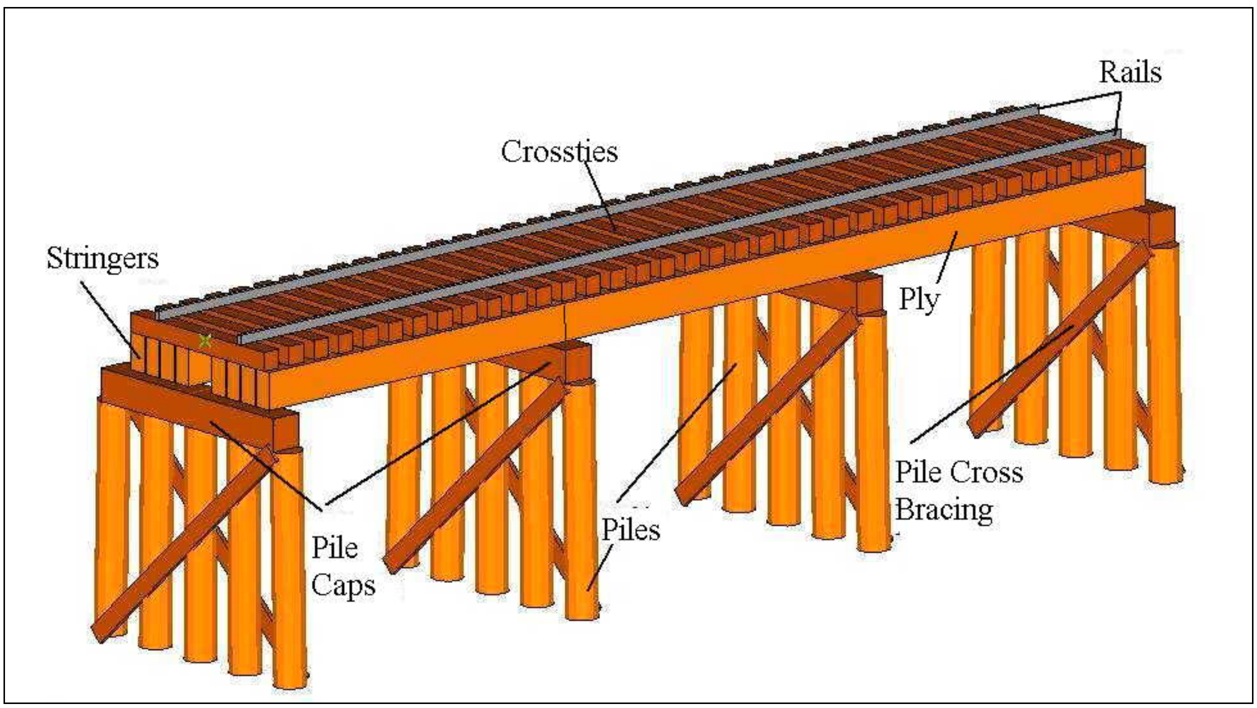

Figure 2.3 Illustration of the main components of an open-deck timber trestle bridge.

The substructure supports the superstructure and transfers imposed loads to the ground. The substructure is composed of the timber piles, pile cross bracings, and pile caps. The piles are round timbers with a typical diameter of 12 to 14 inches (31 to 36 cm). Pile lengths vary, as they are dependent on site topography and requirements of ground penetration. The number of piles varies depending on load exposure; trestle bridges typically have three to six piles per bent. The pile cross bracings connect the piles of a bent diagonally to enhance the overall lateral stability and to prevent lateral buckling of piles. The final components of the substructure are the pile caps; the pile cap rests directly atop the piles. Pile caps are solid sawn timbers, usually of cross-sectional dimensions of 12 by 14 inches (31 by 36 cm) to 14 by 14 inches (36 by 36 cm). Pile caps are long enough to extend past the outer piles on either side of the bridge. The pile caps, in turn, directly support the stringers — the first component of the superstructure. The superstructure is composed of the railroad crossties (usually referred to as "crossties" or simply "ties") and the steel rail, in addition to the stringers. The stringers vary between 7 to 10 inches (18 to 25 cm) in width and between 16 to 20 inches (41 to 51 cm) in depth. Stringer lengths can be up to 30 feet (9.1 m), sometimes even longer, and there are three to five stringers per chord. Stringers are either single span or two-span continuous (double span), arranged in an alternating (staggered) pattern so that adjacent stringers do not cross the same two spans. For multiple-span bridges, staggered double-span stringers are used exclusively except for in the end-spans where half of the stringers are single-span, simply supported members. Figure 2.4 illustrates the ply arrangement of a four-ply chord of a four-span bridge.

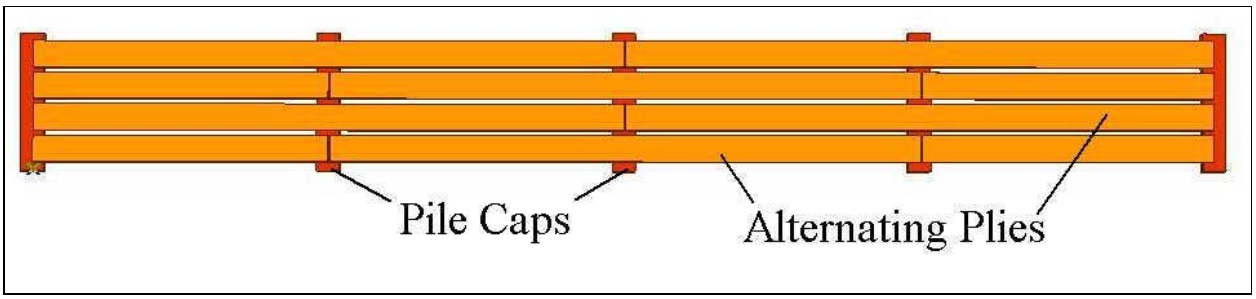

Figure 2.4 Schematic of alternating plies of a four-ply chord of a four-span bridge.

2.2 Description of a Ballast-Deck Timber Bridge

A section view of a typical ballast-deck timber bridge is shown in Figure 2.5.

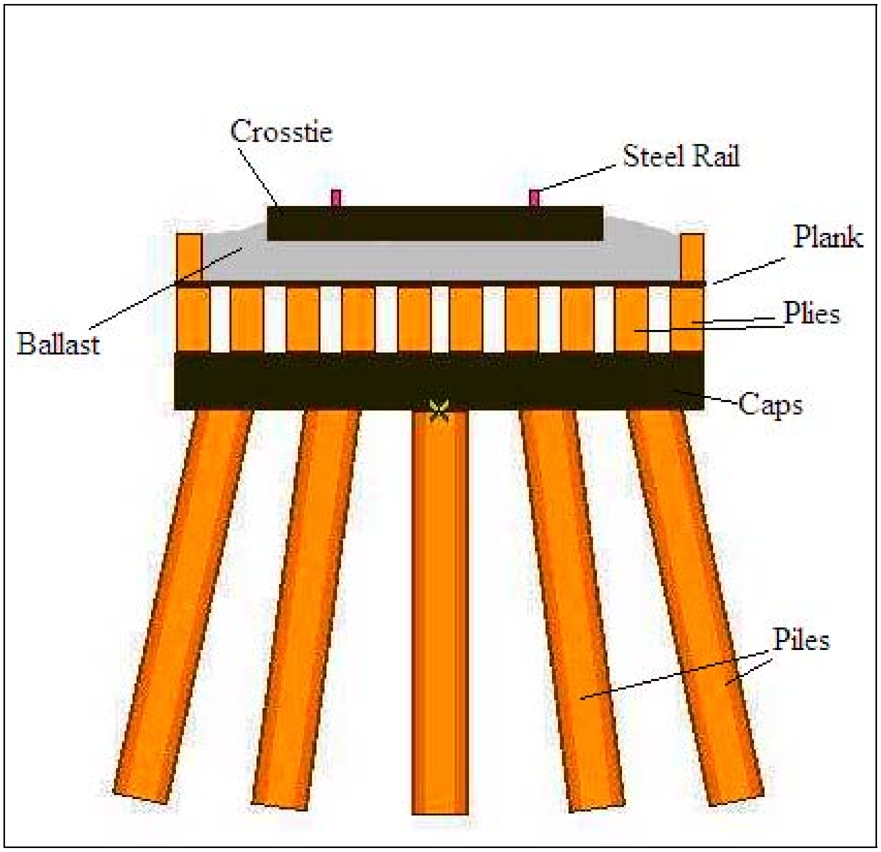

Figure 2.5 Cross-section depicting the main components of a typical ballast-deck timber bridge.

Much like a trestle bridge, the superstructure of a ballast-deck bridge is supported by a substructure consisting of timber pile caps resting atop timber piles. The caps support the plies, and the plies support the above ballast-deck, ballast, planks, crossties, and steel rail. The ballast-deck prevents the ballast from falling through the plies and is made up of stacked boards that rest on the underneath plies. The ballast typically consists of a granular material, such as crushed stone or volcanic ash. The permeable ballast allows for efficient drainage, and the irregular shapes of the ballast constituents provide an interlocking connection to evenly distribute the loads to the underlying ballast-deck plies. The planks, which are nailed to the plies underneath, run along the entire length of the bridge and provide lateral confinement of the ballast. The crossties, which are of similar size to those of a trestle bridge, are embedded in the ballast and spaced at specified intervals. The steel rail sits on rail plates, and the rail and plates are nailed to the crossties by rail spikes.

3. BACKGROUND

3.1 Background to the Research Study

Several investigations involving timber trestle bridges, or components thereof, which have been conducted by researchers at Colorado State University (CSU) are described in this chapter. Issues that have been researched and that are of relevance to this study are load testing and structural behavior of timber railroad bridges ─ both in the field [32, 53-54] and in the laboratory [23]. Also of relevance are investigations of the structural behavior of timber bridges strengthened by the addition of helper plies [23, 32]. Of particular interest are investigations into the structural behavior of bridge components strengthened by the process of shear spiking [15-16, 49-52, and 55-57]. As these investigations of shear spiking are germane to the work described herein, some details are provided.

3.2 Shear Spiking

The first study by CSU researchers investigating the effects of shear spiking was conducted by Radford et al. [49-52]. This research resulted in a comprehensive report published in conjunction with the Mountain Plains Consortium (MPC) [49], along with parallel technical papers [50-52]. The process of shear spiking was further developed in this study for application to structural timbers. The approach entailed adding shear spikes to timber beams of a relatively low aspect ratio as a means to rejuvenate, i.e. stiffen and/or strengthen, them. The reinforced timbers had aspect ratios comparable to those of full-scale railroad bridge span timbers, albeit on a small member size scale.

First, sets of layered, 48 inch (122 cm) long, nominal two-by-twos (actual dimensions of 1.5 by 1.5 inches [38 by 38 mm]) were studied in various interconnections. For example, in one set the layers were interconnected to twelve pairs of ordinary nails centered about the mid-point, creating longitudinally symmetric halves. The insertion order and final layout of the shear spikes is shown in Figure 3.1, where R1 was inserted first, followed by R2, and R6. This approach produced an average increase in effective flexural stiffness of about 81% as compared to stacked, but not interconnected, beams of identical size. The individual values ranged between 58% and 156%.

For comparison, a second set of layered two-by-twos were interconnected by twelve pairs of ⅛ inch (3.2 mm) diameter shear spikes, six on either side of the longitudinal centerline. The shear spikes were installed incrementally, and an epoxy resin was incorporated during installation. The shear spike pairs were placed in the same pattern as the nailed specimens, i.e. as in Figure 3.1. The average increase in effective stiffness from utilization of the shear spikes and epoxy resin, as compared to the unattached two-by-twos, was found to be approximately 160%, essentially double the effect of ordinary nails. The individual values ranged between 75% and 194%. Other two-by-two configurations were tested, and the reader is referred to Radford et al. [49-58] for details and results.

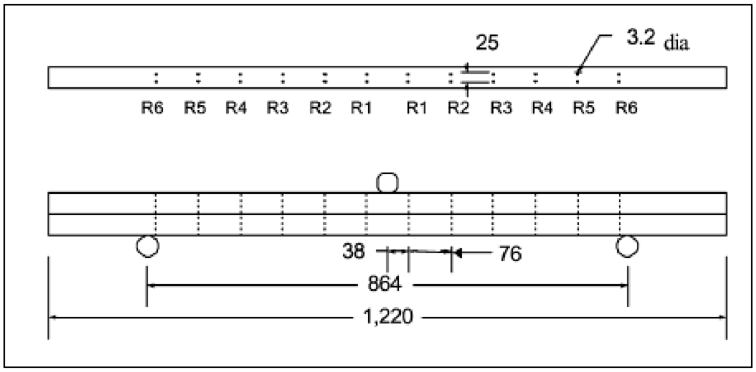

Figure 3.1 Shear spike layout and installation process (all dimensions in mm). Courtesy of Radford et al.

The next phase of the Radford et al. study [49-52] involved shear spiking of solid sawn, 48 inch (122 cm) long, nominal two-by-fours (actual dimensions of 1.5 by 3.5 inches [38 by 89 mm]). The two-by-fours were sawn longitudinally along the neutral axis from one end to within 2 inches (51 mm) of mid-span. Sawing the beams in this manner was done to mimic severe splitting. In one set of specimens, twelve pairs of shear spikes were then installed to both the sawed and non-sawed specimens, using the same spike installation procedure used to attach the stacked two-by-twos as previously described. The geometry of the specimens and spike placement are depicted in Figure 3.2 Sawing caused a drop off in effective stiffness of about 40-60%; shear spiking produced a recovery to about 75% of the effective stiffness of the (un-cut) members.

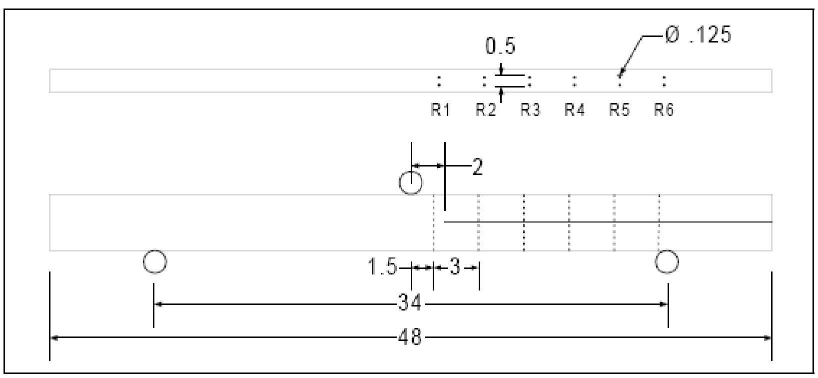

Figure 3.2 Shear spike layout and installation process (all dimensions in mm). Courtesy of Radford et al.

Additional two-by-four specimen configurations were studied and the reader is referred to Radford et al. [49-52] for details and results.

A continuation of the research done by Radford et al. [49-52] was conducted by Schilling et al. [55-57]. The researchers used ½-inch (13 mm) shear spikes in conjunction with an epoxy resin to rejuvenate deteriorated full-scale railroad crossties. A sample population of 35 Douglas fir crossties was available. The ties were divided into five groups; each group was based on physical appearance and measured flexural stiffness. The physical appearance rating incorporated surface conditions of the ties, extent of surface cracking (if any), and general size of the surface cracks. Crossties were categorized as high quality (5), medium quality (17). or low quality (13). The flexural stiffness was found from load testing, and based on the results, the ties were again categorized as high quality (8), medium quality (15), or low quality (12). The number in parenthesis indicates the number of ties in each category. Based on a combination of results from the two sorting methods, each crosstie was placed into one of five categories.

The five resulting combined categories were high-high quality (1), medium-high quality (7), medium quality (10), medium-low quality (12), and low quality (4).

A set of 10 crossties from the medium (3), medium-high (5), and high (2) quality groups were selected for shear spike strengthening. Another set of 10 crossties from the medium-low (6) and low (4) quality groups were also selected for shear spike strengthening. The shear spike installation procedure used was similar to that used by Radford et al. [49-52]. The final shear spike layout of one longitudinal crosstie half is illustrated in Figure 3.3 below. Five pairs of spikes were incrementally installed in each crosstie, symmetric about the longitudinal center line. The first increment of shear spikes was installed near the respective end locations of the beam, with successive installations moving toward the mid-point with a longitudinal spacing of 7.2 inches (18 cm). One installation increment consisted of two pairs of shear spikes ─ one pair on either side of the longitudinal centerline. An epoxy adhesive was installed into the pre-drilled holes via refillable caulking tubes. After installation of one set of shear spikes, the epoxy was allowed to cure for at least two days before load testing. This installation procedure was repeated until all 10 pairs (five pairs on either side of the mid-point) were installed.

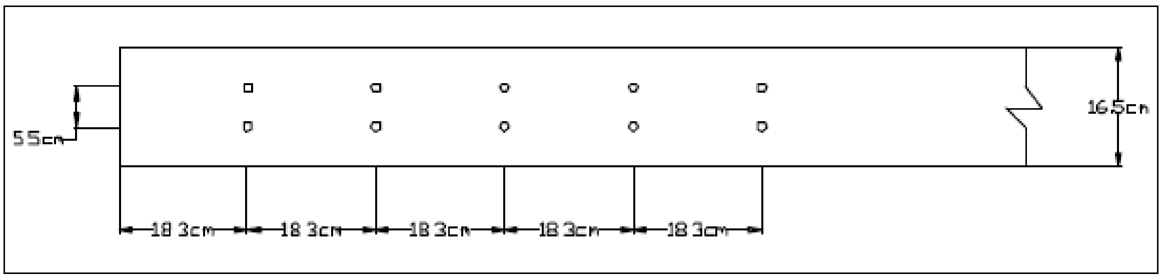

Figure 3.3 Final shear spike layout. Courtesy of Schilling.

The specific property measured in this research study for comparison of effects from strengthening by shear spiking and was the stringer EI, herein termed the “effective flexural stiffness.” The effective flexural stiffness is a product of the modulus of elasticity (E) and the area moment of inertia. The EI, rather than the E alone, was used for comparison for two main reasons. First, the specimens had slightly varying cross-sectional dimensions along their lengths, and thus variations in I. Second, since the E is a material property, it does not change from infliction of damage by cutting.

Load testing was performed before any shear spike installation and after each increment of shear spikes had been installed. A mid-span ramp load was applied by a hydraulic actuator, and load and corresponding deflections were recorded at intervals during both loading and unloading. The load was ramped from zero to a maximum load of approximately 6.5 kips (29 kN) and then unloaded. The EI of the crossties was determined from each load test by substituting the slope of the load versus deflection ($\delta P/\delta \Delta$) curve into the Euler beam equation for a single span simply supported beam with a concentrated load at mid-span.

The average increase in EI of the 10 crossties in the higher quality group was found to be 51% in the fully shear-spiked case as compared to the respective virgin specimens. The corresponding increase in EI of the lower quality group was 66%. It was concluded that specimens with a greater degree of deterioration had a greater potential of being rejuvenated from shear spiking. This research study resulted in an M.S. thesis [55], a comprehensive report published by the Mountain Plains Consortium (MPC) [56], and a technical paper [57].

In a continuation research study, Burgers et al. [15-16] performed laboratory testing of a full-scale, three-span open-deck, timber trestle railroad bridge chord that was strengthened through shear spiking. The chord was composed of a total of four single-span and four double-span stringers, where the single-span members were placed in the end spans and were alternated with the double span stringers to create a standard staggered configuration. The lateral open-deck spacing of 2.0 inches (50 mm) was provided by metal spacers and transverse steel tie rods. A total of five tie rods, two near each support location and at mid-span, were used per span. The researchers sought to improve the shear and flexural performance after the chord was intentionally damaged to simulate deterioration. The specimen was “partial” in the sense that the only components of the chord were the timber stringers and steel tie rods. The substructure was simulated by a steel support frame. The three-spans each measured 13-foot - 2-inch (158 inches [4.0 m]), and the stringers were of an approximate average cross-section of 7.9 inches (20 cm) by 15.8 inches (40 cm). The modulus of elasticity (MOE) of each stringer was determined from a four-point load test. The average value of all stringers used was 1.52 x 10^6 psi (10,500 MPa).

The researchers intentionally damaged the center span by cutting the stringers horizontally along the neutral axis. The end span halves of the double span stringers and the single span stringers were not cut. First, the south segment of the center span was cut with a chainsaw. The chainsaw blade, however, was not wide enough to cut through the entire width of the chord; approximately 1 to 2 inches (2.5 to 5.1 cm) of material of the inner two stringers could not be reached. To have the damage extend into the uncut portions, the chord was loaded with the intention of having a controlled crack propagate through these remaining undamaged portions. However, the cracking that occurred not only propagated through the intended regions, but also propagated into the center segment of the span. The south segment and center segment of the center span were then strengthened through shear spiking. Next, the north end of the center span was intentionally damaged and then strengthened. This time, however, the researcher cut the inner portions, unreachable by the chainsaw, with a two-man handsaw. In other words, portions of the longitudinal halves of the double span stringers located in the center span were damaged. The chainsaw cuts were shimmed so that closing and opening of the gaps would be minimized during loading (see Figure 3.4).

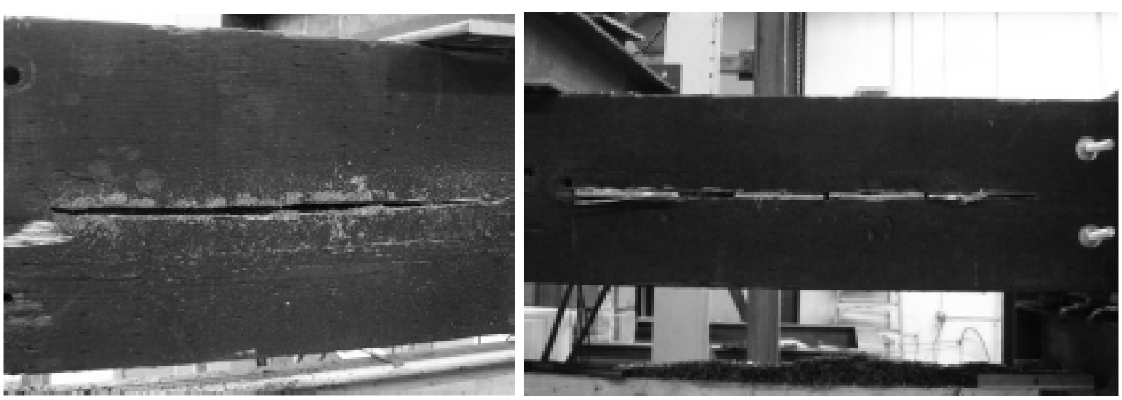

Figure 3.4 Un-shimmed and shimmed chainsaw damage. Courtesy of Burgers.

The shear spikes were cut to length of 16 inches (41 cm) from a ¾ inch (1.9 cm) diameter base stock. The holes for the shear spikes were not drilled through the entire stringer depth; instead, at the bottom approximately ½ inch (1.3 cm) of wood was left in place to ensure containment of the epoxy resin. The length of the shear spikes was such that approximately ½ inch (1.3 cm) protruded from the top face of the stringer after installation. The epoxy adhesive used was the same as that used by Schilling et al. [55-57].

A “set” of shear spikes refers to one pair in each of the four stringers, i.e. a total of eight shear spikes across the full width of the chord. The two shear spikes of each pair were located at the third points of the respective stringer width. After initial load testing of the damaged chord, shear spikes were installed in three phases. The chord was load tested after installation of each set of shear spikes.
In Phase I, the south end of the center span was strengthened. A total of 11 sets of shear spikes were installed in Phase I. Phase II of the strengthening process consisted of five sets of shear spikes installed in the middle segment, three sets of shear spikes installed between already installed pairs, two sets to continue the 4-inch (13 cm) longitudinal spacing. After completion of Phase I and II, a total of 16 sets of shear spikes had been installed. The intent of the shear spikes installed inside the two-load application points was to repair the unintentional crack propagation that occurred during load testing of the damaged, but not strengthened, specimen. The layout of shear spikes of Phase I and Phase II, excluding the three south-most sets of Phase I which were installed outside the distributor beams, are shown in Figure 3.5.

The third and final phase, Phase III, consisted of five sets of shear spikes installed in the north segment, as shown in Figure 3.5. The total number of shear spikes installed in Phases I, II, and III totaled 21 sets, or 42 shear spikes in each of the four stringers.

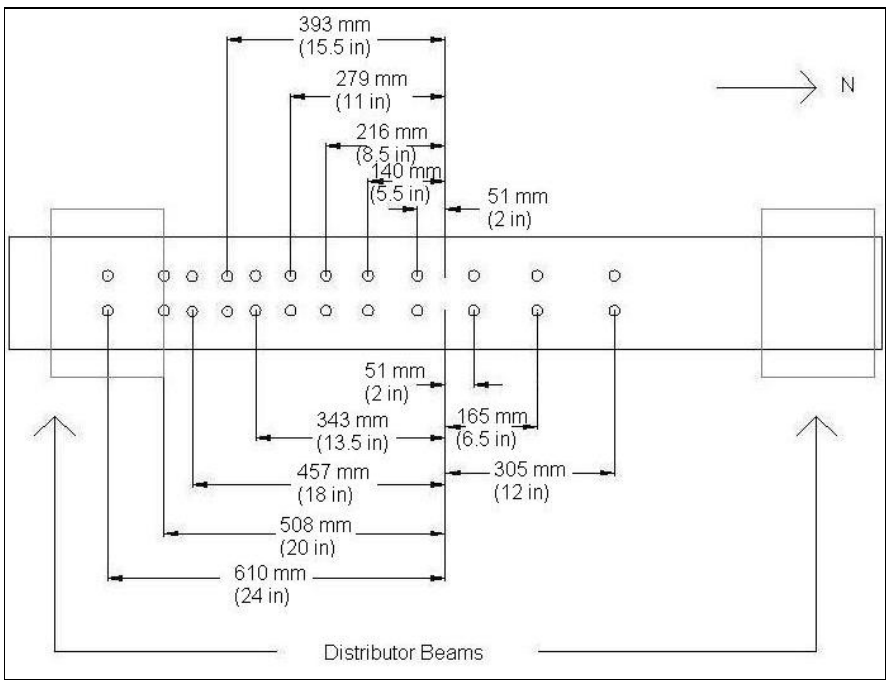

Figure 3.5 Plan view of final shear spike layout of south end (Phases I and II) to repair the unintentional damage. Only the shear spikes installed between (inside) the distributor beams are shown; the four south-most sets of shear spikes of Phase I are thus not shown. Courtesy of Burgers.

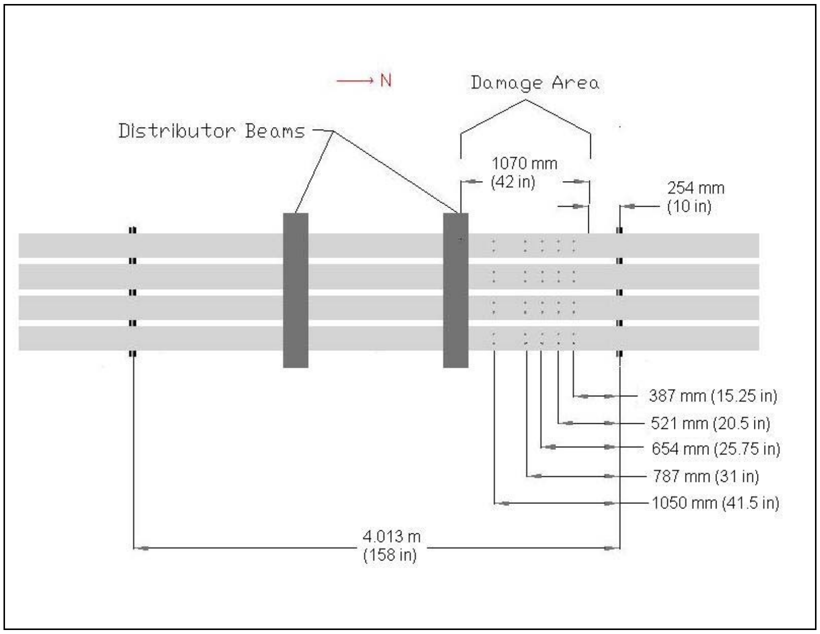

Figure 3.6 Plan view of final shear spike layout of Phase III, installed north of (outside) the north distributor beam. Courtesy of Burgers.

A ramp loading was applied to the chord by two hydraulic actuators, attached to an overhead steel frame. The loads were applied to the respective third-points of the center span and were laterally distributed to all four stringers of the chord by steel spreader beams. The maximum load applied after damage had been inflicted was 15 kips (67 kN) per actuator. Vertical deflections at the mid-span of all three spans of each stringer were recorded at specified load increments, during both loading and unloading, by string potentiometers.

As with work by Schilling et al. [55-57], the effectiveness of the strengthening process was the based on effective flexural stiffness, EI. In this study the EI was determined by substituting the slope of the load versus deflection curve ($\delta P/\delta\Delta$) into the Euler-Bernoulli beam equation for a two-span continuous beam with the load applied at the third-points of one span and corresponding vertical deflection measured at mid-span of the loaded span. The main observations from load testing were as follows:

- All four stringers in the loaded span exhibited linear load versus deflection behavior up to the imposed load level, both before and after insertion of shear spikes.
- After installation of all five sets of shear spikes (Phase III) in the north half of the center span, a 91.6% recovery of chord flexural stiffness, as compared to the undamaged specimen, was observed.
- Repair of the unintentionally-damaged (crack propagation under load) region (Phase I and Phase II) by the higher shear spike density increased the flexural stiffness of all four stringers of the chord. However, there was not enough data to quantify this increase in stiffness.
- The shear spikes, in combination with the epoxy resin, developed significant interlayer shear transfer between the top and bottom layers in the intentionally-damaged area.
- By not drilling holes through the entire depth of the stringer, the majority of epoxy was retained since none was pushed out the bottom. Beads of epoxy were observed at some locations on the outside stringers; it was concluded that the epoxy had migrated from the drilled hole through voids and cracks, which is an added contribution to the stiffening of the stringers.

- The results were consistent with those found by Radford et al. [49-52] and by Schilling et al. [55-57], albeit on a larger member size scale.

The investigation resulted in an M.S. thesis [15] and a comprehensive research report published by the MPC [16].

4. EXPERIMENTAL TEST SETUP AND PROCEDURE

4.1 Description of Timber Stringers

The objective of the research study described is to examine the behavior of shear spike strengthened main members of a timber railroad bridge. Similar to Burgers et al. [15-16], it was decided that the stringers were the only components to be load tested, and that the stringers were to be tested individually. By not using a complete bridge chord, e.g. three to five stringers, rail, rail plates, tie rods, and crossties, many of the variables involved in analysis of the test results were eliminated. Also, by testing the stringers individually, rather than a complete chord, the load required to achieve a desired deflection was greatly reduced.

The majority of the stringers was salvage material; the remainder was new, previously unused stringers. The stringers were donated to CSU by the Association of American Railroads (AAR) in 1996 for use in two prior research studies. In the first study, Doyle [23] researched the effects of adding helper plies to a bridge chord. The stringers were load tested at levels well below their ultimate strength capacity in that study.

In the second study, Burgers et al. [15-16] researched effects of strengthening, through the process of shear spiking, intentionally-damaged stringers of a four-ply, three-span bridge chord. The study was described in Section 3.2. The bridge chord consisted of a total of eight stringers: four double-span (labeled 5 through 8 in Figure 4.1) and four single-span stringers (labeled 1 through 4 in Figure 4.1).

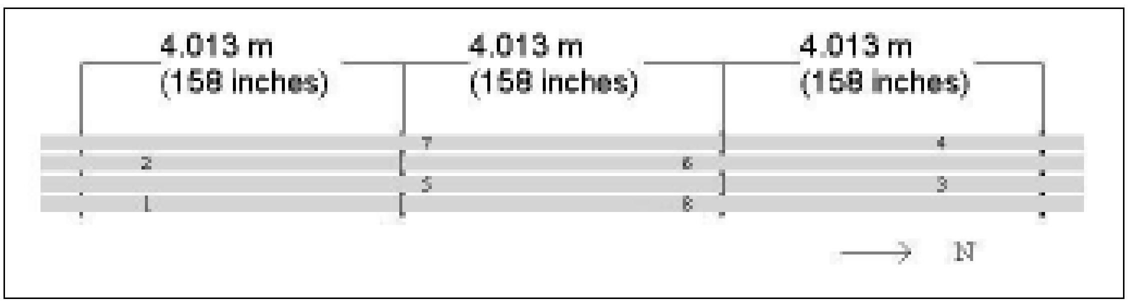

Figure 4.1 Plan view of the chord used by Burgers. Courtesy of Burgers.

The single-span stringers and the half lengths of the double-span stringers that were located in the end spans were salvaged for the study described in this thesis work. The damaged center span (the half length of each of the four double-span stringers) was cut off and discarded. Since the timbers used in this study were located in the end spans, they were never directly loaded themselves, and a visual inspection showed that no significant damage had been imposed on them.

4.2 Loading Setup

Numerous load tests in this study investigated the effects of inflicted damage and subsequent strengthening — and particularly the effects of durability loading on the strengthened stringers. "Durability loading" is defined herein as continuous, cyclic loading of the stringers. The total load cycle count is at least 10,000 if referred to as "durability loading." The load configuration used throughout this study was two equidistant loads, applied at the third-points of the clear span as shown in Figure 4.2. The measured clear span was 159 inches (4.0 m). An MTS hydraulic actuator was used to apply a point load at mid-point. This point load was then transformed via a distributor beam into two equal (in magnitude) line loads (oriented perpendicular to the length of the stringer), applied at the clear span third-points. The distributor beam was centered atop 8 inch (20 cm) square, ½ inch (1.3 cm) thick steel plates, which transferred the imposed load to the top face of the stringer. Identical size steel plates were used at the support points.

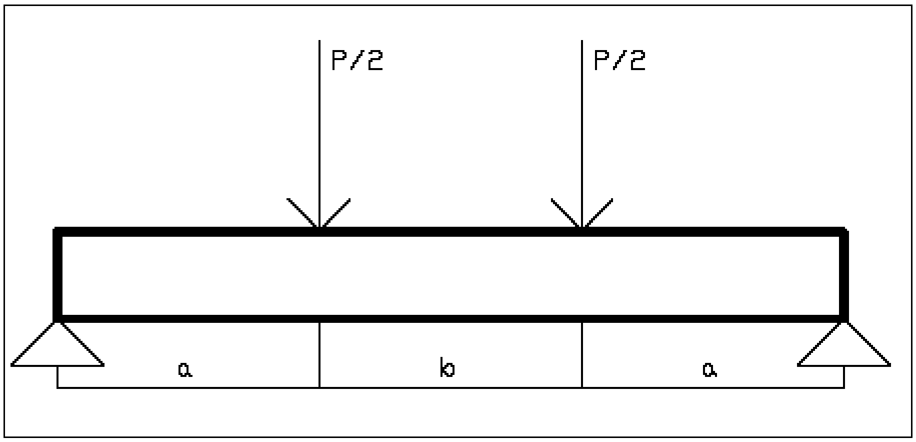

Figure 4.2 Simply supported beam with two equidistant point-loads; a = b = L/3, where L is the clear span length.

Loading was applied by a hydraulic actuator, which was attached to an overhead steel frame that was moveable along the length of the below described concrete pad. Another actuator was attached to the overhead steel frame, and the frame therefore had to be off-centered for the one actuator used to be longitudinally centered at mid-span, as evident from Figure 4.3. The steel support frame was made of lateral crossbeams, bolted to vertical columns, which were in turn welded to lateral framing members. The framing members were anchored into an existing 8-foot 7-inch (2.6 m) wide concrete pad that sat on the laboratory floor. The steel crossbeams supported the stringer from underneath, thus mimicking pile caps; the vertical steel columns substituted for the piles. The load cell had a maximum rated load capacity of 100 kips (445 kN). The actuator was controlled, and load data was recorded, by an MTS 406 controller.

Figure 4.3 Photograph of test setup.

4.3 Material Properties

The stringers were solid sawn, creosote treated Douglas fir timbers. Length, cross-sectional dimensions, and wood moisture contents of each stringer are given in Table 4.1. The stringer lengths varied from 170 to 175 inches (4.3 to 4.5 m), with an average length of 174 inches (4.4 m). This resulted in an overhang of 6.15 to 8.55 inches (16 to 22 cm) at each support. The average stringer cross-section, as measured at mid-point, was 7.9 by 16.1 inches (20 by 41 cm). The moisture content of each stringer was measured with an electrical resistance meter [22]. The wood moisture contents ranged from 5.7% to 8.8%, with an average of 7.1%.

Table 4.1 Stringer dimensions and moisture contents

Beam	Length [in]	Height [in]	Width [in]	Length [cm]	Height [cm]	Width [cm]	Wood Moisture Content
1P-A	174.9	16.3	7.8	444.2	41.3	19.7	7.0%
1P-B	173.2	16.1	7.8	439.9	41.0	19.8	7.4%
2P-A	171.0	16.1	8.1	434.3	40.8	20.7	7.5%
2P-B	175.1	15.8	7.9	444.8	40.2	20.2	8.8%
1F-A	175.0	16.0	7.8	444.5	40.7	19.8	6.6%
1F-B	175.0	16.5	8.0	444.5	42.0	20.4	6.4%
2F-A	170.3	15.8	8.1	432.4	40.2	20.5	5.7%
2F-B	174.8	16.1	7.8	443.9	41.0	19.7	7.5%
Average	173.6	16.1	7.9	441.1	40.9	20.1	7.1%

4.3.1 Timber Stringers

Before infliction of damage and subsequent strengthening, ramp load tests were performed on all eight stringers to determine their virgin effective stiffness. A total of seventy-six (76) load tests were performed. In each case, a ramp load was applied to the specimen and the stringer EI was determined from the resulting load-deflection behavior. The actuator was operated using stroke control at the rate of 0.015 in/s (0.4 mm/s). When a desired load increment was reached, the stroke was held constant and stringer deflection recorded. Equal point loads were applied by the actuator, via the distributor beam, to the one-third points of the 13-foot 2-inch (4.0 m) span. The applied load and corresponding mid-span deflection were measured at intervals of approximately 0.25 to 0.30 kips (1.1 to 1.3 kN), starting at 0 kips (0 kN) to a maximum load ranging from 7.1 to 7.9 kips (32 to 35 kN). This load level ensured that the wood stayed well within its linear-elastic range.

The EI-values reported herein are determined from the slope of the load versus mid-span deflection curve of the load tests. This slope is calculated as change in load (δP) [kips or kN] divided by change in vertical deflection (δΔ) [in or cm] of each load increment, i.e. δP/ δΔ. Data points outside of (+/-) one standard deviation of the mean are excluded. A new mean δP/δΔ was then calculated from the "inbound data." This inbound mean δP/δΔ is used in Equation 4.1 to calculate the effective stiffness, EI. Equation 4.1 is the Euler beam equation for a simply supported beam with two equidistant point-loads applied at third-points.

$$\frac{\delta\Delta}{\delta P} = \frac{3L^2 a - 4a^3}{48EI} \Leftrightarrow EI = \frac{\delta P}{\delta\Delta}\frac{3L^2 a - 4a^3}{48} \qquad (4.1)$$

In Equation 4.1, "δP/δΔ" is the average slope of the load versus mid-span deflection curve, "L" is the clear span length (158 inches [401.3 cm]), and "a" is the distance from either end to the point of load application (L/3 = $52^2/_3$ inches [134 cm]). Raw data from ramp load testing of stringer 1P-A is given in Table 4.2.

Table 4.2 Load-deflection data of stringer 1P-A, virgin state

Specimen 1P-A, Virgin

Actual Load [kips]	δP [kips]	Mid-Span Deflection [in]	δΔ [in]	δP/δΔ [kips/in]	Data Analysis	Bounded Data
0.00	0.00	0.0000	0.0000	-		
0.22	0.22	-0.0039	-0.0039	-55.74	FALSE	
0.39	0.17	-0.0081	-0.0042	-40.88	TRUE	-40.88
0.58	0.19	-0.0128	-0.0047	-40.32	TRUE	-40.32
0.78	0.20	-0.0177	-0.0049	-40.83	TRUE	-40.83
0.89	0.11	-0.0192	-0.0015	-74.79	FALSE	
1.08	0.19	-0.0239	-0.0048	-39.96	TRUE	-39.96
1.27	0.19	-0.0291	-0.0052	-36.57	FALSE	
1.48	0.21	-0.0343	-0.0052	-40.59	TRUE	-40.59
1.69	0.21	-0.0383	-0.0040	-52.84	TRUE	-52.84
1.87	0.18	-0.0413	-0.0031	-58.90	FALSE	
2.08	0.21	-0.0461	-0.0048	-43.81	TRUE	-43.81
2.27	0.19	-0.0506	-0.0045	-42.36	TRUE	-42.36
2.49	0.22	-0.0562	-0.0056	-39.43	TRUE	-39.43
2.69	0.20	-0.0606	-0.0044	-45.71	TRUE	-45.71
2.91	0.22	-0.0648	-0.0042	-52.16	TRUE	-52.16
3.08	0.17	-0.0685	-0.0037	-46.26	TRUE	-46.26
3.30	0.22	-0.0732	-0.0048	-46.03	TRUE	-46.03
3.47	0.17	-0.0779	-0.0047	-36.42	FALSE	
3.69	0.22	-0.0821	-0.0041	-53.13	TRUE	-53.13
3.86	0.17	-0.0850	-0.0030	-57.28	FALSE	
4.10	0.24	-0.0887	-0.0037	-64.81	FALSE	
4.29	0.19	-0.0920	-0.0033	-57.47	FALSE	
4.49	0.20	-0.0975	-0.0055	-36.42	FALSE	
4.69	0.20	-0.1025	-0.0050	-40.32	TRUE	-40.32
4.92	0.23	-0.1071	-0.0047	-49.35	TRUE	-49.35
5.12	0.20	-0.1112	-0.0041	-49.09	TRUE	-49.09
5.32	0.20	-0.1155	-0.0042	-47.06	TRUE	-47.06
5.50	0.18	-0.1198	-0.0043	-41.82	TRUE	-41.82
5.71	0.21	-0.1248	-0.0050	-42.09	TRUE	-42.09
5.93	0.22	-0.1291	-0.0043	-51.08	TRUE	-51.08
6.12	0.19	-0.1336	-0.0045	-41.96	TRUE	-41.96
6.32	0.20	-0.1377	-0.0041	-49.33	TRUE	-49.33
6.50	0.18	-0.1414	-0.0037	-48.60	TRUE	-48.60
6.70	0.20	-0.1461	-0.0047	-42.52	TRUE	-42.52
6.91	0.21	-0.1512	-0.0051	-41.24	TRUE	-41.24
7.10	0.19	-0.1548	-0.0036	-52.52	TRUE	-52.52

Average	-47.21
Std Dev	8.44
100%	8.44
Average + Std Dev	-38.77
Average - Std Dev	-55.65

Average, Inbound Data	-45.233
New StDev	4.625

For purposes of illustration, the following computation clarifies how the EI is determined from Equation 4.1. The data used is from virgin load testing of stringer 1P-A: δP/δΔ = 45.233 kip/in, L = 158 inches, and a = 52 $^{2}/_{3}$ inches.

$$EI_{eff} = 45.233\,kip/in \times \frac{3 \times (158\,inches)^2 \times (52\,{}^2\!/_3\,inches) - 4 \times (52\,{}^2\!/_3\,inches)^3}{48} = 3.17 \times 10^6\,kip-in^2$$

By dividing the above calculated EI by the stringer's area moment of inertia, I, a stringer's apparent modulus of elasticity is calculated. The moment of inertia is calculated using Equation 4.2:

$$I = \frac{b \times h^3}{12} \qquad (4.2)$$

In Equation 4.2, "I" is the area moment of inertia, "b" is the stringer width, and "h" is the stringer's height. The virgin stiffness (EI), area moment of inertia (I), and modulus of elasticity (E) of all stringers used in this study are given in Table 4.3.

Table 4.3 EI, I and E of stringers

Stringer	EI [kip-in^2]	I [in^4]	E [lbs/in^2]	EI [kN-cm^2]	I [cm^4]	E [kN/m^2]
1P-A	3.17E+06	2789	1.14E+06	9.09E+07	1.16E+05	7.83E+06
1P-B	2.94E+06	2740	1.07E+06	8.43E+07	1.14E+05	7.39E+06
2P-A	3.51E+06	2813	1.25E+06	1.01E+08	1.17E+05	8.61E+06
2P-B	3.36E+06	2615	1.29E+06	9.65E+07	1.09E+05	8.86E+06
1F-A	3.58E+06	2688	1.33E+06	1.03E+08	1.12E+05	9.19E+06
1F-B	2.94E+06	3025	9.71E+05	8.43E+07	1.26E+05	6.70E+06
2F-A	3.53E+06	2667	1.32E+06	1.01E+08	1.11E+05	9.13E+06
2F-B	3.83E+06	2718	1.41E+06	1.10E+08	1.13E+05	9.71E+06
Average	3.36E+06	-	1.22E+06	9.63E+07	-	8.43E+06

The empirical E values were compared to those given in the 2001 edition of the National Design Specification (NDS) for Wood Construction Supplement, Table 4D [1]. The tabulated E values for Douglas fir (-larch, -larch north and -south), category timbers, and stringers, range from 1.00 x 10^6 to 1.70 x 10^6 psi (6.89 x 10^6 to 1.17 x 10^7 kPa), dependent on structural grade. The E values reported herein thus fall within the lower half of that range.

4.3.2 Shear Spikes

The pultruded rods used in the study were manufactured by Liberty Pultrusions of West Mifflin, Pennsylvania. The rods are composed of thin, unidirectional (oriented in the longitudinal direction) fiberglass strands, bonded together with polyglass polyester resin by process of pultrusion. The rods are graded for general purpose use for in-place temperatures of up to 311˚F (155˚C). Some notable mechanical properties of the pultruded rods, at room temperature, are ultimate strength of 70.0 ksi (483 MPa), flexural strength of 70.0 ksi (483 MPa), and compressive strengths of 20.0 ksi (138 MPa) and 40.0 ksi (276 MPa) perpendicular and parallel to fiber-strand orientation, respectively. The E of the rods is 3,000 ksi (2.1 x 10^4 MPa) and the specific gravity is 1.95, approximately one-quarter the specific gravity of structural steel.

4.3.3 Epoxy Resin Adhesive

The epoxy adhesive was supplied by West Systems, Inc. of Bay City, Michigan. The cured epoxy resin/hardener/filler mixture yields a high-strength, moisture resistant solid. At 72°F (22°C), the pot life of this epoxy-hardener mix is 20 to 25 minutes. The cure time to solid state is nine to 12 hours, and cure time to maximum strength time is one to four days. The times stated above are highly dependent on ambient temperature and humidity. If the ambient air temperature is higher (lower) than that recommended by the manufacturer, the cure time can greatly decrease (increase) due to the increased (reduced) heat available for the exothermic reaction between the epoxy resin and hardener. The manufacturer specifies a recommended temperature range of 60° to 90°F (16° to 32°C). The temperature was held well within this temperature range during shear spike installation; the ambient room temperature ranged from 70.3° to 84.7°F (21.3° to 29.3°C), and the average ambient humidity ranged from 5% to 44%, with an average of 22.2%.

Mechanical properties of the cured epoxy are dependent on mix ratio, curing conditions, etc; specific values of mechanical properties therefore vary greatly. Load testing was conducted to determine the shear strength of the epoxy bond between the shear spikes and the wood fibers of the crosstie. The epoxy bond strength was found from six load tests, and varied from 0.68 to 1.85 ksi (4.7 to 12.8 MPa) with an average strength of 1.26 ksi (8.7 MPa).

4.4 Damaging the Timber Stringers

The stringers used in this study were considered structurally intact, in good physical condition, and not in need of strengthening. The stringers were, therefore, intentionally damaged prior to shear spiking. The damage was intended to replicate the loss of stiffness, related to a loss of shear capacity that is often observed in the deteriorated span timbers of railroad bridges (Radford et al. [51]). The average depth, width, and length of the stringers tested in this study were 16.1, 7.9, and 174 inches (40.9, 20.1, and 441 cm), respectively. The eight stringers were randomly paired into four groups, and similar damage was inflicted on the stringers of each pair.

All stringers were saw cut horizontally at the neutral axis location, and half the sample population were also saw cut horizontally at the quarter distance above the bottom face. All saw cuts extended lengthwise from the stringer ends to the respective third-point, relative to span length. The longitudinal middle-third thus remained uncut in all stringers. For half the sample population, the horizontal saw cut(s) extended through the entire width of the member. For the other half of the sample population, the saw cuts were 3 inches (7.6 cm) deep, measured from either side face. The center approximately 2 inches (5.1 cm) of the stringer width thus remained uncut for the latter described stringers. The four pairs of stringers were damaged and labeled as follows:

- The group with damage inflicted by one saw cut (at the neutral axis location), and the cut extending through only a portion of the width of the stringer will be referred to as the “one partial cut,” or simply the “1P” group (top-left cross-section in Figure 4.4).
- The group with damage inflicted by one saw cut (at neutral axis location), and the cut extending through the entire width of the stringer will be referred to as the “one full cut,” or simply the “1P” group (bottom-left cross-section in Figure 4.4).
- The group with damage inflicted by saw cuts at two locations (at neutral axis location and quarter depth), and cuts extending through only a portion of the width of the stringer, will be referred to as the “two partial cuts,” or simply the “2P” group (top-right cross-section in Figure 4.4).
- Finally, the group with damage inflicted by saw cuts at two locations (at neutral axis location and quarter depth), and cuts extending through the entire width of the stringer, will be referred to as the “two full cuts,” or simply the “2F” group (bottom-right cross-section in Figure 4.4).

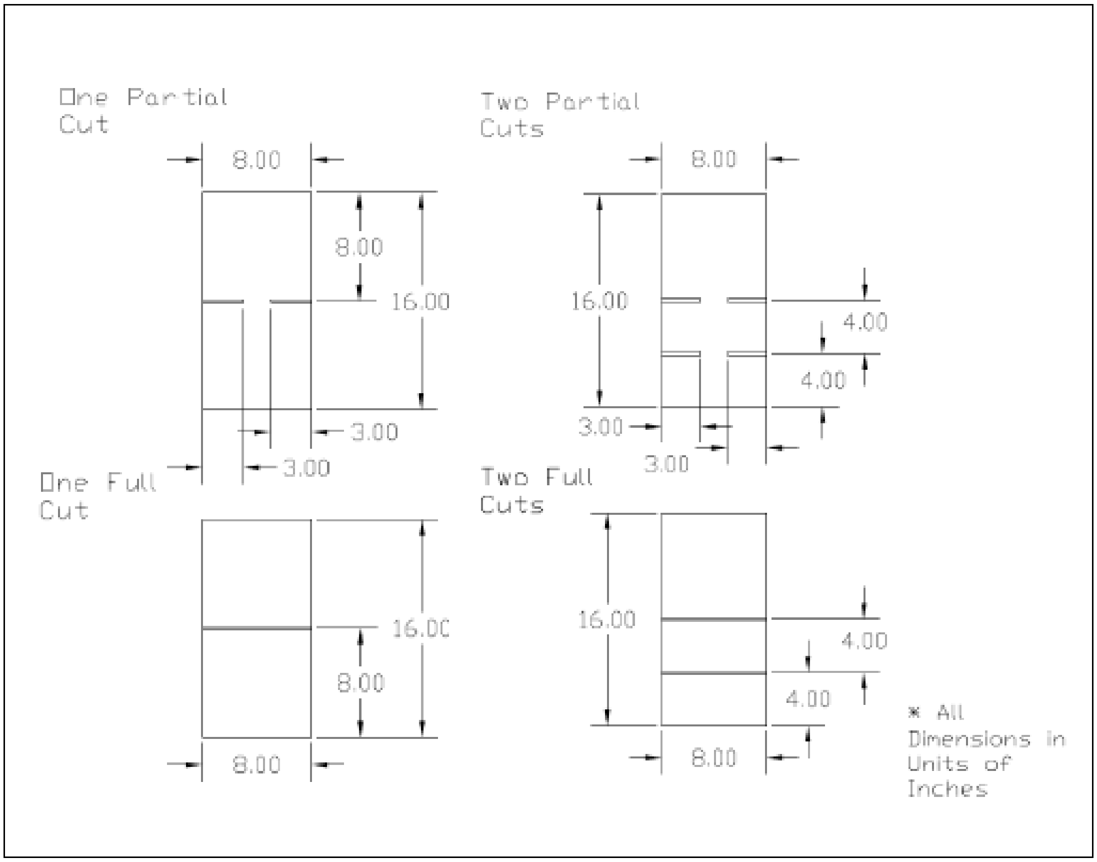

Figure 4.4 Cross-sections depicting location(s) of saw cuts, based on an 8" by 16" cross-section.

A circular saw with a cut depth of 3 inches (7.6 cm) was used to saw the partial cuts. These cuts were sawed from both sides of the stringer, leaving approximately (depending on stringer width) the middle 2 inches (5.1 cm) of the section uncut. For the full cuts, which extended through the entire stringer width, the circular saw was first used in the same manner as for the partial cuts. The uncut center section was cut using a reciprocating saw. The cuts from both the circular saw and the reciprocating saw created vertical gaps of less than $^1/_8$ inch (3.2 mm).

4.5 Shear-Spike Installation

The shear spikes were cut from a 96-inch (2.44 m) long, ¾-inch (19 mm) diameter, base rod stock. As show in Figure 4.5, the shear spikes were cut to a length of 16 inches (40.6 cm) ― approximately the same depth as the stringers. The last 1 inch (25 mm) of the leading edge of each spike was beveled to a sharp point using an angle grinder. This was done to reduce the force required to drive the shear spike into the pre-drilled hole in the stringer and to avoid scraping off the epoxy adhesive from the sides of the hole by the sharp edge of the original cut during installation.

Figure 4.5 Photograph of cut and beveled shear spikes.

The shear spikes were installed in a manner similar to that of Burgers et al. [15]; vertical holes were drilled from the top face of the stringer at the intended shear spike locations. Four sequential steps were involved in the drilling process, as illustrated in Figure 4.6.

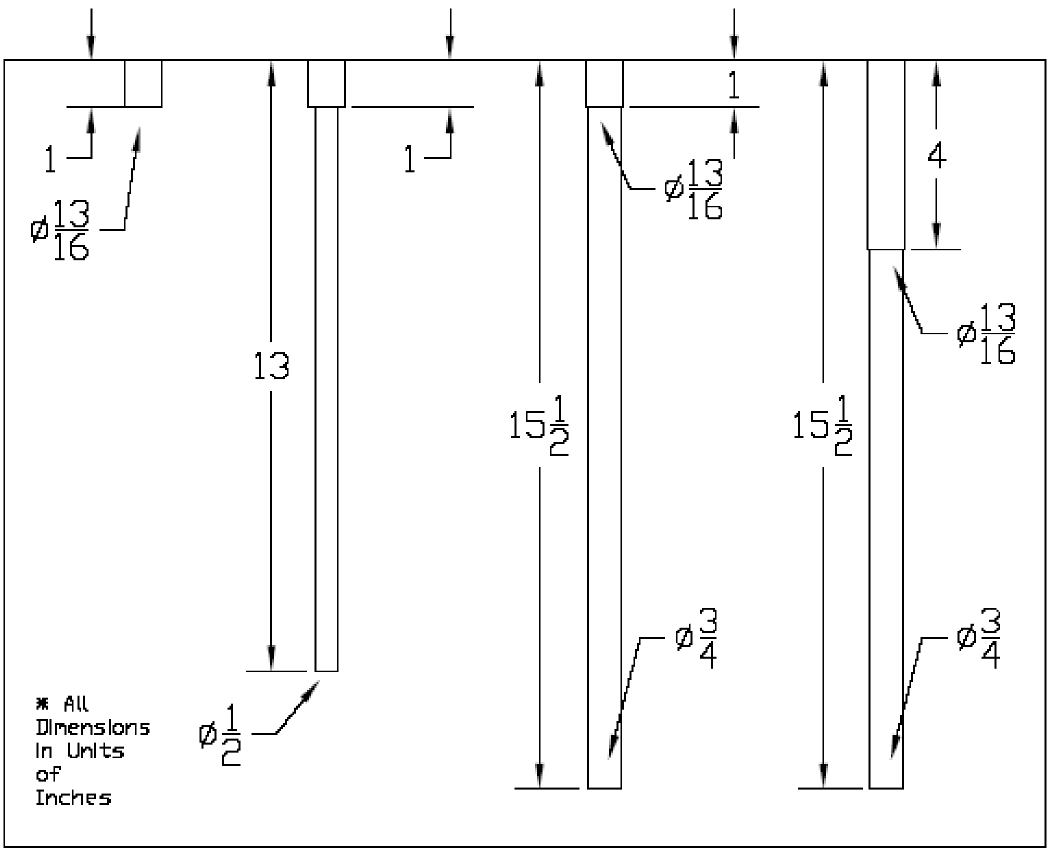

Figure 4.6 Sequence (left-to-right) of drilling process.

First, a 1-inch (25 mm) deep, $^{13}/_{16}$-inch (21 mm) diameter countersunk was drilled using a paddle drill bit. Next, a ½-inch (13 mm) diameter auger drill bit was used to drill a 13 inch (320 mm) deep pilot hole for the more flexible ¾-inch (19 mm) diameter auger drill bit used next. The ¾-inch (19 mm) hole was drilled to an approximate depth of 15½ inches (39.4 cm) but varied as these holes were drilled to approximately ½-inch (13 mm) less than the full depth of the stringer. Next, the $^{13}/_{16}$-inch (21 mm) diameter countersunk was extended to a depth of 4 inches (102 mm). Finally, a modified ¾-inch (19 mm) diameter drill bit, where the driving tip had been removed, was use to clean out any wood fiber debris from the hole.

The three-part epoxy system used to bond the shear spikes to the wood fibers was the same as that used by Burgers et al. [15] and by Schilling et al. [55]. The three components of the system were the epoxy resin, hardener, and filler. The epoxy resin used was the “105 Epoxy Resin (Part 1).” This is a low-viscosity liquid epoxy resin designed specifically to wet out and bond with wood fibers and fiberglass. The hardener used was the “206 Slow Hardener (Part 2)” ― a low-viscosity liquid curing agent used to extend the pot and cure times of the epoxy-hardener mix. The epoxy-hardener was combined in a five-to-one ratio ― five parts epoxy to one part hardener (by either weight or volume).

The epoxy and hardener were mixed by use of a paint stick. The 5:1 mix ratio was closely monitored to ensure a consistent quality and strength of the epoxy adhesive. Finally, the epoxy-hardener mix was combined with the “406 Colloidal Silica Adhesive Filler”, a thickening additive used for viscosity control. The silica filler is designed for general bonding and filleting. The exact amount of filler added was not directly measured. Instead, filler was added until an acceptable viscosity was reached ― approximately the consistency of room-tempered maple syrup. The mix could not be too viscid to allow for it to flow into and fill decay voids and cracks near the shear spike insertion point, but at the same time it had to viscid enough so that all adhesive mixture would not flow directly to the bottom of the hole during shear spike installation. Approximately 2.5 fluid ounces (74 mL) of epoxy/hardener/filler mix was used per shear spike.

First, the epoxy adhesive was poured into the pre-drilled hole, as shown in Figure 4.7. Then, the shear spike was driven into the hole using a 2½-pound dead blow hammer, as depicted in Figure 4.8. A dead blow hammer was used, rather than a steel hammer, to prevent the trailing end of the shear spike from fracturing during the driving process. After installation, the epoxy adhesive was allowed to cure for at least 48 hours, as specified by the manufacturer, prior to any load testing. A total of twenty shear spikes were installed in each stringer after load tests of the virgin specimen and in the subsequently damaged state.

Figure 4.7 Photograph of pouring of epoxy into pre-drilled hole.

Figure 4.8 Photograph of driving shear spike into pre-drilled hole.

The shear spikes were installed in pairs; in each pair spikes were installed at respective third-points of the crosstie width. The first pairs of spikes, one pair at each end, were installed 5¼ inches (130 mm) inside of the two respective support locations (R1 in Figure 4.9). Additional pairs of spikes were installed 10½ inches (270 mm) closer to the mid-span. Shear spiking continued at this 10½-inch (270 mm) spacing, and the final two pairs of spikes (R5 in Figure 4.9) were installed approximately 5¼ inches (130 mm) outside of the respective third-points. A longitudinal shear spike spacing of 10½ inches (270 mm) was chosen because an open-deck trestle bridge with 8-inch (203 mm) wide, typically spaced crossties would allow for installation of shear spikes between crossties if this approximate shear spike spacing was used. Figure 4.9 illustrates the final shear spike layout and installation sequence. In half the sample population (one stringer per pair of stringers, where pairing was based on degree of inflicted damage), ramp load testing was performed after each shear spike installation increment. The ramp load testing was performed to determine the effectiveness in flexural stiffness as related to reinforcement ratio. In the other sample population, one-half of all 20 shear spikes were installed in one day, without performing any load testing of the stringer between each installation sequence.

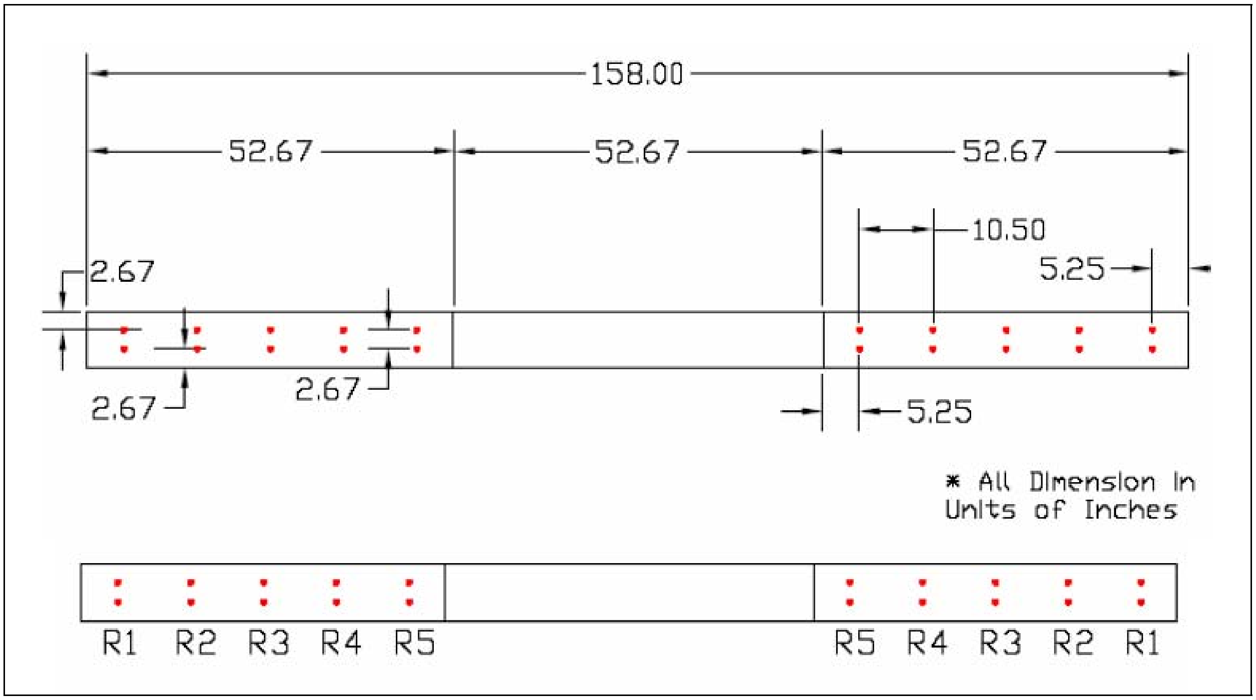

Figure 4.9 Plan view of a stringer, illustrating final shear spike layout (typical spacing) and installation sequence.

In the case of the stringers with shear spikes installed incrementally, each increment consisted of four shear spikes, giving a total of five increments per stringer. Installation was initiated by installing two pairs of two spikes each, located 5¼ inches (130 mm) inside of the respective support locations. This installation and loading process was followed for all five shear spike increments: insert two pairs of shear spikes, cure for at least 48 hours, and then load test the stringer. Since the installation sequence was mirrored about the longitudinal mid-point of a stringer, reinforced specimens were symmetric, with respect to shear spike reinforcement, at all times.

4.6 Durability (Cyclic) Loading

A sinusoidal load signal was used during the durability loading. The flowchart of Figure 4.10 illustrates the imposed load level and number of load cycles of the respective stringers during durability loading. It also depicts which stringers were incrementally load tested during shear spike installation and which stringers were subsequently ramp load tested to failure.

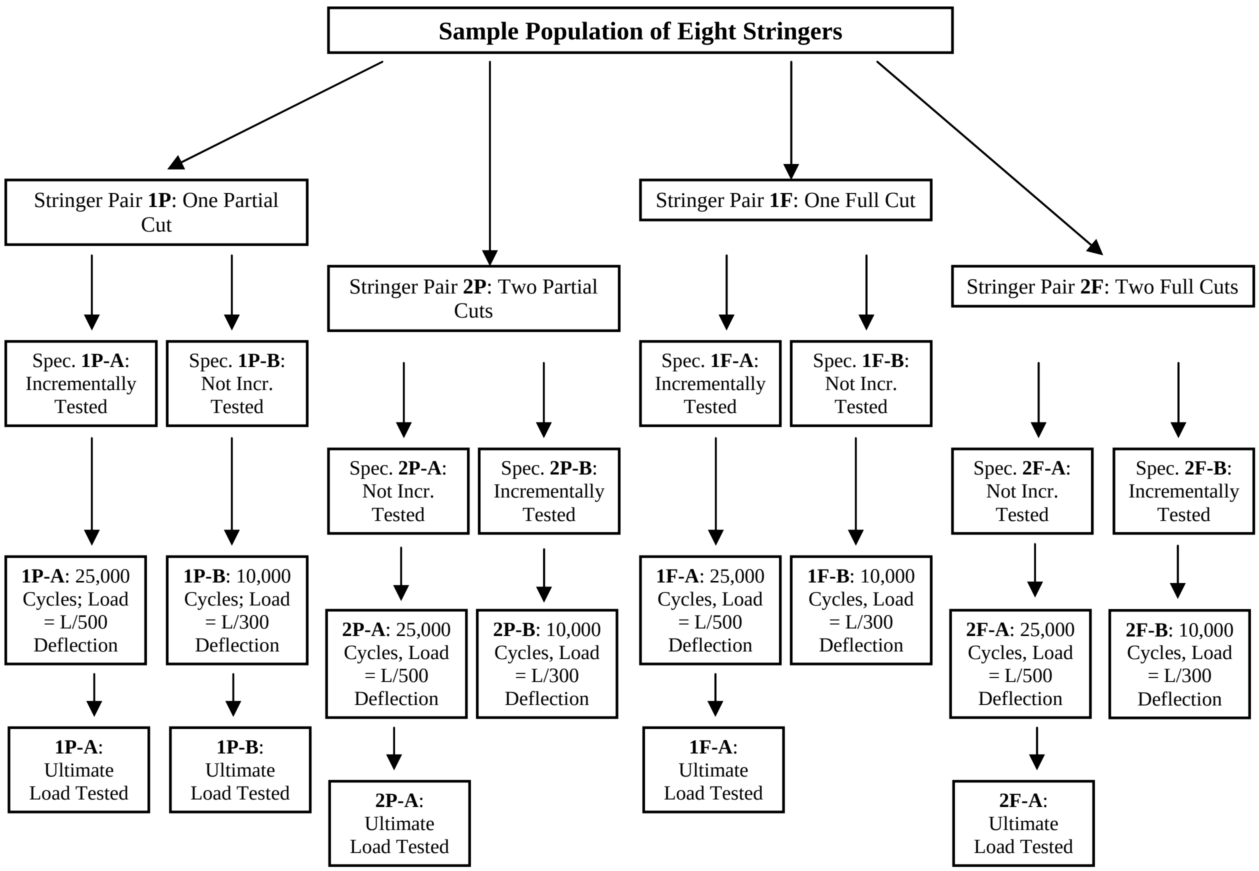

Figure 4.10 Flowchart illustrating how respective stringers were load tested.

The maximum load imposed during durability loading was that corresponding to a mid-span deflection of clear span divided by 300 (158”/300 = 0.53 inches [1.34 cm]) for half the sample population and clear span divided by 500 (158”/500 = 0.32 inches [0.80 cm]) for the other half of the sample population. During the cyclic loading, a minimum load of approximately 10% of the maximum imposed load was used to minimize any stringer movement relative to the support frame. The load rate during durability loading was 0.25 load-cycles/second (Hz). During durability loading, half the sample population (one beam per pair) was loaded to 10,000 cycles. The maximum load for these specimens corresponded to a mid-span deflection of 0.53 inches (1.34 cm). The other half of the sample population was loaded to 25,000 cycles at an imposed maximum load corresponding to a mid-span of deflection of 0.32 inches (0.80 cm). The durability loading was interrupted at certain intervals to perform intermediate ramp load tests to determine if the flexural stiffness had been adversely affected by the durability loading.

4.7 Ramp Load Testing to Failure

After completion of the durability loading, five of the eight stringers were load tested to failure. The other three stringers had partial failures during the durability loading. These three stringers were retained and later dissected in the plane of shear spikes to determine the failure mode. The results of this sub-investigation are given in section 5.2.4.

During ramp load testing to failure, the load was increased until catastrophic failure occurred. The stroke rate was 0.015 in/s (0.4 mm/s) and the load was increased in increments of approximately 1.0 kips (4.5 kN). Load and mid-span deflection was recorded at each increment. If something indicative of stringer failure occurred, such as a cracking sound or sudden increase in deflection, the stroke was held constant and load and deflection measurements taken. Vertical deflections of the stringers were measured by Celesco cable-extension positional transducers, also called “string” potentiometers.

The flowchart of Figure 4.10 illustrates how the respective stringers were load tested. “Incrementally Tested” indicates that the stringer was load tested after each row of installed shear spikes. “Not Incr. Tested” indicates the stringer was load tested only before and after all twenty shear spikes were installed. The next row of the flowchart explains the imposed load level and number of load cycles during the durability loading phase. The final row indicates whether or not the stringer was tested to failure after completion of the durability loading.

5. RESULTS

After load testing of the undamaged specimens, the four previously-described damage configurations were inflicted on the sample population. The specimens were then again ramp load tested to determine the magnitude of loss of flexural stiffness. The average flexural stiffness losses, as compared to the respective stringer's virgin state, for stringers with "one partial" cut (1P-A and 1P-B), "two partial" cuts (2P-A and 2P-B), "one full" cut (1F-A and 1F-B), and "two full" cuts (2F-A and 2F-B) are 6.4%, 17.1%, 59.5% and 69.2% for each pair of stringers respectively. The percent loss of each individual stringer is given below in Figure 5.1.

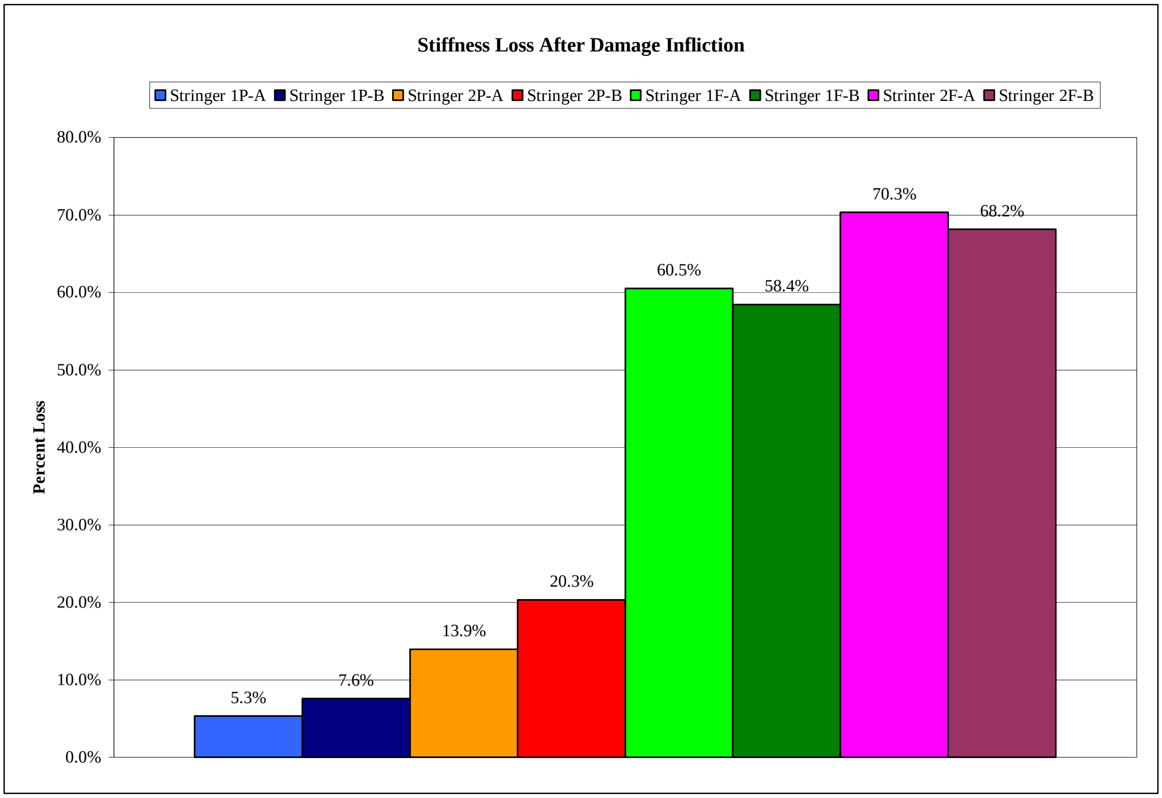

Figure 5.1 Percent loss in EI, relative to virgin state, after damage infliction.

Imposing either one or two partial cuts has a relatively small detrimental effect on stringer flexural stiffness (up to 20.3% loss for specimen 2P-B). By comparing average losses in specimens with two partial cuts (2P-A and 2P-B) to losses in specimens with one partial cut (1P-A and 1P-B), it can be seen the average flexural stiffness loss almost triples (from 6.4% to 17.1%). In the stringers with full cut(s), rather severe losses in flexural stiffness are observed; from 58.4% for specimen 1F-B to 70.3% for specimen 2F-A. There is also a loss of area moment of inertia from the removal of material from the saw cutting, which adds to the loss in flexural stiffness. An approximately 10% higher loss in flexural stiffness was observed in samples with two full cuts compared to stringers with one full cut.

5.1 Effectiveness of Shear Spike Repair

After load testing of the intentionally damaged specimens, all stringers were shear spike reinforced with five rows of shear spikes each. The “fully reinforced state” refers to when five rows of shear spikes had been installed in a stringer. Moreover, half the sample population was ramp load tested after each successive row of shear spikes installed. In Figure 5.2, losses in flexural stiffness and subsequent regains from shear spiking at the fully reinforced state are presented.

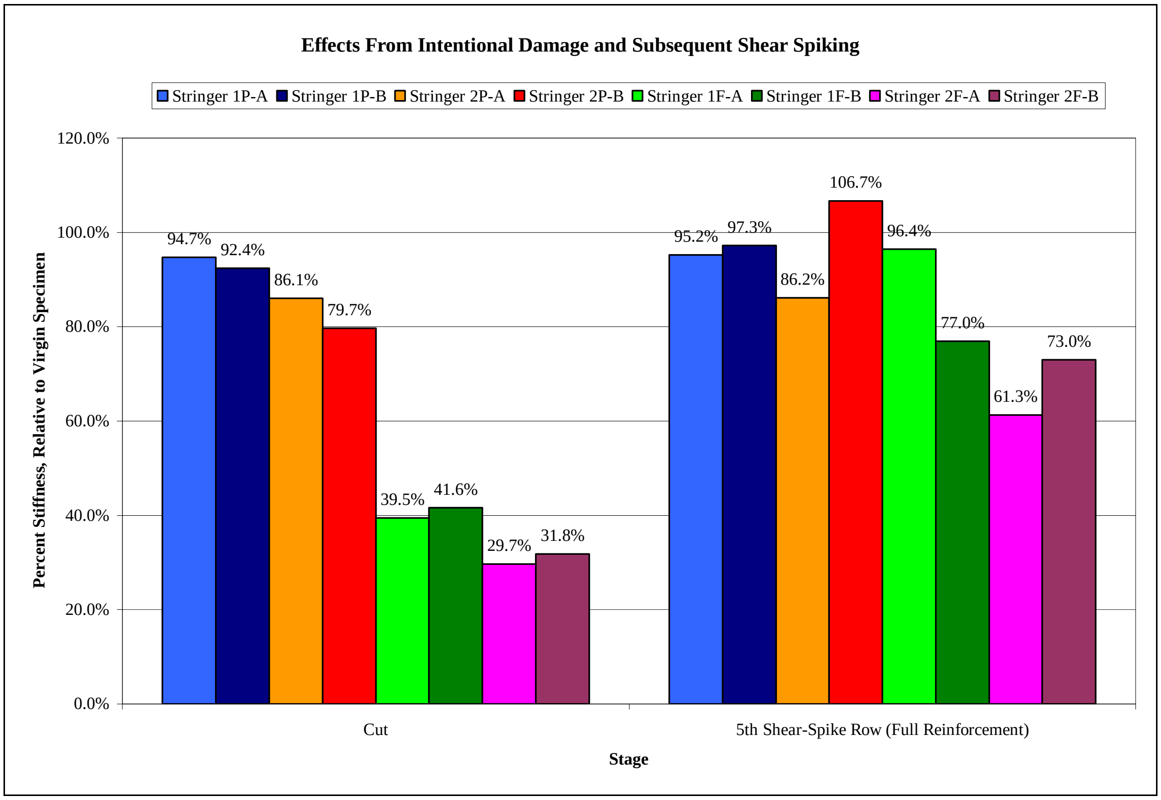

Figure 5.2 Effects on flexural stiffness from intentional damage and subsequent shear spiking.

Some general trends can be observed from comparing the flexural stiffness of damaged states to fully reinforced states of the respective stringers. Shear spiking of timbers that are in relatively good structural condition, that is stringers with partial cuts(s), have a relatively small absolute return in terms of improved flexural stiffness. It appears the flexural stiffness of the virgin state provides an upper limit on attainable stiffness of the shear spike strengthened specimen. However, stringer 2P-B had its stiffness after full reinforcement exceeded its virgin stiffness by 6.7%.

The larger gain, which is the greatest differential between damaged and fully reinforced states, is observed in specimens with full cut(s). These four stringers were all rather severely damaged, with losses of flexural stiffness from intentional damage in the region of 58.4% to 70.3% of the virgin stiffness. In the fully reinforced state, three of the four stringers have their flexural stiffness at least doubled from the damaged state, with the fourth stringer having its flexural stiffness rejuvenated from 41.6% to 77.0%. The stringers with one full cut have their flexural stiffness restored to 96.4% and 77.0% of the respective virgin state stiffness flexural (from 39.5% and 41.6% in the damaged state). Corresponding values for specimens with two full cuts are 61.3% and 73.0% (from 29.7% and 31.8%). Accordingly, strengthening through the process of shear spiking of appreciably damaged/deteriorated timbers is highly effective, whereas shear spiking of timbers that are in relatively good (or better) structural condition may not be very beneficial.

Nonetheless, if one looks at the relative flexural stiffness recovered in each respective stringer, i.e. the stiffness that was lost due to intentional damage compared to the flexural stiffness regained from shear spiking, some interesting observations can be made, as detailed in Table 5.1 and depicted in Figure 5.3. The relative recovery of flexural stiffness in stringer 1P-A is in fact more than 10%. Approximately two-thirds of the stiffness lost from intentional damage of stringer 1P-B is recovered. Stringer 2P-A, however, shows very little relative recovery; less than 1%. Stringer 2P-B has all its lost stiffness recovered, plus some additional stiffening; the flexural stiffness of the repaired stringer exceeds the flexural stiffness of the virgin specimen by nearly 7%.

Table 5.1 Relative Flexural Stiffness Lost and Recovered (kips-in^2) (SS = Shear Spike)

Stiffness Lost and Regained at Damaged and Fully Reinforced State, Respectively									
Stringer	1P-A	2P-B	1F-A	2F-B		1P-B	2P-A	1F-B	2F-A
EI Lost	1.68E+05	6.83E+05	2.17E+06	2.61E+06		2.22E+05	4.90E+05	1.72E+06	2.48E+06
EI Regained	1.77E+04	9.07E+05	2.04E+06	1.57E+06		1.41E+05	3.99E+03	1.04E+06	1.12E+06
5th SS Row	10.5%	132.9%	94.1%	60.3%		63.7%	0.8%	60.6%	45.0%

The average flexural stiffness relative recovery for specimens with partial and full cut(s) is 52.0% and 65.0%, respectively, and the average of all eight stringers is 58.5% of the stiffness that was lost from intentional damage. Therefore, it seems a higher portion of the flexural stiffness can be recovered in more severely damaged/deteriorated specimens, even though less damaged/deteriorated specimens can benefit significantly from shear spiking, on a relative percent regain basis.

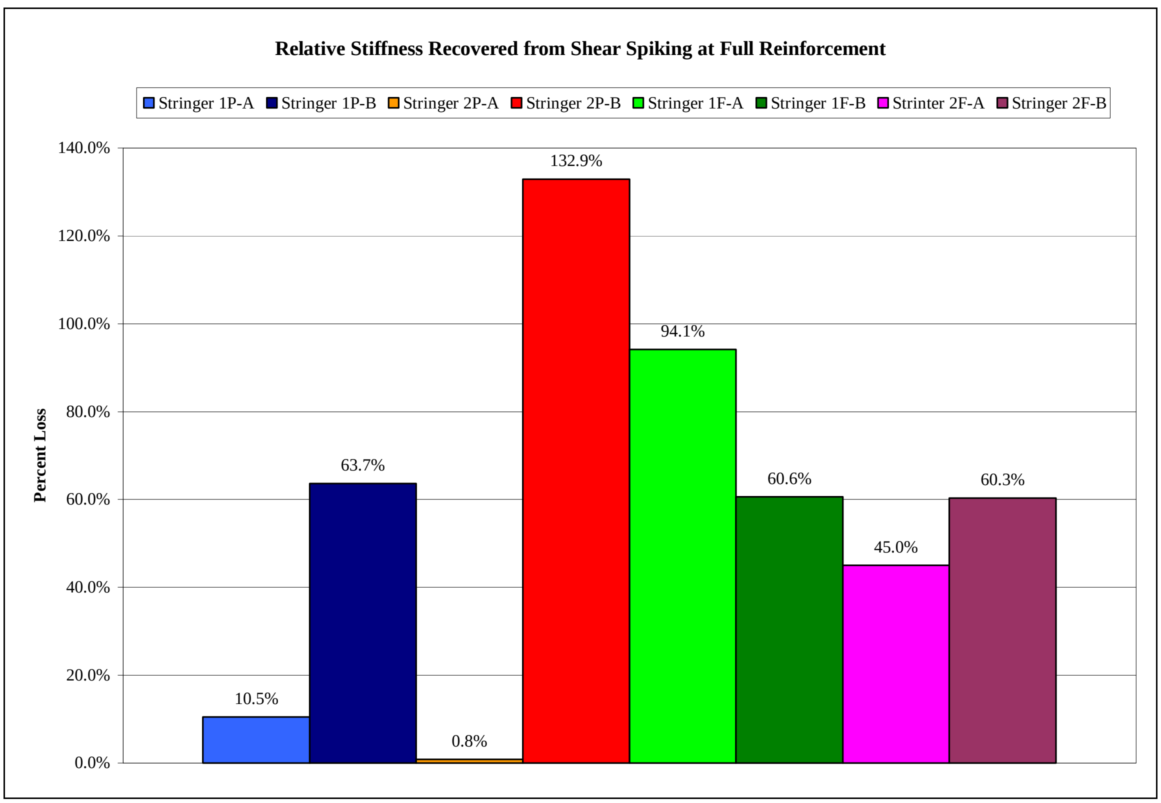

Figure 5.3 Relative flexural stiffness regained from shear spiking, at the fully reinforced state.

A complete summary of losses of flexural stiffness from intentional damage and regains from shear spiking of all stringers is given below in Tables 5.2 and 5.3. Table 5.2 gives the measure of stiffness-values.; Table 5.3 gives the corresponding percentages, relative to the respective virgin state.

Table 5.2 Flexural Stiffness (kips-in^2) (Dam. = Damaged, SS = Shear Spike)

Stiffness (kips-in^2)									
Stringer	1P-A	2P-B	1F-A	2F-B		1P-B	2P-A	1F-B	2F-A
Virgin State	3.17E+06	3.36E+06	3.58E+06	3.83E+06		2.94E+06	3.51E+06	2.94E+06	3.53E+06
Dam. State	3.00E+06	2.68E+06	1.41E+06	1.22E+06		2.71E+06	3.02E+06	1.22E+06	1.05E+06
1st SS Row	2.97E+06	2.80E+06	2.36E+06	1.78E+06		-	-	-	-
2nd SS Row	2.91E+06	3.13E+06	2.65E+06	2.29E+06		-	-	-	-
3rd SS Row	3.02E+06	3.60E+06	2.87E+06	2.54E+06		-	-	-	-
4th SS Row	3.08E+06	3.60E+06	3.25E+06	2.53E+06		-	-	-	-
5th SS Row	3.02E+06	3.59E+06	3.45E+06	2.79E+06		2.86E+06	3.03E+06	2.26E+06	2.16E+06

Table 5.3 Flexural Stiffness, as Percent of Respective Virgin Stiffness (Dam. = Damaged, SS = Shear Spike)

Percent Flexural Stiffness Relative to Virgin Specimen									
Stringer	1P-A	2P-B	1F-A	2F-B		1P-B	2P-A	1F-B	2F-A
Virgin State	100.0%	100.0%	100.0%	100.0%		100.0%	100.0%	100.0%	100.0%
Dam. State	94.7%	79.7%	39.5%	31.8%		92.4%	86.1%	41.6%	29.7%
1st SS Row	93.9%	83.4%	65.9%	46.4%		-	-	-	-
2nd SS Row	91.9%	93.2%	74.1%	59.8%		-	-	-	-
3rd SS Row	95.2%	107.0%	80.2%	66.2%		-	-	-	-
4th SS Row	97.3%	107.0%	90.8%	66.1%		-	-	-	-
5th SS Row	95.2%	106.7%	96.4%	73.0%		97.3%	86.2%	77.0%	61.3%

The specimens with one partial cut, 1P-A and 1P-B, show relatively small losses from the intentional damage. After damage infliction, the average flexural stiffness of these specimens is 93.6% of their average virgin stiffness (i.e. a 6.4% loss). In the fully reinforced state, the flexural stiffness is recovered to 96.2% on average. Figure 5.4 illustrates the magnitude of the flexural stiffness at various states for specimens 1P-A. For specimen and 1P-B, which was not incrementally tested, the data between "Cut" and "5th Shear-Spike Row" is linearly interpolated, as represented by the dashed line in Figure 5.4. Results from the incremental (1st, 2nd, 3^{rd,} and 4th shear spike row) load testing are described later.

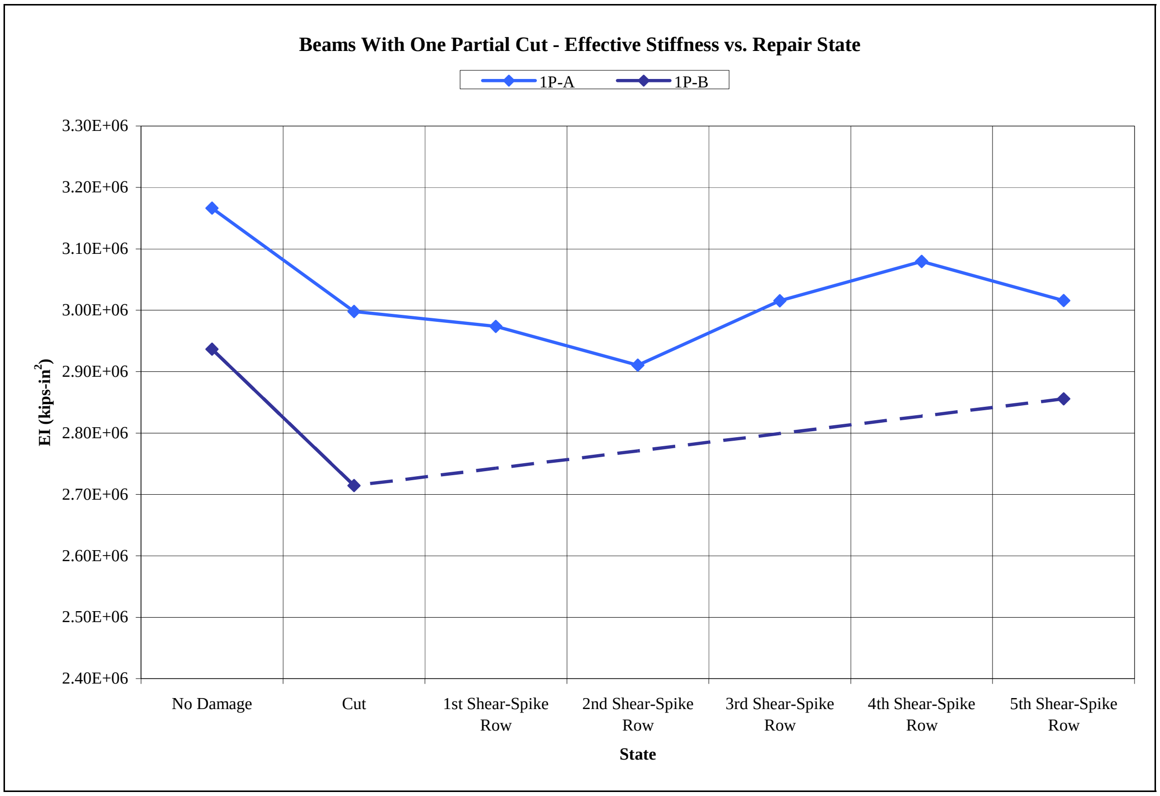

Figure 5.4 Flexural stiffness (EI) versus state for beams with one partial cut.

For the specimens with two partial cuts (2P-A and 2P-B), the average loss of flexural stiffness from the intentional damage and subsequent regain from shear spiking are 82.9% and 96.4%, respectively. It is interesting to note that specimen 2P-B suffered a flexural stiffness loss of 20.3% after damage, but the stiffness of its fully reinforced state exceeds the virgin state by 6.7% (e.g. flexural stiffness 106.7% relative to the virgin state). Specimen 2P-A, on the other hand, lost only 13.8% of its flexural stiffness because of intentional damage, but shows barely any rejuvenation in the fully reinforced state; 86.1% relative flexural stiffness after damage, 86.2% relative flexural stiffness after full shear spike reinforcement. Effects on flexural stiffness at various states for these two specimens are illustrated in Figure 5.5, including the linear assumption for the trend of specimen 2P-A. Again, results from the incremental (1^{st}, 2^{nd}, 3^{rd}, and 4^{th} shear spike row) load testing are described later.

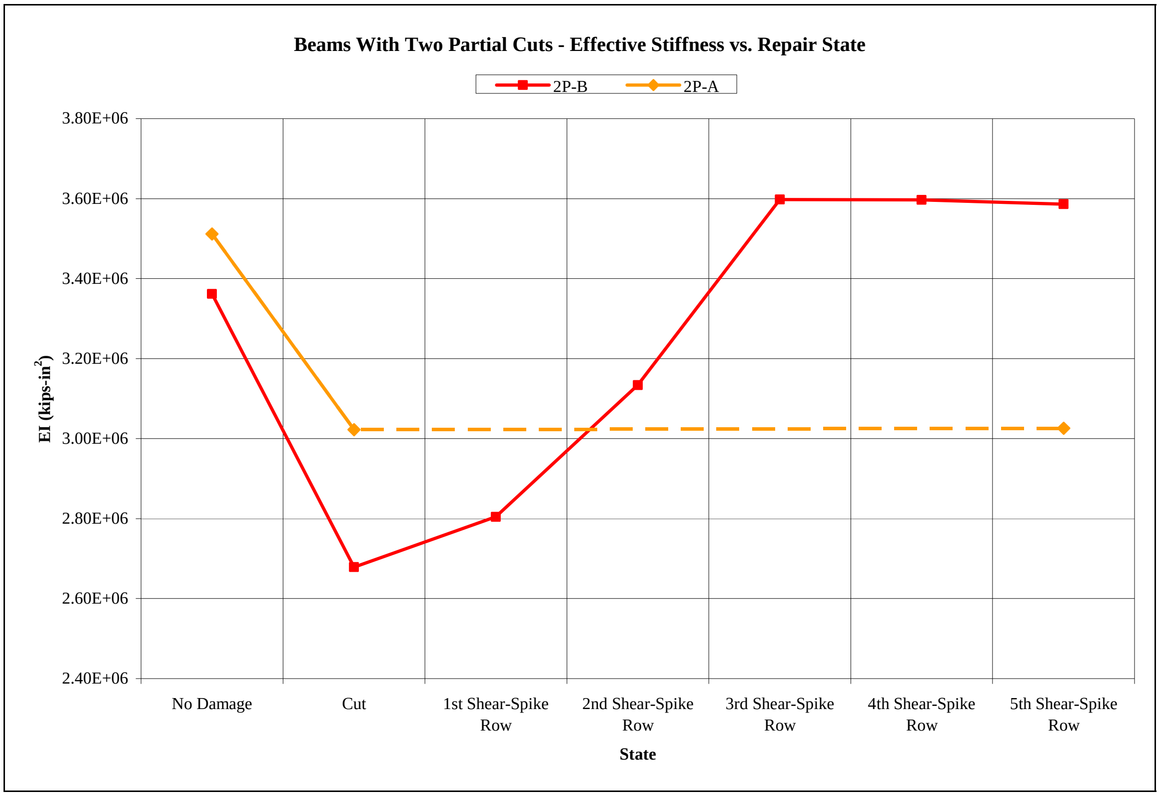

Figure 5.5 Flexural stiffness (EI) versus state for beams with two partial cuts.

For the specimens with one full cut, flexural stiffness losses from the intentional damage are rather significant; 60.5% and 58.4% of the flexural stiffness is lost compared to the respective virgin specimens of stringer 1F-A and 1F-B. However, both these specimens have much of their flexural stiffness regained from shear spiking, especially stringer 1F-A, which has its flexural stiffness restored to 96.4%. Specimen 1F-B regained 77.0% of the virgin flexural stiffness in the fully reinforced state. Effects on flexural stiffness at various states of these specimens are given in Figure 5.6, where the dashed line of specimen 1F-B represents linear interpolation.

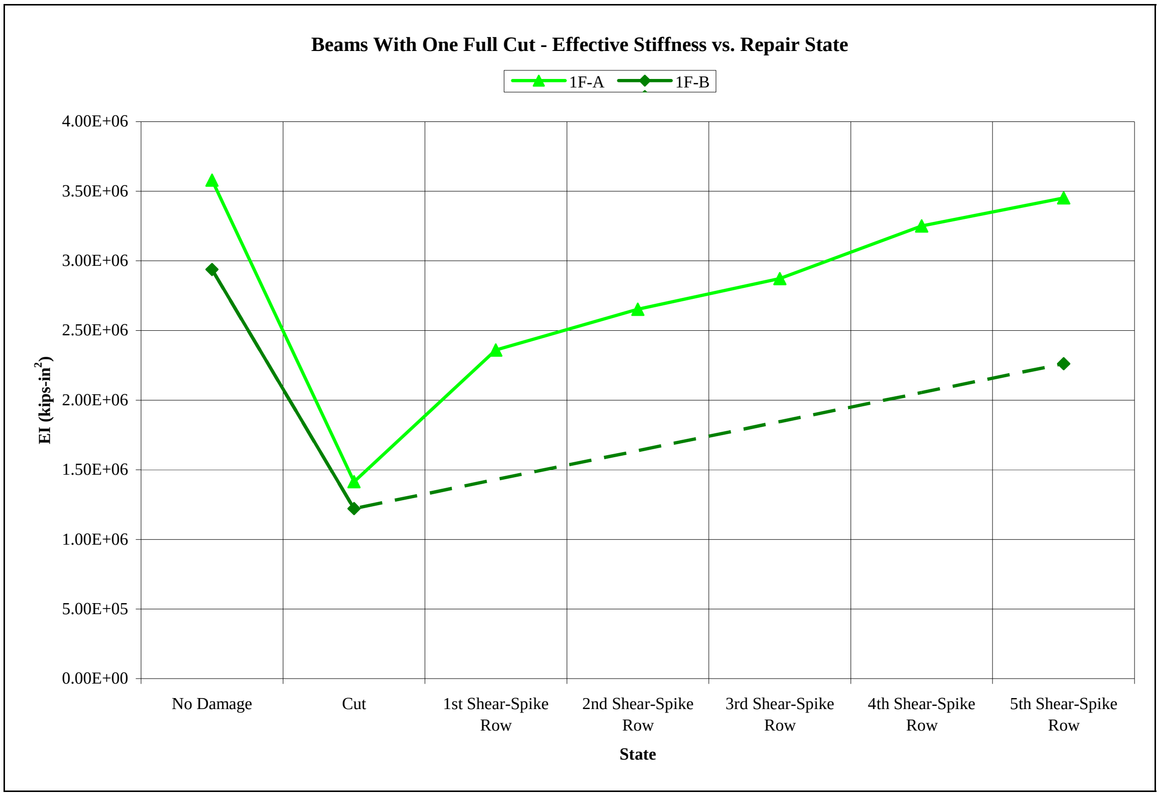

Figure 5.6 Flexural stiffness (EI) versus state for beams with one full cut.

The most severely damaged specimens, 2F-A and 2F-B, have their flexural stiffness reduced to 31.8% and 29.7% of their virgin flexural stiffness, respectively, after intentional damage. These specimens have relatively similar percentage rejuvenation in the fully reinforced state; specimen 2F-A has its flexural stiffness recovered to 73.0% (from 31.8%); specimen 2F-B has its flexural stiffness restored to 61.3% (from 29.7%). The effects at various states on the flexural stiffness are presented in Figure 5.7 for these two specimens; the dashed line of specimen 2F-A represents linear interpolation.

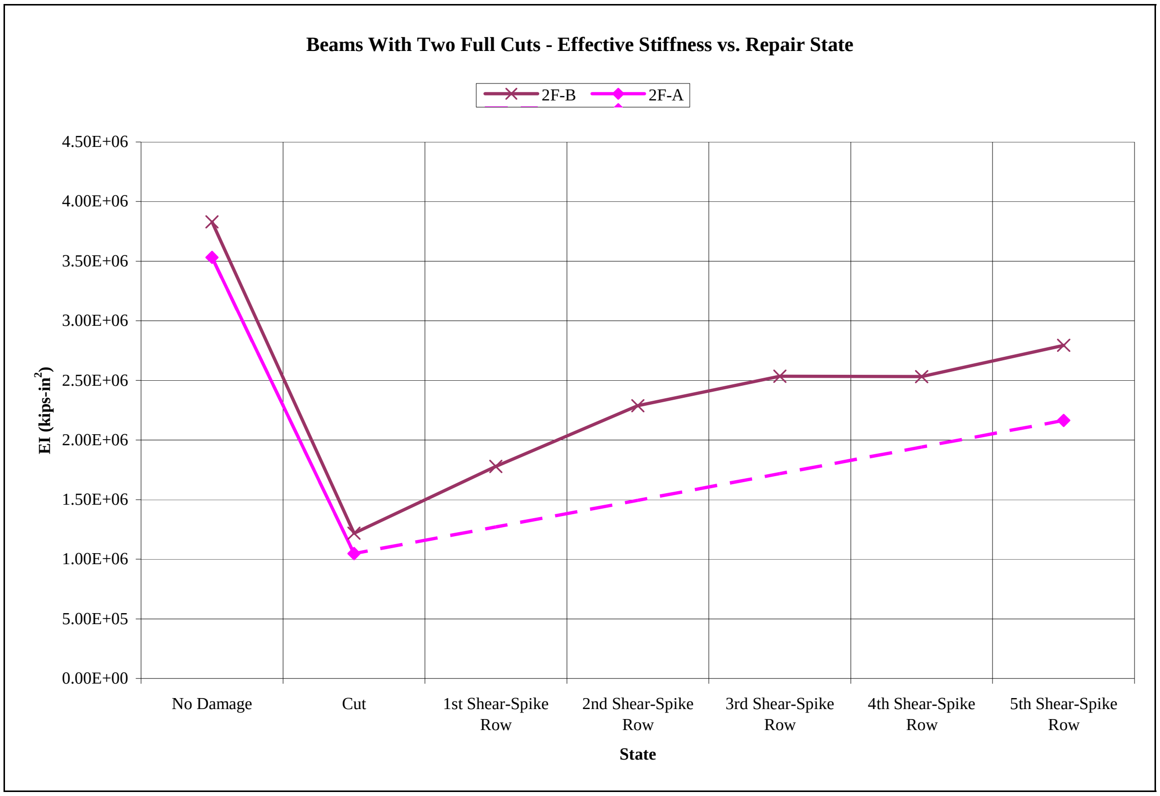

Figure 5.7 Flexural stiffness (EI) versus state for beams with two full cuts.

As can be seen from Tables 5.2 and 5.3 and from Figures 5.4 to 5.7, half the sample population was load tested after each successive row of shear spikes installed; the other sample population half was load tested only after all five shear spike rows had been installed. Incremental load testing of the stringers was performed to quantify the relative flexural stiffness gain as a function of reinforcement ratio. Again, the respective stringer virgin flexural stiffness corresponds to 100%. Figure 6.8 shows the effects from each successive row of shear spikes installed in the specimens that were load tested incrementally. These flexural stiffness percentages are also depicted on an individual basis in Figures 5.4 to 5.7.

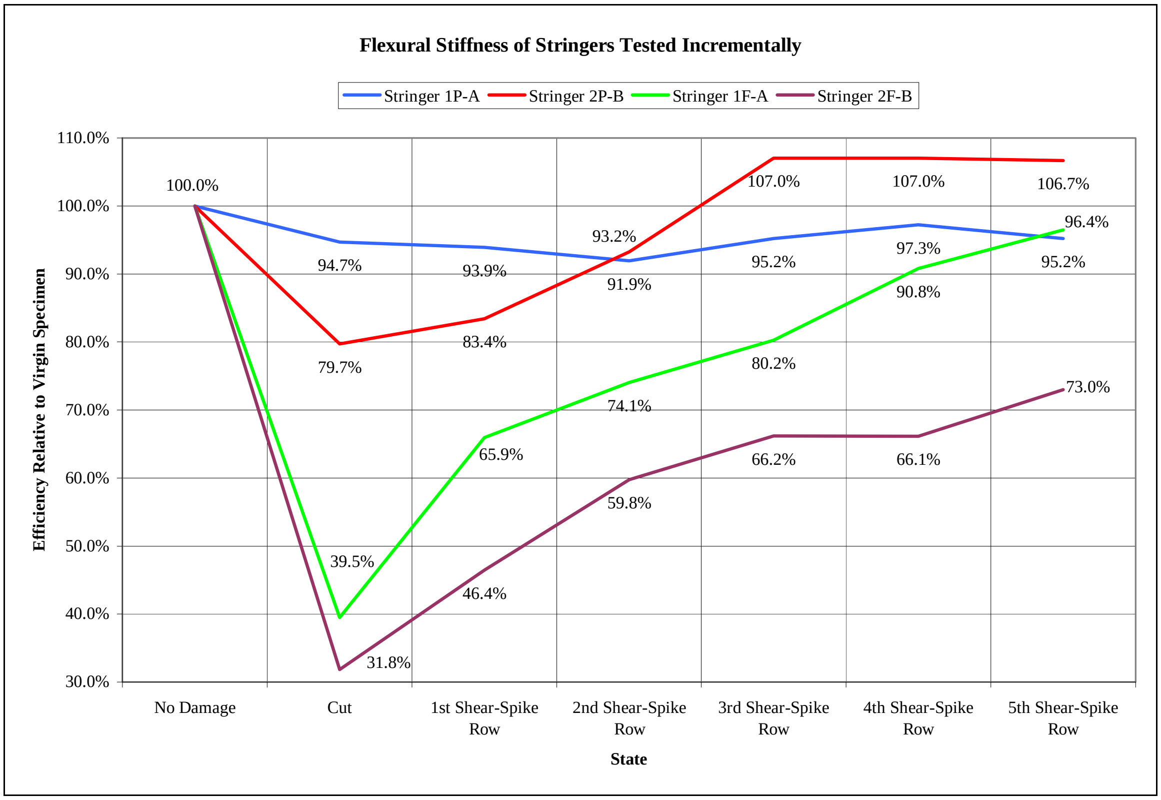

Figure 5.8 Effects from successive rows of shear spikes installed.

From Figure 5.8, two prominent trends can be observed; in the specimens with more severe damage inflicted (1F-A and 2F-B), the stiffness increases more or less linearly with each successive row of shear spikes installed. Moreover, there is no indication of this increase in flexural stiffness reaching a plateau state. Therefore, for more severely damaged/deteriorated members, a higher reinforcement ratio may be beneficial.

In the specimens with less prominent damage inflicted (1P-A and 2P-B), it seems a plateau state relative to increase in flexural stiffness from shear spiking is reached after the third and fourth row of shear spikes, respectively. As previously mentioned, stringer 1P-A has its fully reinforced flexural stiffness exceed its virgin state stiffness; a flexural stiffness of 107.0% is reached already after the third shear spike row. The fourth and fifth shear spike rows have very little effect on the flexural stiffness; there is in fact a small loss from the fourth to the fifth shear spike row. Finally, for stringer 1P-A there iss little overall gain from shear spiking. Small losses in flexural stiffness are actually observed after the first, second and fifth row of shear spikes. However, the flexural stiffness is improved from the third and fourth rows of shear spikes. These negative effects from shear spiking are believed to be due to a loss of properties from drilling out sound wood exceeding what is gained from shear spiking at these locations. This interesting phenomenon was also occasionally observed in previous studies, i.e. Radford et al. [49-52], Schilling [55-57], and Burgers [15-16].

5.2 Durability Loading

After the stringers had been fully reinforced, the specimens labeled with an "A" (i.e. XX-**A**) were durability loaded to 25,000 load cycles at a load level corresponding to an absolute mid-span deflection of clear span length divided by 500, or 0.316 in. (8.0 mm). The sample population half labeled with a "B" (i.e. XX-**B**) was durability loaded to 10,000 load cycles, but at a significantly higher load level; corresponding to an absolute mid-span deflection of clear span length divided by 300, or 0.527 in. (13.4 mm). Since all eight stringers had different measured flexural stiffness values in the fully reinforced state, it was decided that loading stringers to a specific deflection would provide a better basis for comparison than if identical load magnitudes were imposed. All stringers were ramp load tested at intervals of at least 5,000 cycles to determine if there had been any adverse effect on the structural integrity of the stringers from the cyclic loading.

5.2.1 Durability Loading to 25,000 Cycles at L/500

During durability loading, no physical indications of detrimental effects on stringer 1P-A from the cyclic loading were observed. These observations were verified from load test results, where no apparent detrimental effect from the repeated loading was evident. As can be seen in Figure 5.9, there are small variations in measured flexural stiffness after 5,000, 10,000, 15,000, 20,000, and finally after 25,000 load cycles. These variations are believed to be due to variables other than the mechanical properties of the strengthened stringer itself. Rather, slight movement of the stringer relative to its support locations during the durability loading and/or opening and closing of vertical gaps at damage locations during ramp load testing are believed to have contributed to these minute fluctuations in measured stiffness. In Figure 5.9, 100% on the left-hand y-axis corresponds to the flexural stiffness in the fully reinforced state. The right-hand y-axis depicts the corresponding measured flexural stiffness values, in units of kips-in.^{2}; this is also the case in subsequent Figures 5.10 to 5.12 and Figures 5.14 to 5.17.

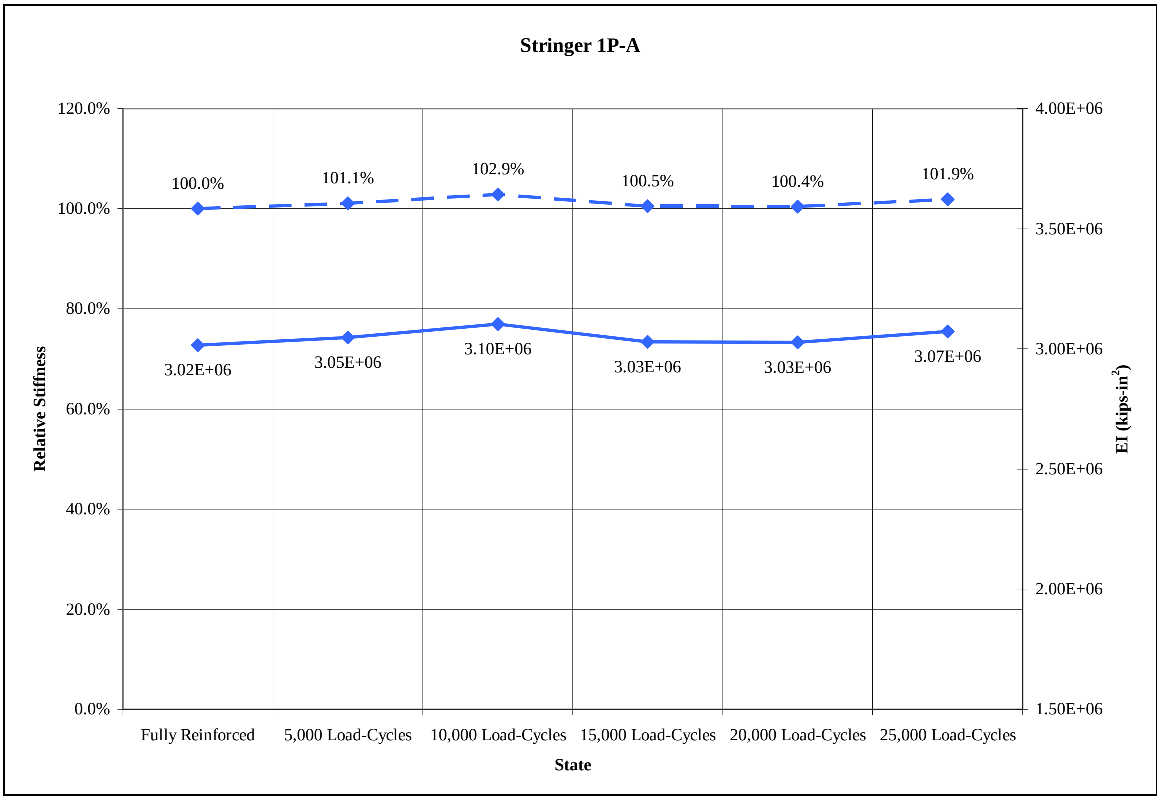

Figure 5.9 Stiffness of specimen 1P-A at various stages during durability loading.

Results from ramp load testing of specimen 2P-A are presented in Figure 5.10. Similar to stringer 1P-A, no detrimental effect resulted on specimen 2P-A from the durability loading.

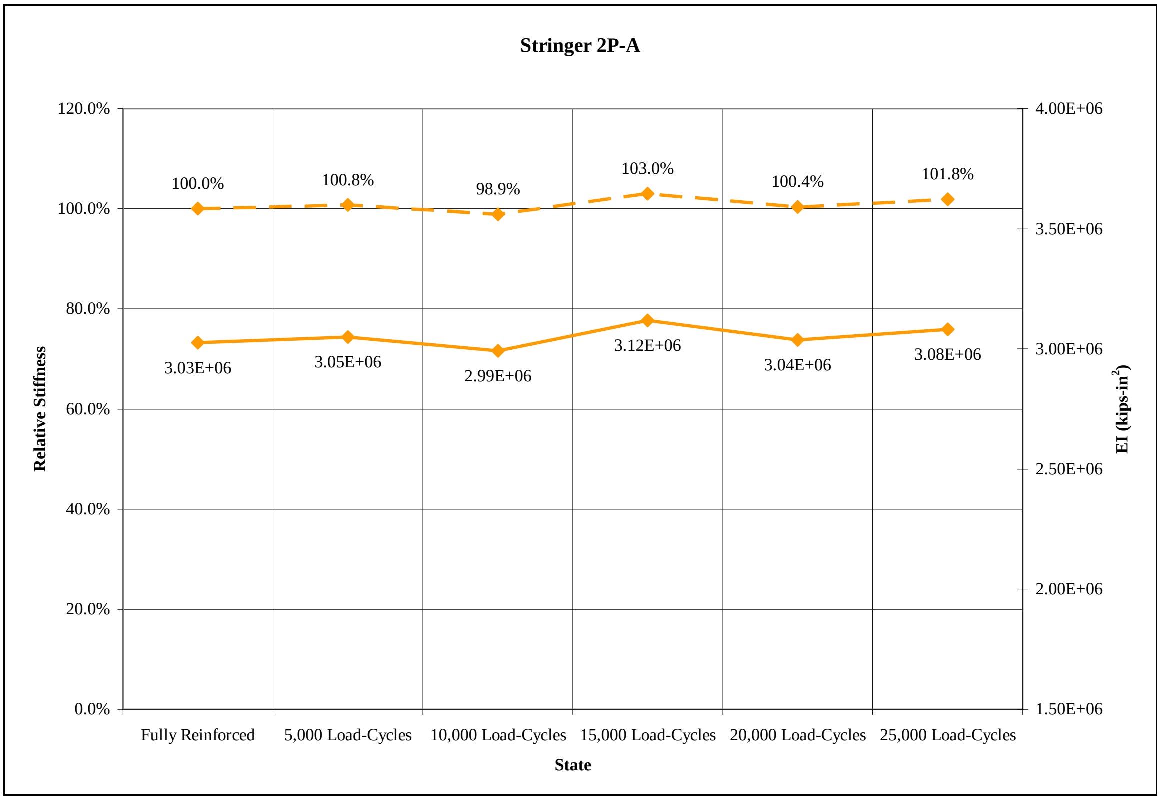

Figure 5.10 Stiffness of specimen 2P-A at various stages during durability loading.

As can be seen from Figure 5.11, ramp load testing of stringer 1F-A shows no effects from the repeated loading up to 20,000 load cycles. The minute fluctuations that can be observed in Figure 6.11 are again believed to be due to external factors. However, there is a notable drop in flexural stiffness between 20,000 cycles and 25,000 cycles (from 3.56×10^6 to 3.40×10^6 kips-in^2 [1.02×10^4 to 9.76×10^3 kN-m^2]). However, when the stiffness after 25,000 load cycles is compared to that at full reinforcement but before any durability loading (3.40×10^6 vs. 3.45×10^6 kips-in^2, [9.76×10^3 vs. 9.90×10^3 kN-m^2]), this drop is small enough to be believed to result from the previously described external effects rather than an actual loss of flexural stiffness.

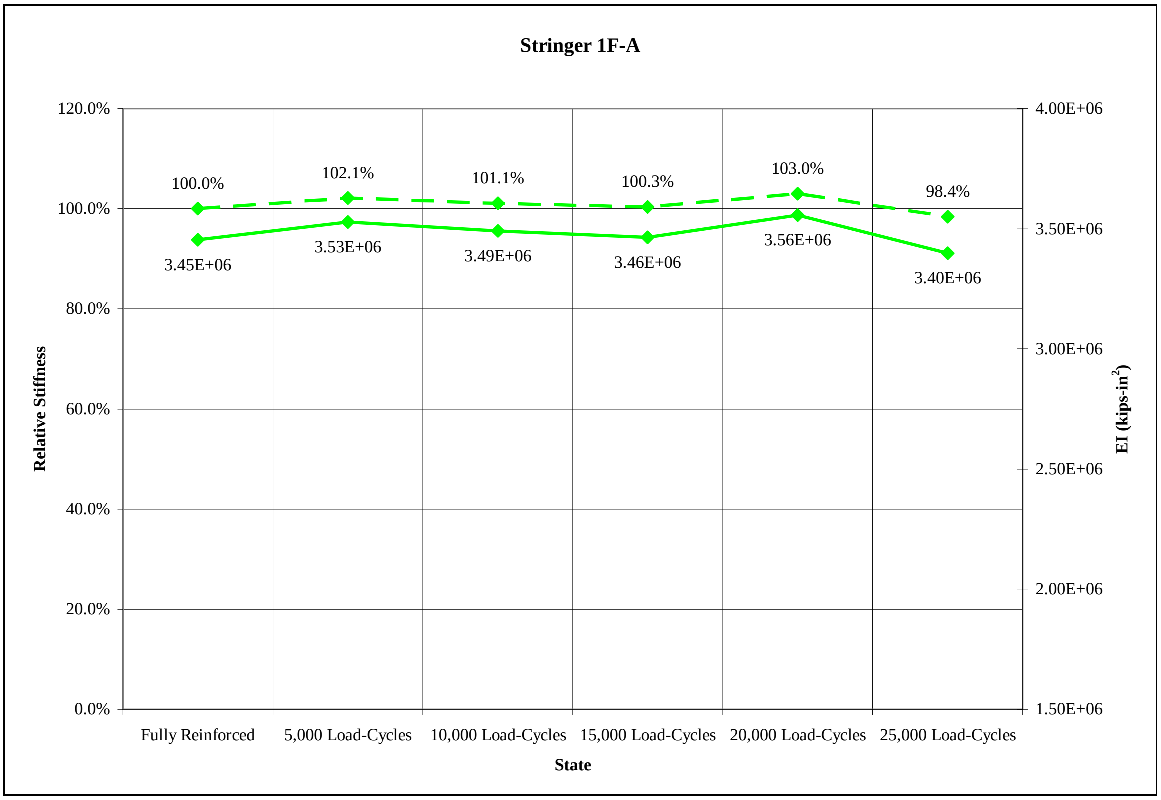

Figure 5.11 Stiffness of specimen 1F-A at various stages during durability loading.

In contrast to the other three specimens exposed to a durability load level corresponding to a mid-span deflection of L/500, specimen 2F-A exhibits a trend of lost flexural stiffness resulting from the repeated loading, as can be seen in Figure 5.12. Already after 5,000 load cycles, the measured flexural stiffness is down to 93.8% of the fully reinforced state stiffness. Relative flexural stiffness after 10,000 and 15,000 load cycles, however, show no indication of further loss. Quite opposite, there is actually a small rebound in flexural stiffness after 10,000 and again after 15,000 load cycles, as compared to the measured flexural stiffness at 5,000 load cycles. However, the magnitude of "restored" flexural stiffness is small enough to be believed to be due to external factors or possibly an anomaly of a measurement error itself for the 5,000 cycle data point. Another noticeable drop in flexural stiffness occurs from 15,000 to 20,000 load cycles. The flexural stiffness drops by 7.2%, from 95.2% down to 88.0%. Yet, there is no apparent further loss in flexural stiffness from 20,000 to 25,000 load cycles. The loss in flexural stiffness that is observed at 20,000 load cycles is too large to be solely attributed to external factors; it is thus believed that the repeated loading does contribute to the reduction. Lateral movement of the upper relative to the lower half in the south half of stringer 2F-A was evident during durability loading post 15,000 load cycles. In other words, interlayer slip occurred at the south lengthwise half of the beam where the neutral axis cut acted as a slip plane.

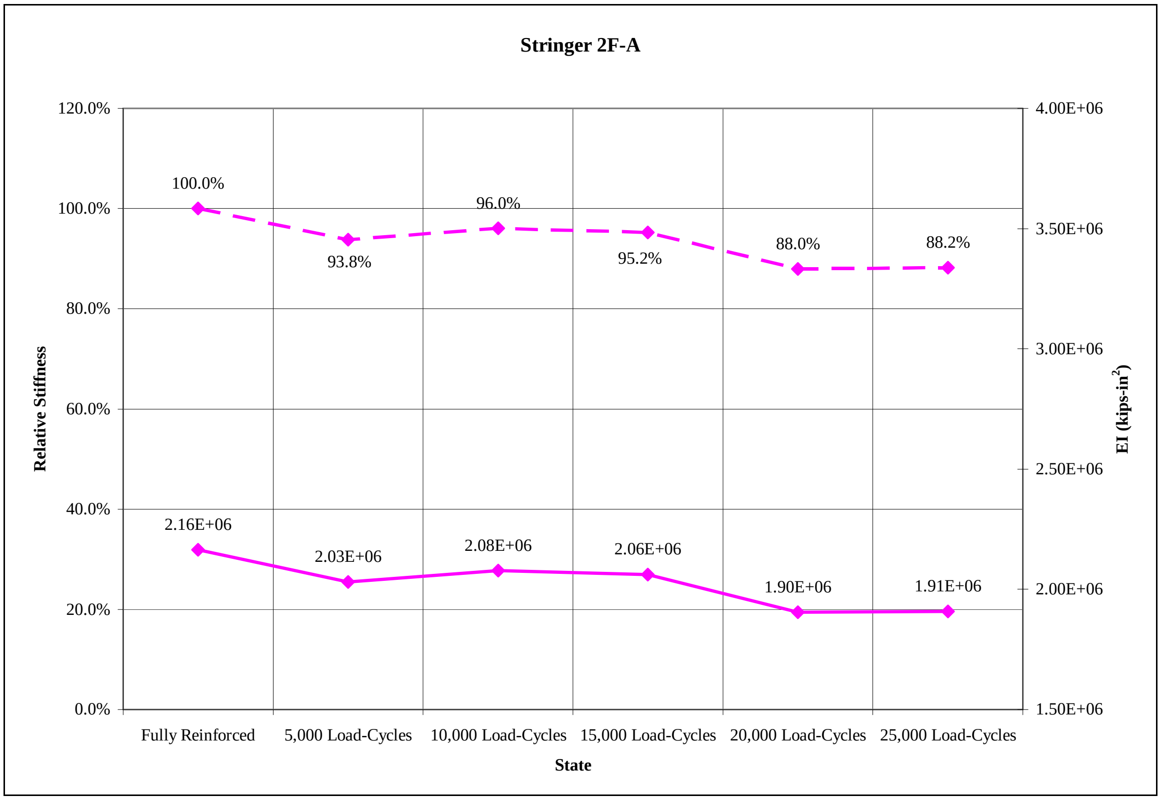

Figure 5.12 Stiffness of specimen 2F-A at various stages during durability loading.

It is evident that the relative flexural stiffness remains near 100% for all stringers except specimen 2F-A. The two drops in flexural stiffness of specimen 2F-A, at 5,000 and 20,000 load cycles, are easily observed in Figure 5.13, which summarizes the results for all four specimens. All specimens (1P-A, 2P-A, 1F-A, and 2F-A) were ramp load tested to failure after conclusion of the durability loading, as described subsequently in Section 5.3.

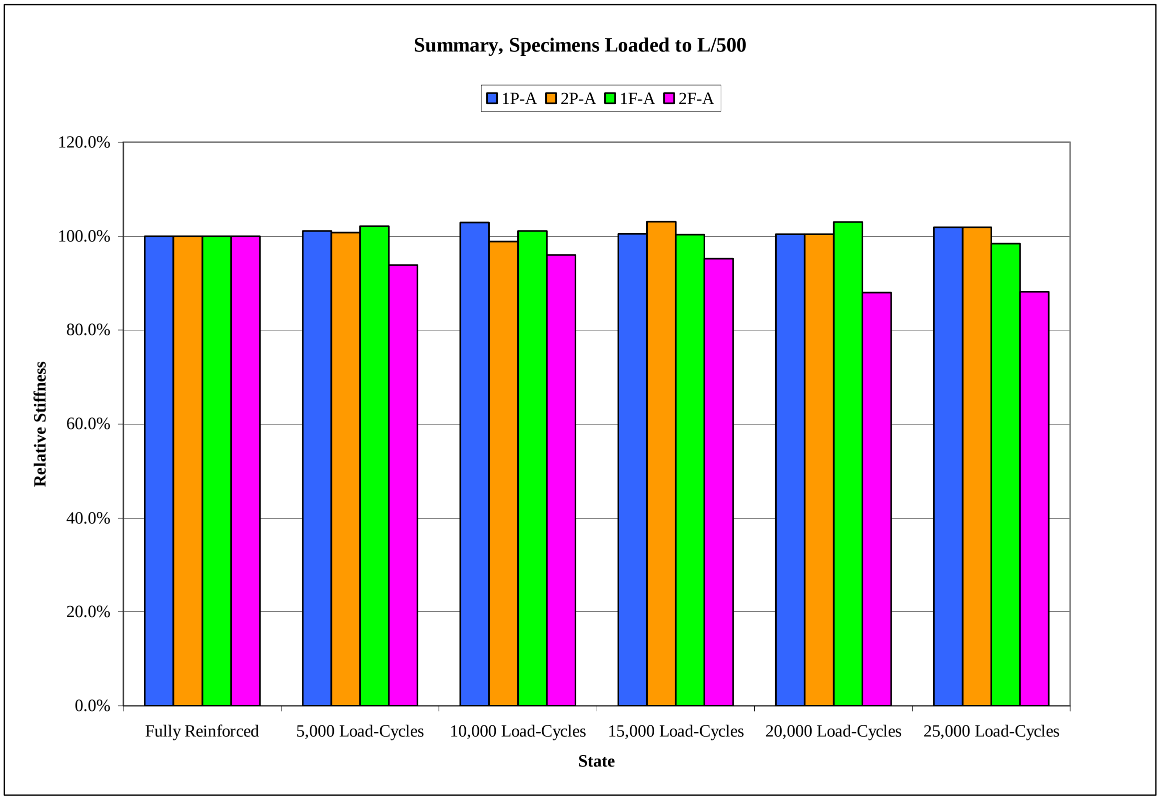

Figure 5.13 Summary of effects from repeated loading on specimens loaded to mid-span deflection corresponding to L/500.

5.2.2 Durability Loading to 10,000 Cycles at L/300

Figure 5.14 illustrates the results for specimen 1P-B. Specimen 1P-B shows no effect whatsoever from the durability loading. The percent flexural stiffness lingers very near 100%, i.e. the stiffness before any repeated loading, after both 5,000 and 10,000 load cycles. Stringer 1P-B was ramp load tested to failure after conclusion of the durability loading, as described subsequently in Section 5.3.

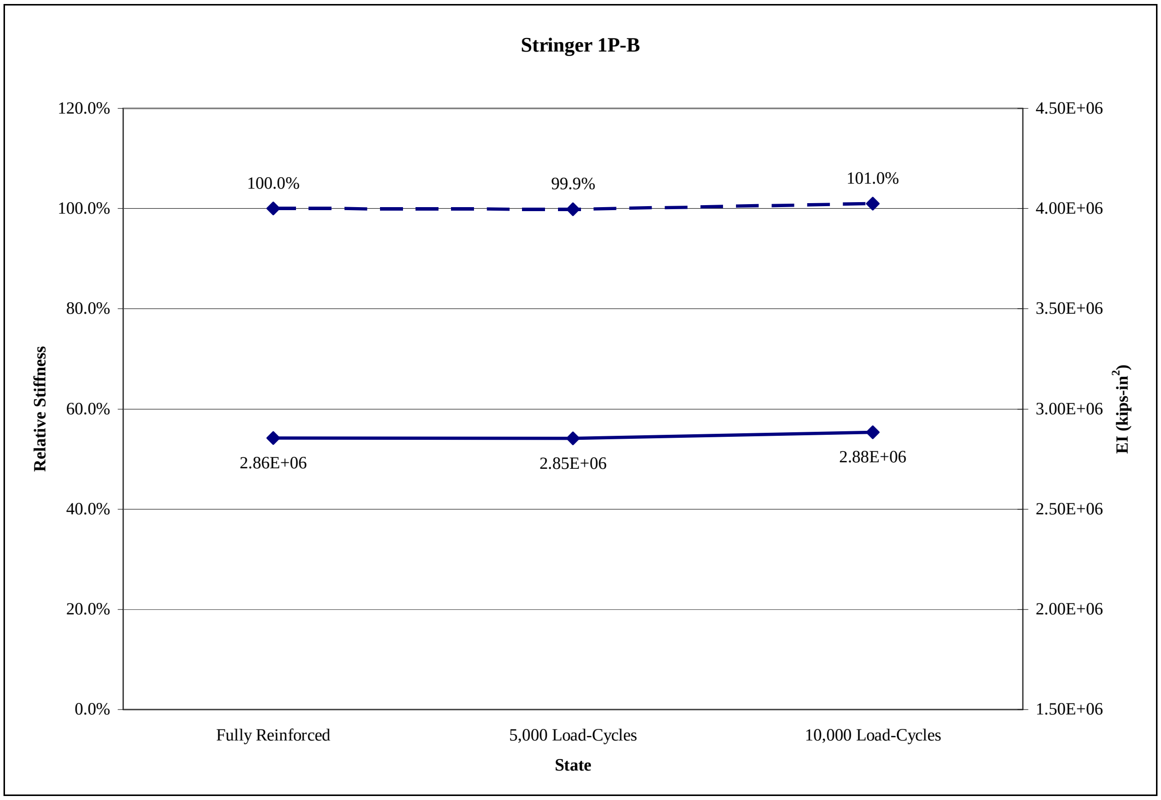

Figure 5.14 Stiffness of specimen 1P-B at various stages during durability loading.

Stringer 2P-B showed physical signs of diminished structural integrity early on in the durability loading; already after fewer than 100 load cycles. Diagonal shear cracks at both butt ends became evident. These shear cracks had propagated between the two imposed partial cuts. During durability loading, significant interlayer slip occurred in the plane of these cuts. Since the shear failures were evident early on in the durability loading, it is believed that the failure stemmed from the load capacity being exceeded rather than resulting from the repetitive nature of the loading. Figure 5.15 depicts the effects from durability loading on specimen 2P-B. The flexural stiffness shows a significant drop between 5,000 to 10,000 load cycles, which suggests that after the initial shear failure(s), the repetitive loading further diminished the structural integrity, probably causing the initial failure to further propagate. Moreover, at the 5,000 load cycle mark, over 40% of the stiffness of the reinforced stringer had been lost. After 10,000 cycles, the flexural stiffness had been reduced by another 12.5% (to 52.5%). Because of this rather significant loss of flexural stiffness, it was determined that the stringer was not to be load tested to failure. The specimen was instead dissected to, if possible, determine the failure mode. Because of this diminished flexural stiffness, it was decided that subsequent specimens were to be ramp load tested at shorter load cycle increments (e.g. also after 100, 1,000, 2,500, and 7,500 load cycles).

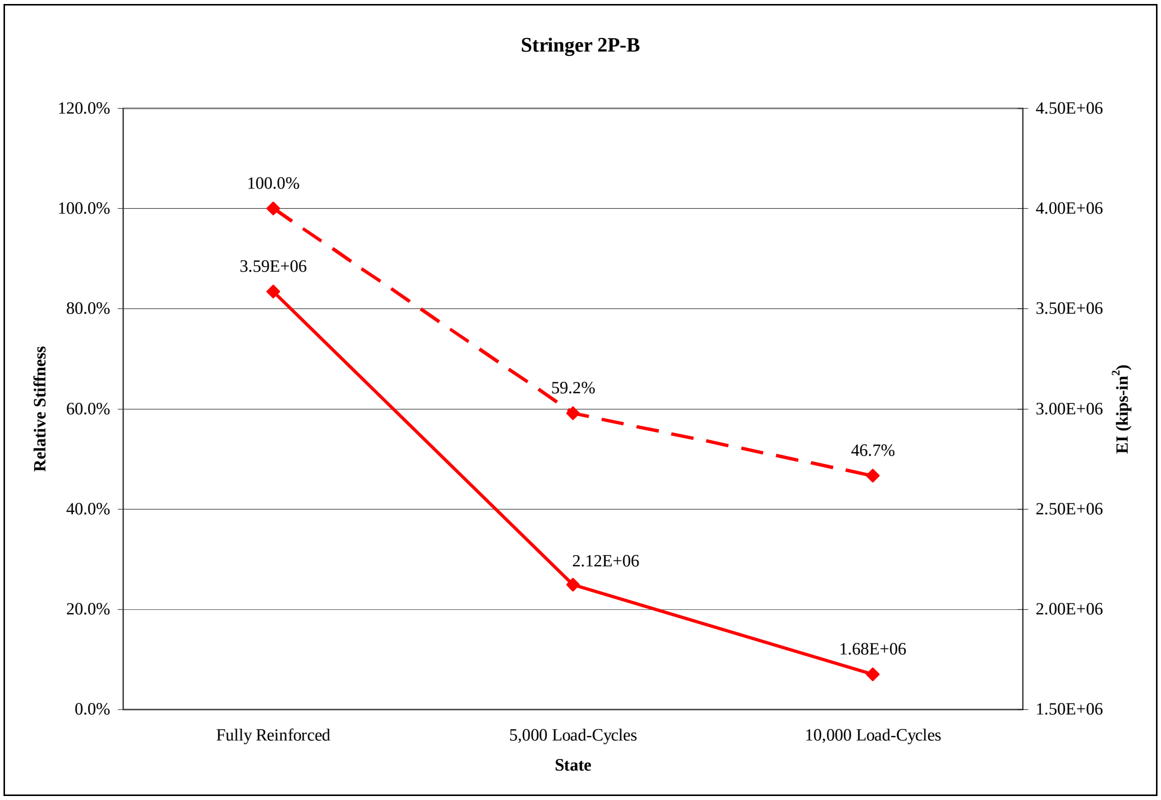

Figure 5.15 Stiffness of specimen 2P-B at various stages during durability loading.

Much like specimen 2P-B, stringer 1F-B experienced an interlayer shear failure early on in the durability loading process. This shear failure became apparent almost immediately, and interlayer slip occurred between the two vertical halves separated by the intentional cut at the neutral axis location in both the south and north stringer end. Moreover, a shear crack propagated into the center-third of the beam from its south end. This horizontal crack commenced where the intentional horizontal cut had been terminated and made its way all the way to near the stringer midpoint. Figure 5.16 is a plot depicting the effects of durability loading on specimen 1F-B. There is an approximate linear loss of flexural stiffness up to 2,500 load cycles, after which the flexural stiffness remains fairly constant. It can also be seen that the flexural stiffness is reduced by more than 10% already after 100 load cycles. After 1,000 load cycles, the flexural stiffness is down to 85.6%, as compared to the fully reinforced state prior to any repetitive loading, and after 2,500 load cycles the flexural stiffness is reduced to 77.9%. However, there seems to be little detrimental effect from further repetitive loading since only an additional 1% loss in stiffness is observed from 2,500 to 10,000 load cycles. Specimen 1F-A was later dissected to determine its failure mode; it was therefore not ultimate load tested.

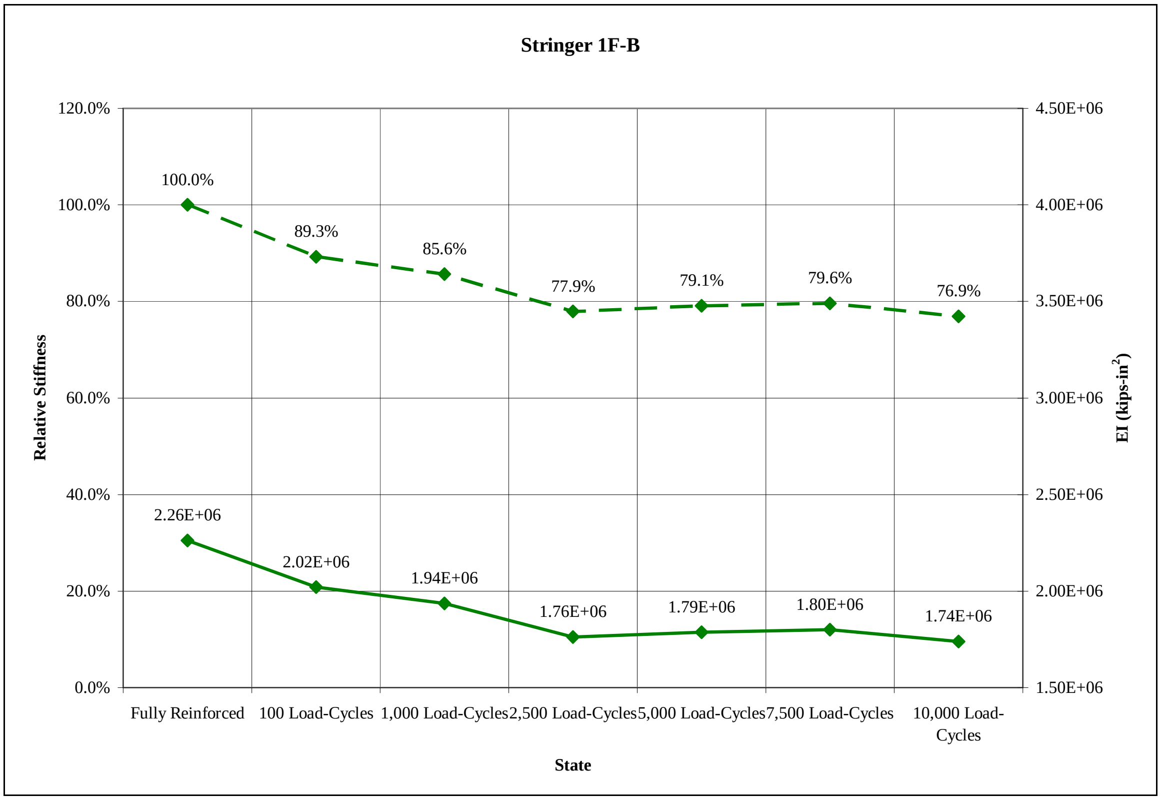

Figure 5.16 Stiffness of specimen 1F-B at various stages during durability loading.

Stringer 2F-B had apparent shear failures at the neutral axis cuts, at both ends, and significant interlayer slip occurred in the early stages of durability loading; the north end shear crack extended into the middle-third of the stringer. The interlayer slip became evident almost immediately during the repetitive loading process, and became much more pronounced after approximately 500 load cycles. Figure 5.17 is a plot of its relative stiffness versus number of load cycles. There is a flexural stiffness loss of 5.9% already after 100 cycles. What is more interesting is the significant loss in stiffness from 100 to 1,000 load cycles. The measured flexural stiffness drops from $2.63\text{x}10^6$ to $2.02\text{x}10^6$ kips-in^2 ($7.55\text{x}10^3$ to $5.80\text{x}10^3$ kN-m^2) from 100 to 1,000 load cycles; a loss corresponding to 21.7%. However, post 1,000 load cycles show little effect on the stiffness from the repetitive loading. The stiffness remains fairly constant up to 5,000 load cycles, after which a 6.9% drop is observed over the next 5,000 load cycles. At the conclusion of durability loading, stringer 2F-B was dissected to determine the failure mode(s); it was therefore not load tested to failure.

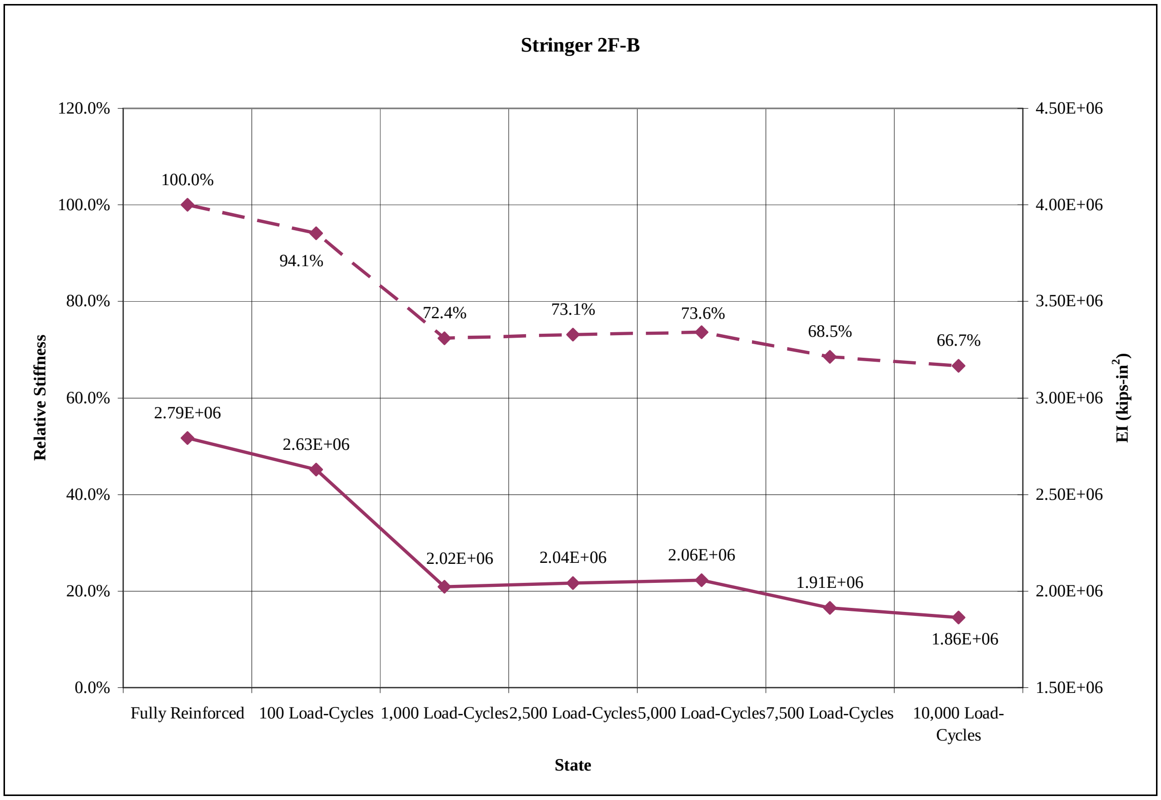

Figure 5.17 Stiffness of specimen 2F-B at various stages during durability loading.

A summary of the results from load testing of specimens exposed to a repetitive load corresponding to a mid-span deflection of L/300 is given in Figure 5.18. Note again that stringers 1P-B and 2P-B were not ramp load tested at 100, 1,000, 2,500 and 7,500 load cycles; these increments are therefore not shown in Figure 5.18. It is evident that specimen 1P-B shows no effect from the durability loading. The other three stringers (2P-B, 1F-B and 2F-B), however, all exhibit significant stiffness losses from the durability loading. In specimens 1F-B and 2F-B it can be seen that the majority of loss has already taken place at 2,500 load cycles. Specimen 2P-B was not intermediately load tested; it is therefore not known if there was a sudden drop in stiffness somewhere between 1 and 5,000 load cycles or if this loss was relatively continuous. Nonetheless, since the bulk of loss in stiffness seems to have taken place before the 2,500 load cycle mark was reached, it is believed that the diminishing flexural stiffness resulted from overloading of the stringers rather than resulting from the repetitive nature of the loading.

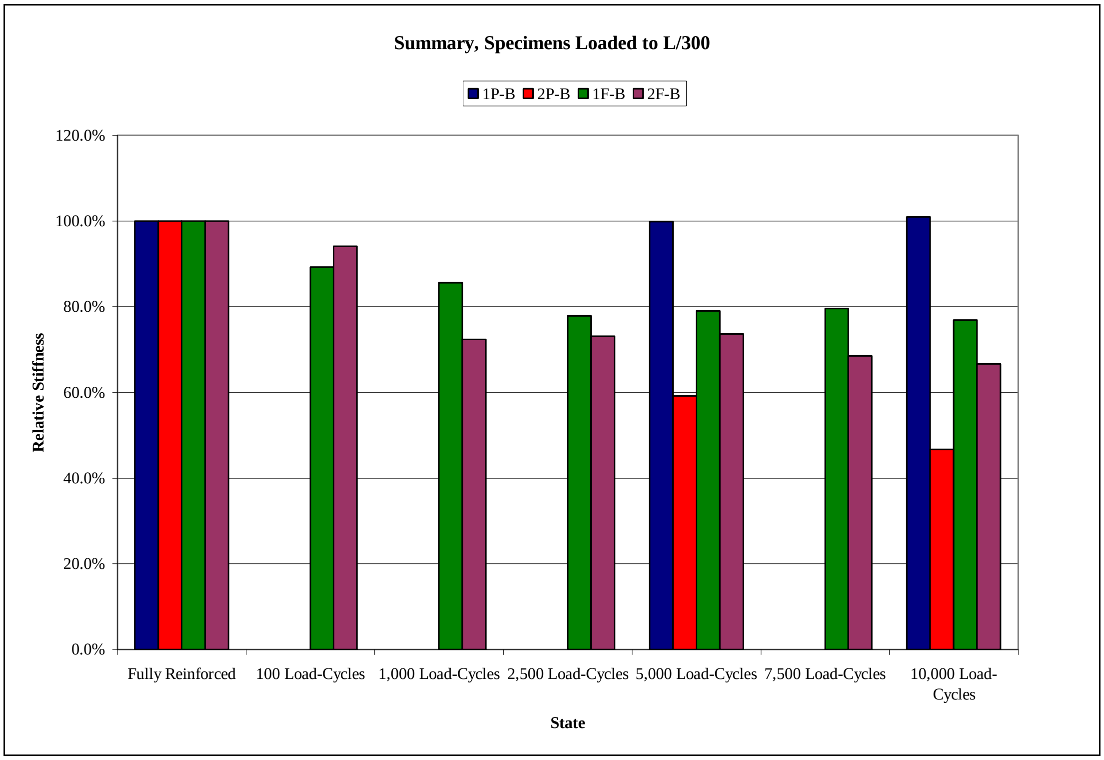

Figure 5.18 Summary of effects from repeated loading on specimens loaded to mid-span deflection corresponding to L/500.

5.2.3 Comparison of Durability Loading Configurations

The effect of dissimilar load exposure on paired (matched) specimens is discussed in this section. Figure 5.19 depicts effects of cyclic loading on the two specimens with one partial cut. It can be seen that the specimens with one partial cut (1P-A and 1P-B) display almost identical responses from the durability loading. Both these specimens lingered at or near their respective virgin stiffness throughout durability loading. Also, as is discussed in Section 5.3, these two specimens exhibit similar structural responses and failure modes from the ramp load tests conducted to failure.

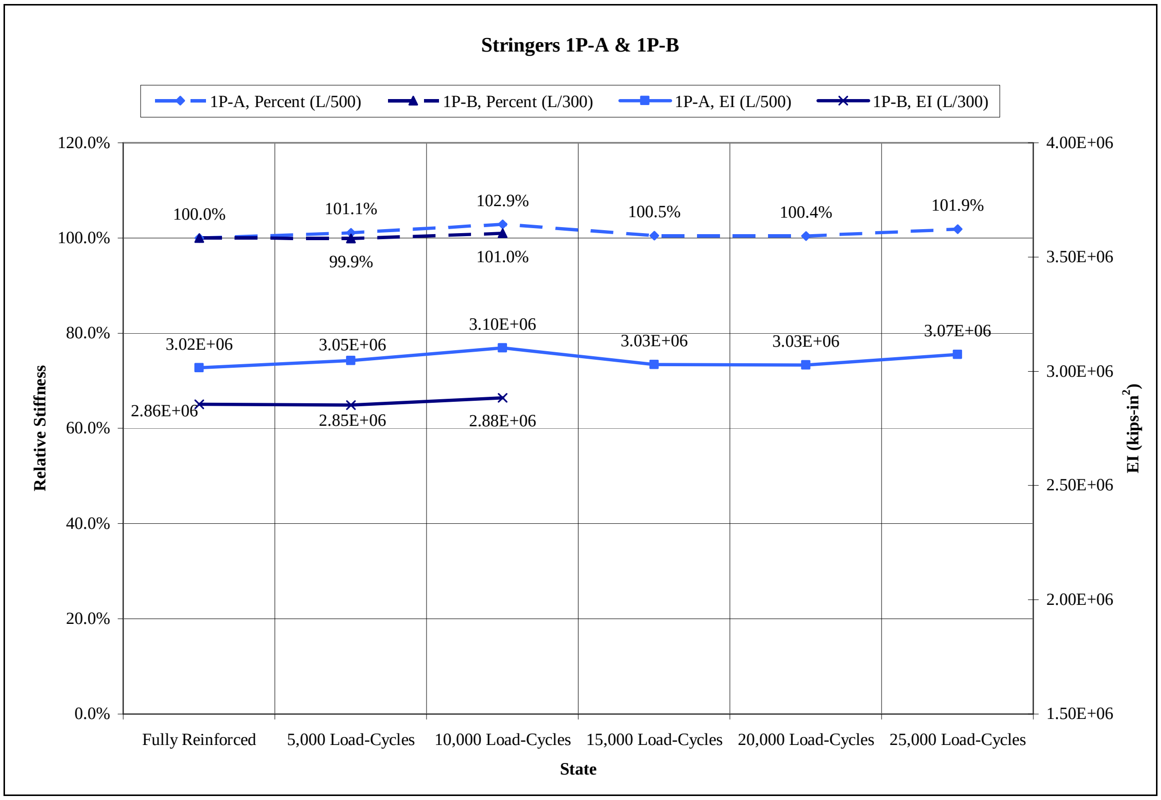

Figure 5.19 Comparison of effects of different durability loading configurations of stringers with one partial cut.

A clear distinction in effect of the durability loading was displayed by specimens 2P-A and 2P-B, as can be seen in Figure 5.20. Stringer 2P-A, which was durability loaded at the lesser load level than specimen 2P-B (25,000 load cycles at L/500 vs. 10,000 load cycles at L/300) shows little, if any, detrimental effect from the durability loading. Stringer 2P-B on the other hand has its flexural stiffness reduced by over 40% already after 5,000 load cycles, and shows a further reduction of 12.5% from the next 5,000 load cycles.

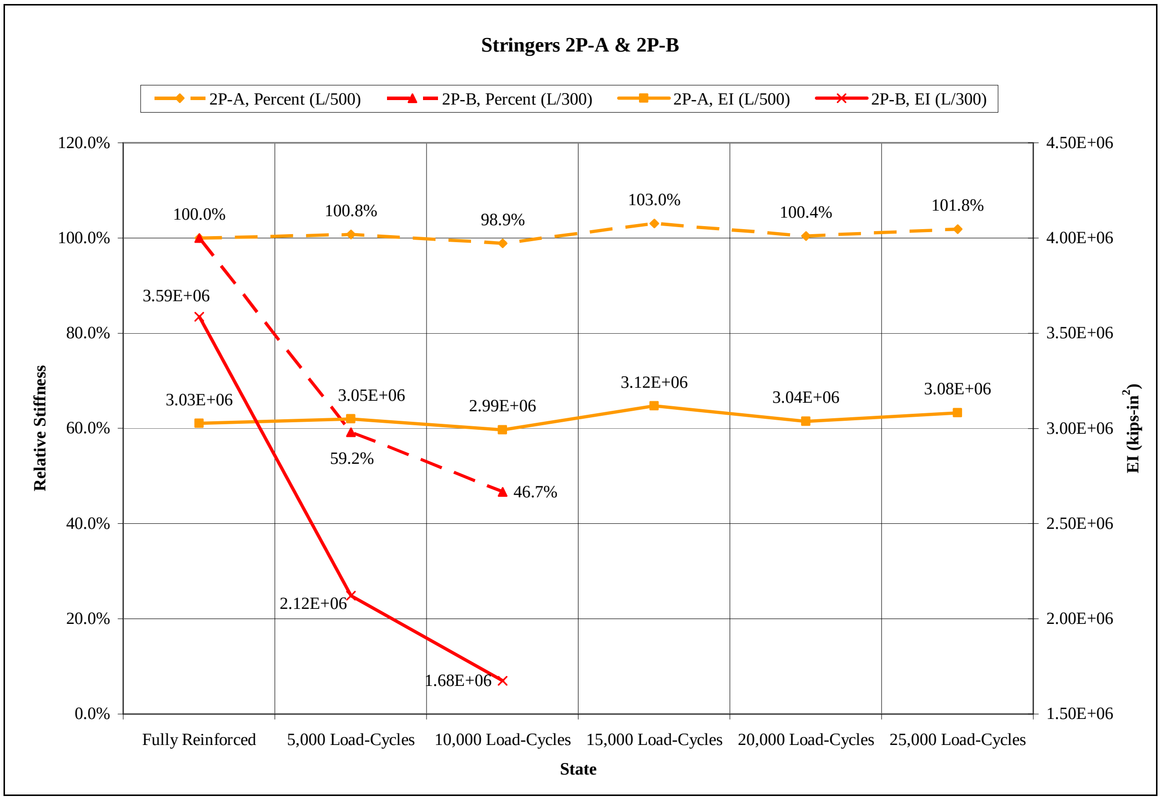

Figure 5.20 Comparison of effects of different durability loading configurations of stringers with two partial cuts.

A similar trend is noted in specimens 1F-A and 1F-B, as shown in Figure 5.21. Specimen 1F-A exhibits no appreciable loss from the durability loading, whereas stringer 1F-B has a loss in flexural stiffness of over 20% at 5,000 load cycles. However, there is little further loss in flexural stiffness of stringer 1F-B from 5,000 to 10,000 load cycles.

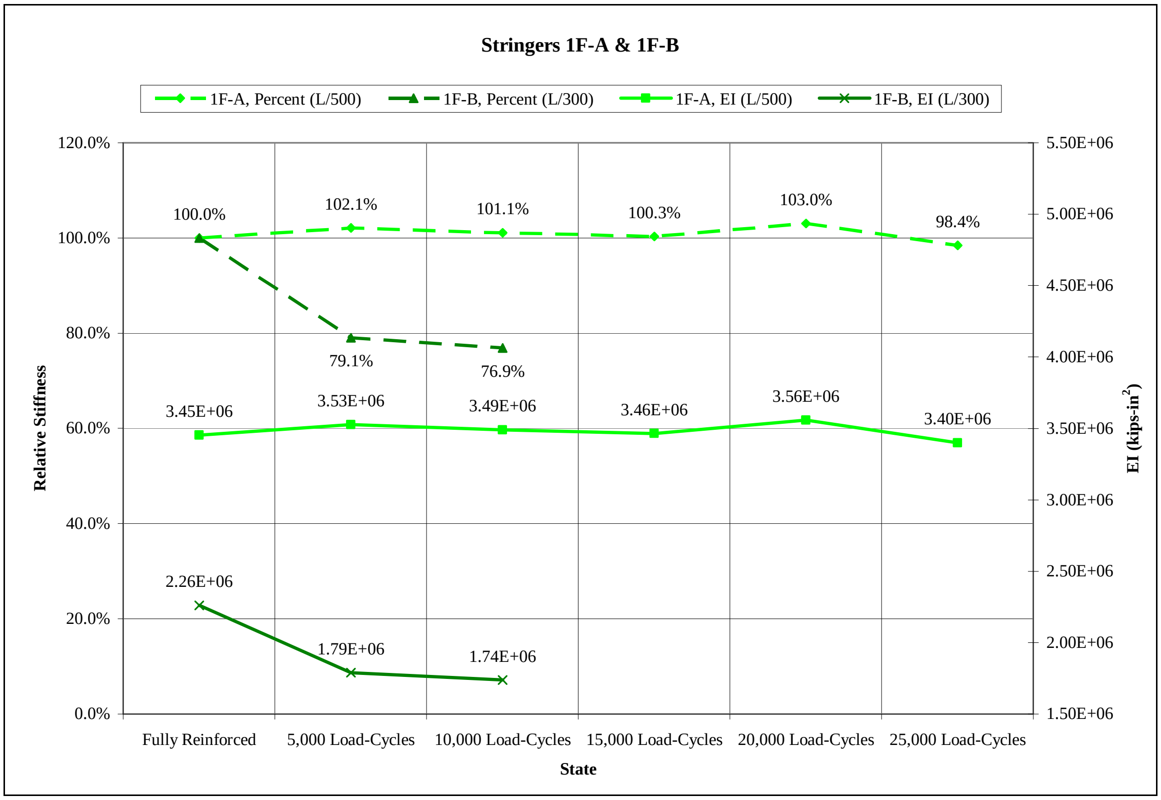

Figure 5.21 Comparison of effects of different durability loading configurations of stringers with one full cut.

The stringers with two full cuts (2F-A and 2F-B) both show appreciable losses of flexural stiffness in the early stages of durability loading; a 6.4% and 26.4% loss at 5,000 load cycles, respectively. It is interesting to note in Figure 5.22 that there is a trend in both specimens where after 5,000 cycles, the rate of flexural stiffness loss, relative to number of load cycles, seems to level off. A similar settling trend after 5,000 load cycles can also be observed in stringer 2P-B (see Figures 5.15 and 5.20) and particularly in stringer 1F-B (see Figures 5.16 and 5.21). However, since only one of the specimens (2F-A) that displayed detrimental effects from the repetitive loading was loaded beyond 10,000 load cycles, it is unknown if these “asymptotic trends” would continue as the number of load cycles increases.

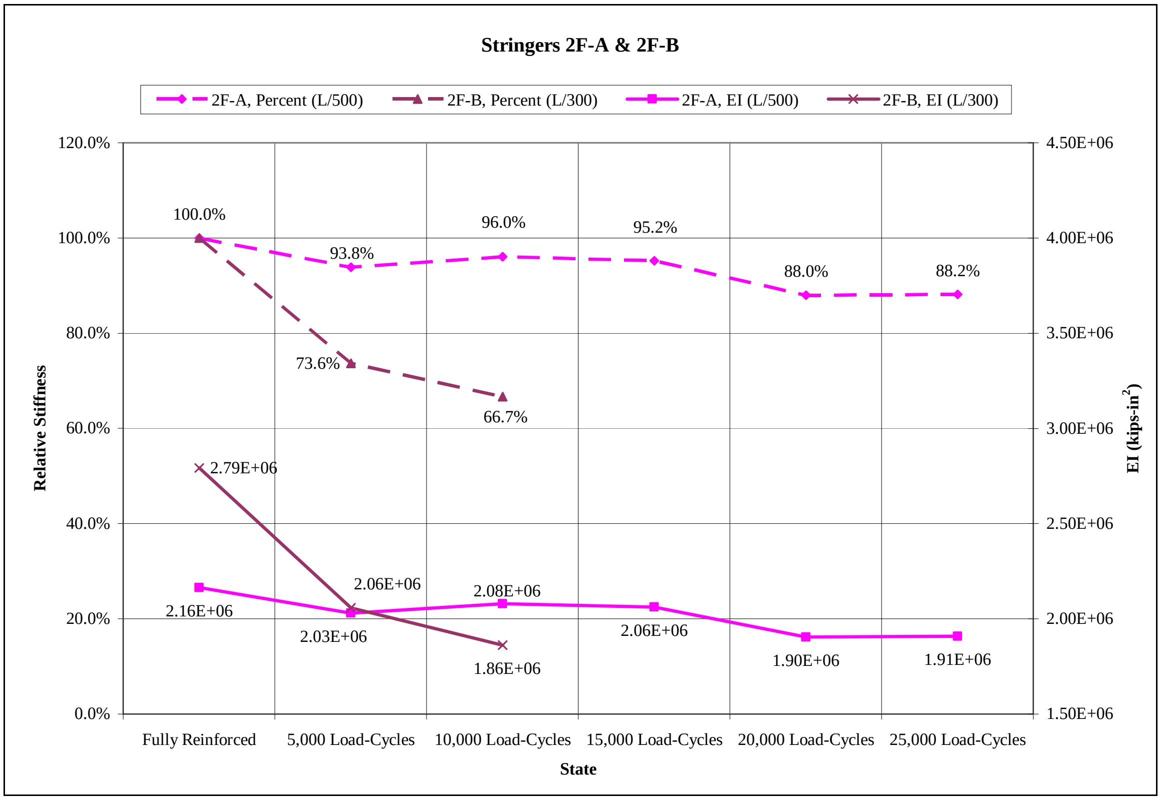

Figure 5.22 Comparison of effects of different durability loading configurations of stringers with two full cuts.

Since these losses in flexural stiffness generally took place in the early stages of durability loading, it is suspected that overloading was the cause, rather than the repetitive nature of the durability loading. Of the specimens that suffer losses in flexural stiffness from the durability loading, only one specimen (2P-B) has its flexural stiffness reduced below the flexural stiffness level after damage (but before any shear spiking). In all other specimens that suffer losses in stiffness during the durability loading, the level is still above the flexural stiffness after damage infliction, as can be seen in Figure 5.23.

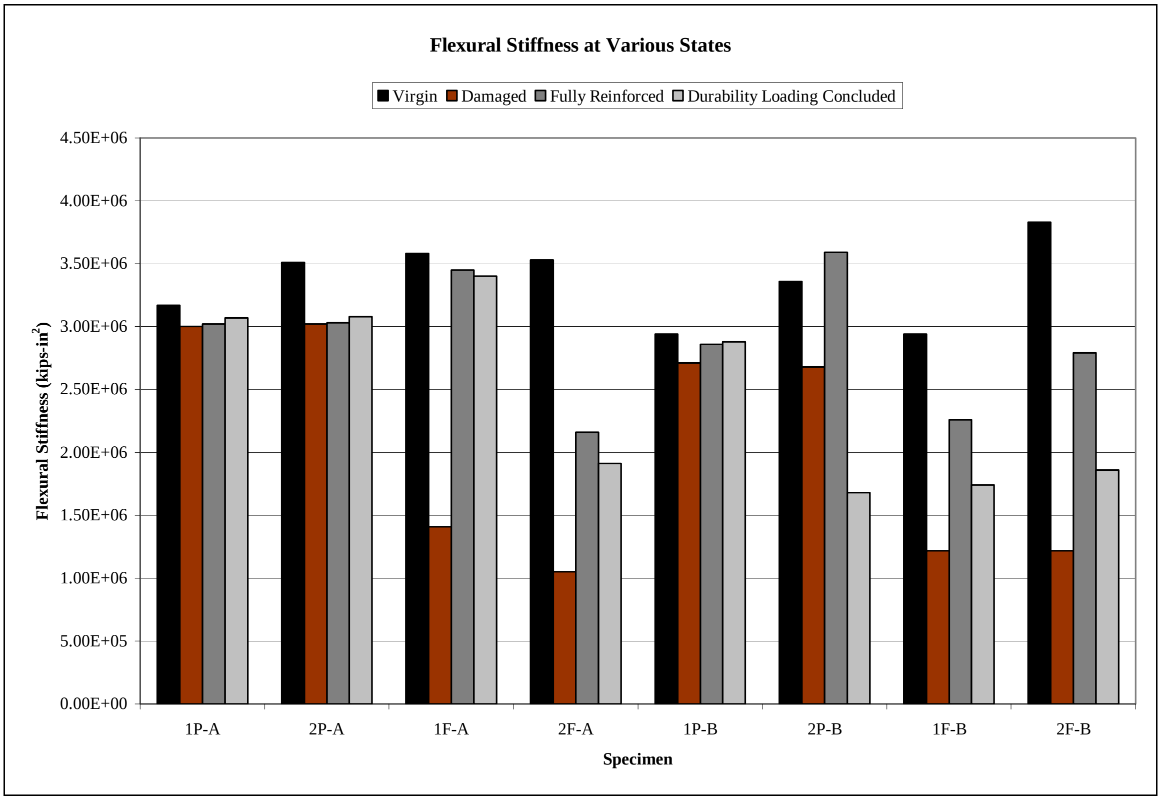

Figure 5.23 Progress of flexural stiffness at various stages.

5.2.4 Dissection of Failed Specimens

Stringers 2P-B, 1F-B, and 2F-B were dissected at the conclusion of durability loading to determine the actual failure mode(s). Dissection was done by cutting a stringer cross-wise, in the plane of a shear spike pair. In doing so, cross-sectional planes of the shear spike, in place, could be scrutinized to determine the failure mode and to inspect the integrity of wood-FRP epoxy bond. Two such cross-sections are shown in Figure 5.24.

Figure 5.24 Dissected cross-sections with shear spikes in place.

It appears that the dissected stringers failed from either a combination of local wood crushing and debonding at the shear spike-epoxy interface or solely from debonding at the shear spike-epoxy interface. A few instances of localized crushing of wood fibers near the shear spike are evident. Consequently, this allows for rigid body rotation of the shear spike during loading of the stringer, even though the wood-FRP bond is intact.

The predominant failure mode is debonding at the epoxy/shear spike interface. From the visual inspections it is evident that, in general, the epoxy resin initially bonded along most of the length of the shear spikes. However, it is also evident that the main cause of lost shear resistance as originally provided by the shear spikes is debonding at the epoxy resin /shear spike interface. Many of the shear spike halves in the dissected specimens can be removed from the cross-section while the cured epoxy bed remains attached to the wood fibers. This debonding is believed to be caused by shearing of the epoxy resin shear spike during durability loading, stemming from opening and closing of gaps at the inflicted cut(s); i.e. relative vertical movement of the top and bottom halves of the beam.

5.3 Ramp Load Testing to Failure

The five stringers that were not dissected were instead ramp load tested to failure at the conclusion of durability loading. The load-deflection curve from ultimate load testing of specimen 1P-A is given in Figure 5.25. Stringer 1P-A exhibits a linear load-deflection behavior up to approximately 29 kips (129 kN), when apparent shear failures near the neutral axis location within both end-thirds occur (at "A" in Figure 5.25). It is evident that the remaining wood in the center portion sheared, since significant interlayer slip is evident within both ends, and shear cracks are clearly discernible in both butt ends. The north end shear crack is highlighted in Figure 5.26. This particular crack propagates from one side face, almost through the entire stringer width, and branches down through the uncut center portion. A sudden drop in load, along with an increase in mid-span deflection, was observed when these shear failures took place. However, the stringer was further loaded up to 31 kips (138 kN) before a catastrophic flexural failure occurred ("B" in Figure 5.25); a diagonal flexural crack across the center third of the tension face resulted.

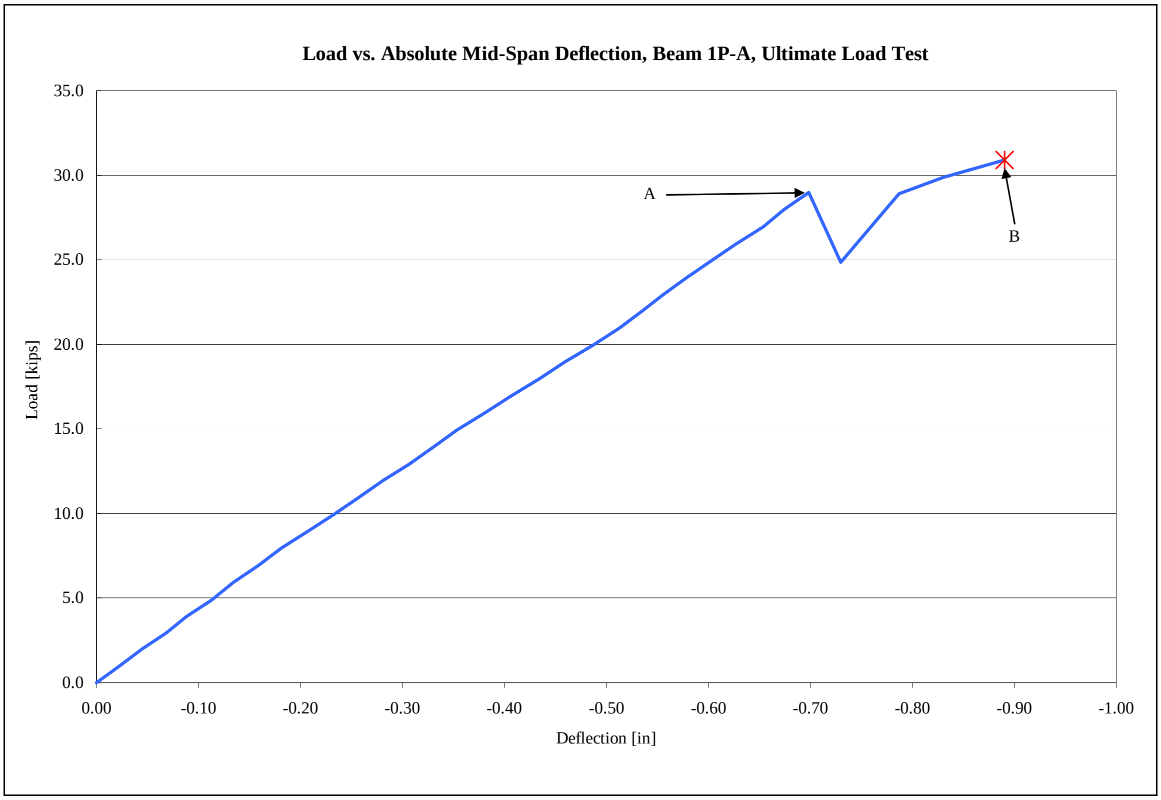

Figure 5.25 Load-deflection curve from ultimate load test of stringer 1P-A.


Figure 5.26 Shear crack (traced) at north end of specimen 1P-A.

The load-deflection curve of stringer 1P-B is given in Figure 5.27. Stringer 1P-B had a more or less linear load-deflection behavior before its sudden and catastrophic failure (at “A” in Figure 5.27), when a deep flexural crack propagated diagonally across the center-third of the tension face, as show in Figure 5.28. This specimen withstood the highest ultimate load of all five stringers; approximately 48.5 kips (216 kN).

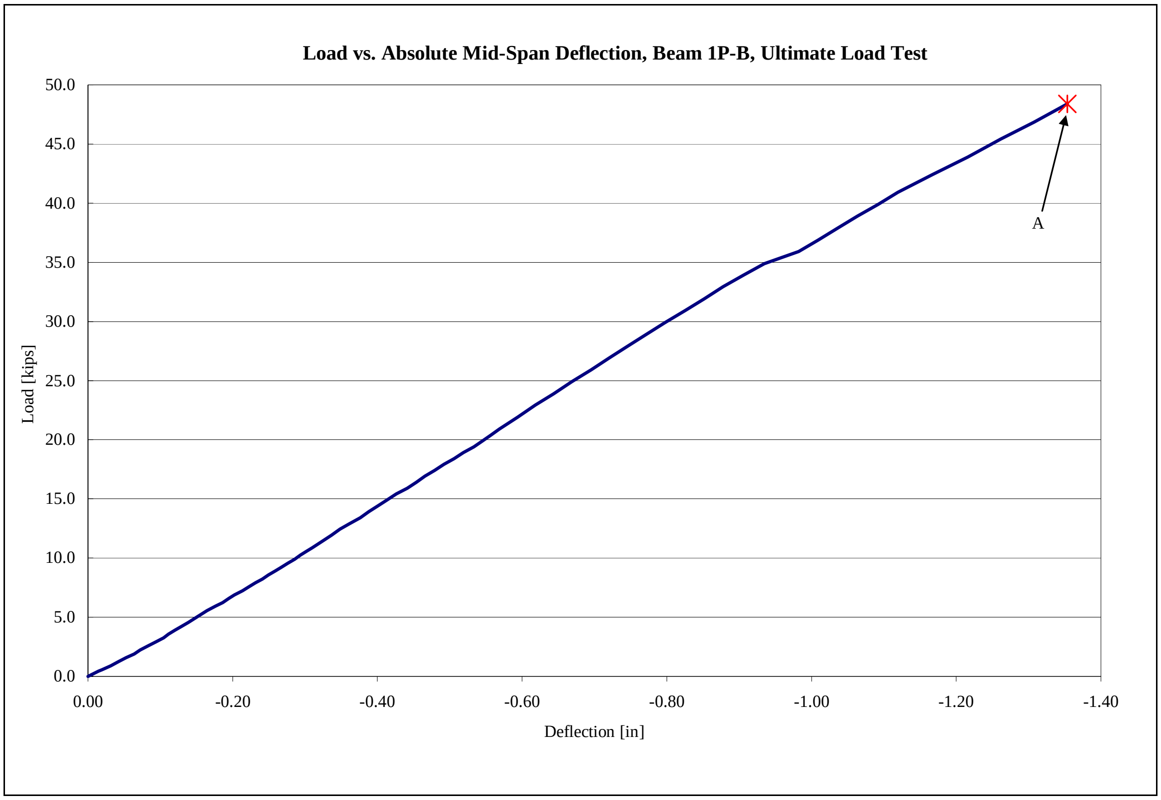

Figure 5.27 Load-deflection curve from ultimate load test of stringer 1P-B.

Figure 5.28 Diagonal flexure crack at tension face of stringer 1P-B.

Stringer 2P-A experienced successive non-catastrophic shear failures in the south end during ultimate load testing (at “A” and “B” in Figure 5.29). These successive shear failures start at a load level of approximately 32 kips (142 kN) (at “A” in Figure 5.29). An “inverted C” shaped slip plane appears between the two partial horizontal cuts in the south stringer third, as can be seen in Figure 5.30. The stringer shows severe interlayer slip in along the “inverted C” shaped slip plane. Note in Figure 5.30 how this “inverted C” shaped crack propagates from the end of one partial cut, through the center portion of the member, and back to the other partial cut.

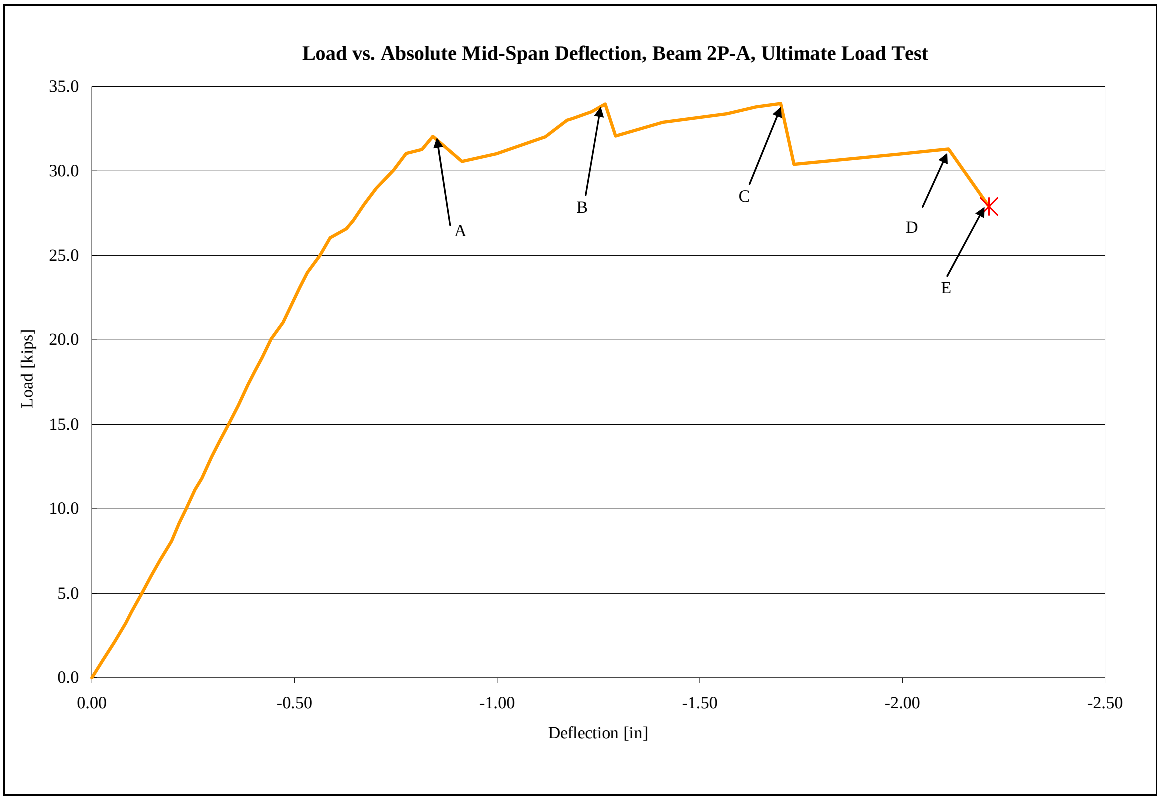

Figure 5.29 Load-deflection curve from ultimate load test of stringer 2P-A.

The stringer retains its load carrying capacity up to a load of approximately 34.5 kips (153 kN), when a perpendicular-to-grain tension failure develops at approximately the south third-point, initiated almost at the neutral axis and propagating upward, towards mid-span at an approximate 45-degree angle (at “C” in Figure 5.29).

Figure 5.30 Traced shear crack at south end of stringer 2P-A.

At point “D,” another non-catastrophic shear failure occurs along with further propagation of the just described perpendicular-to-grain failure. Finally, there is a catastrophic flexural failure in the tension face in the vicinity of the south third-point (at “E” in Figure 5.29). The propagation of this flexural crack is more or less perpendicular to the length of the beam. This ultimate failure occurs at load of 31.5 kips (140 kN).

The load-deflection curve of ultimate load testing of stringer 1F-A is given in Figure 5.31. Specimen 1F-A first shows non-catastrophic shear failure along the neutral axis cuts at a load level of approximately 37 kips (165 kN) (at “A” in Figure 5.32). Significant related interlayer slip was observed at both stringer ends, where slip occurs in the plane of the intentional cuts. The specimen ultimately fails in flexure with a resulting diagonal flexural crack in the tension face, spanning the middle-third of the beam, as shown in Figure 5.32 (“B” in Figure 5.31). The load at failure is 38 kips (169 kN).

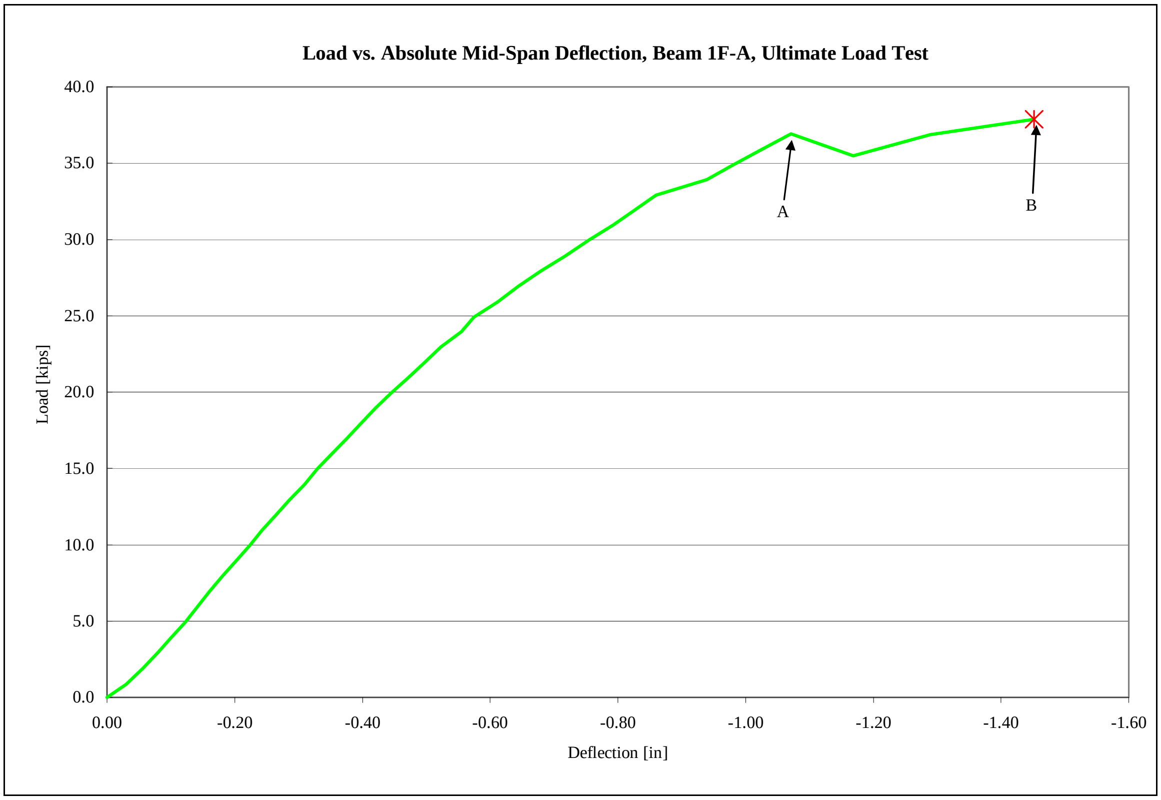

Figure 5.31 Load-deflection curve from ultimate load test of stringer 1F-A.

Figure 5.32 Flexural crack at tension face of stringer 1F-A.

The load-deflection curve of stringer 2F-A is given in Figure 5.33. It shows several successive non-catastrophic shear failures during loading, first along the neutral axis cut and later, at a load of approximately 34 kips (151 kN), it also shows shear failures with corresponding interlayer slip at the quarter-depth cut, along with a non-linear load-deflection behavior as shown in Figure 5.33. This specimen finally fails catastrophically in flexure at a load of 35.5 kips (158 kN) (at "A" in Figure 5.33).

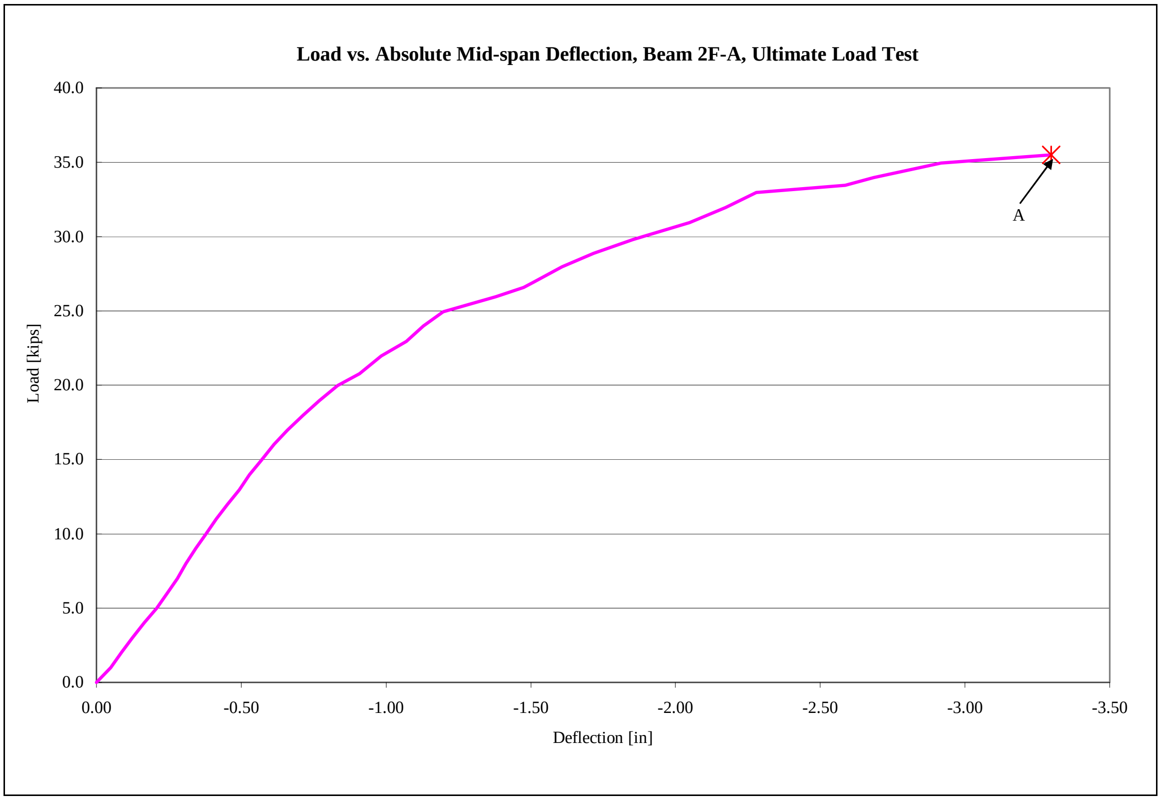

Figure 5.33 Load-deflection curve from ultimate load test of stringer 2F-A.

It is thus noted that despite intermediate shear failure(s) along the inflicted horizontal cuts, as observed in four of the five stringers, the governing (catastrophic) failure mode is a flexural failure in the tension face.

5.4 Cost Analysis

As can be seen in Tables 5.4, 5.5 and 5.6, the material cost per stringer for this study is estimated to be about $80. This cost is based on a total of twenty shear spikes per stringer. The associated approximate labor cost is $130, giving a total of $210 for shear spiking of one single span stringer. It should be noted that this labor cost is based on time required for installation in a laboratory setting. Strengthening in an in situ situation would require additional time (and consequently further costs). Nonetheless, this approximate total cost is far less than the estimated $2,400 to replace a railroad timber bridge stringer, as given by Schilling [55].

While no cost comparison between shear spiking and other FRP strengthening methods is given herein, it is noted shear spiking requires less labor effort. Shear spiking does not necessitate highly skilled workers, and very little training is necessary for laborers. Most importantly, by not requiring removal of structural members, shear spiking is believed to be highly competitive compared to other FRP-based strengthening methods.

Table 5.4 Material Cost per Stringer

	Material Cost, per Stringer		
	Length per Stringer [ft]	Cost per Foot	Cost
FRP (Shear Spike)	26.67	$1.48	$39.47
	Cost per Quantity	Stringers per Quantity	Cost
Epoxy Resin	$78.80	3.0	$26.27
Hardener	$30.70	3.3	$9.30
Silica Filler	$17.95	5.0	$3.59
		Total Cost	$78.63

Table 5.5 Labor Cost, per Stringer

	Labor Cost, per Stringer			
	Hourly Wage	Time Required per Hole [min]	Number of Holes	Cost
Drill Holes	$17.00	10	20	$56.67
Preparation of Epoxy Resin	$17.00	10 min total	-	$2.83
Pouring of Epoxy Resin	$17.00	0.5	20	$2.83
Cutting Shear Spikes	$17.00	2	20	$11.33
Shear Spike Installation	$17.00	10	20	$56.67
			Total Cost	$130.33

Table 5.6 Total Cost, per Stringer

Total Material Cost	$78.63
Total Labor Cost	$130.33
Total Cost	$208.96

6. OBSERVATIONS, CONCLUSIONS AND RECOMMENDATIONS

The main objective of this research study is to investigate effects of repeated loading on shear spike strengthened, full-size timber railroad bridge stringers. The ultimate bending strength and failure mode of the shear spiked stringers are also investigated. Results of this study show that strengthening through the process of shear spiking is highly effective in restoring bending stiffness and strength of ‘deteriorated’ timbers. Moreover, it is shown that shear spiked timbers exhibit little detrimental effect from repeated loading at approximate service load levels. When ultimately load tested, the strengthened stringers fail primarily in flexure, i.e. a wood failure rather than failure of the shear spikes. Some notable points are:

- The flexural stiffness in the undamaged state of a stringer seems to provide an approximate upper limit of stiffness that can be regained from shear spiking of a damaged stringer.
- Attained improvements in effective flexural stiffness are comparable to those measured by Radford [49-52] (in dimension lumber), Schilling [55-57] (in railroad crossties), and Burgers [15-16] (in full scale railroad trestle bridge stringers).
- Driving shear spikes into the pre-drilled holes with a dead blow hammer proves practicable; the spikes show minimal damage from the impact of repeated dead blow hammer blows.
- By not drilling holes for the shear spikes through the full depth of a specimen, no epoxy is pushed out the bottom during installation. On the side faces of the stringers, it is visually evident that beads of epoxy penetrate from the drilled hole through the wood fibers and decay/damage voids. This migration of epoxy further most likely helped in improving the flexural strength and stiffness. From the dissected cross-sections, it is also observed that epoxy resin filled voids near the shear spikes.
  - From dissection of reinforced members, it is visually evident that the epoxy resin does, in general, bond to the entire length and circumference of shear spikes.
- In an in situ situation, shear spike reinforcement does not necessitate removal of structural members to provide access to the members to be strengthened; only portions of the top or bottom surface need to be accessed for insertion of the shear spikes. This method thus provides a highly cost effective bridge rehabilitation method when that access can be made, e.g. in timber trestle railroad bridges.

6.1 Conclusions

- Significant recovery of flexural stiffness and shear strength of full size, deteriorated/damaged timber stringers can be attained from shear spiking, when bonded-in perpendicular to the primary bending axis.
  - On average, the eight stringers in this study lost 36% of their flexural stiffness from the intentional damage. After full shear spike reinforcement, the average flexural stiffness is up to 91%, i.e. a regain of 27%.

- In general, the ‘severely deteriorated’ stringers experienced a dramatic recovery of flexural stiffness, with a corresponding decrease in deflection under load, when all shear spike rows had been installed.
  - The four stringers with full cut(s) inflicted on them had an average loss of flexural stiffness of 61% (i.e. to 39%of the ‘undamaged’ average flexural stiffness) after damage infliction. In the full shear spike reinforced state, the average flexural stiffness of these four specimens is regained to 84%, e.g. 16% below the ‘undamaged’ average flexural stiffness.

- The application of bonded-in, fiberglass pultruded rods, as shear spikes, in specimens with saw cut(s) through their full width produced greater increases in flexural stiffness than did shear spiking of specimens with “partial” saw cuts, i.e. not through the entire specimen width. It is thus concluded that stringers with a greater degree of deterioration show a greater potential to rejuvenate flexural stiffness and interlayer shear resistance.

- The shear spike reinforced specimens showed very little, if any, detrimental effect from the repetitive nature of the durability loading up to 25,000 load cycles; for both the cyclic levels and load levels examined.
    - The few partial failures of specimens that occurred during durability loading are instead believed to have resulted from overloading of the specimens since considerable losses of flexural stiffness generally occurred very early in the durability loading process.
    - Despite these initial partial shear failures, the specimens showed little further detrimental effect from further repeated loading.

- Dissection of specimens that had suffered partial failures during durability loading showed that debonding at the shear spike/epoxy resin interface was the primary cause of failure. The combination debonding and local crushing of wood fibers surrounding the shear spike was also evident in a handful of dissected cross-sections.
    - Vertical shear (in the plane of the shear spikes), resulting from opening and closing of gaps created within a stringer by the intentional saw cuts most likely caused the debonding at the shear spike/epoxy resin interface, which in turn led to the partial shear failures during durability loading.
    - Despite this debonding, the ‘un-bonded’ shear spikes still provided significant shear resistance.

- Flexural failure was the typical failure mode of shear spike reinforced specimens when ultimately load tested. In other words, the strength of wood fibers governed a composite stringers’ ultimate strength, while the strengthening components remained virtually intact.
    - Even with partial shear failures and subsequent interlayer slip within specimens during ultimate load testing, additional loading was necessary to induce catastrophic failure.
    - The shear spiking thus seems to promote a ductile behavior of the strengthened stringers, when loaded to failure.

6.2 Recommendations

- The use of a primer, in conjunction with the epoxy resin, should be investigated as a means to improve the wood/FRP bond. Incorporation of a primer could be particularly beneficial in high humidity environments.

- A polyester resin adhesive should be considered in future research studies. It is believed that a polyester resin would be more compatible with the spikes, compared to epoxy resin, and therefore would provide a stronger and more durable bond.

- A continuation of the study of the shear spike/epoxy resin/wood bond that was conducted by Schilling et al. [55-57] should be considered. The bonding in shear spike should be cyclically loaded to investigate the durability characteristics of the epoxy bond.

- Related parameters to be investigated are the effects of varying humidity and/or temperature exposures on shear spiked timbers. This can be done by conditioning specimens in an environmental chamber to investigate the epoxy resin bond strength under simulated in situ exposure conditions.

- An investigation into the bond performance of shear spikes with roughened surface and/or with an irregular surface configuration, shaped much like steel rebar, is suggested. A non-smooth shear spike surface will presumably improve the FRP/epoxy resin interface and could potentially prevent FRP/epoxy resin interface failures that were observed in this study.

- The feasibility of combining the shear spiking process with pressure injection of epoxy resin should be investigated as a means of filling a greater fraction of decay voids. This would shield the interior portions of the composite member from further environmental exposure and decay. Moreover, any severe surface crack/splits/voids could be hand filled.

- The next rational step in this ongoing research program is shear spike strengthening of either a deteriorated in situ structure or a laboratory study of deteriorated members that have been salvaged from a field bridge.

- To improve the efficiency of strengthening of in situ structures through shear spiking, NDE techniques should be considered to identify locations of decay/deterioration. A combined NDE/shear spike approach might be developed; a standardized NDE based decay classification method, along with guidelines as to when shear spiking (relative to extent of decay) is effective would be highly useful.

REFERENCES

1. American Forest & Paper Association, American Wood Council. "National Design Specification Supplement, Design Values for Wood Construction, Ed. 2001" Table 4D, Design Values for Visually Graded Timbers, pp. 44; 2001.

2. American Railway Engineering Association (AREA).[1] "1995 Manual for Railway Engineering, Chapter 7," Washington DC: AREA, Timber Structures; 1995.

3. Bohannan, B. "Prestressing Wood Members," Forest Products Journal, Volume 12, No. 12, December 1962, pp. 596-602.

4. Breyer, D.E., Fridley, K.J., Cobeen, K.E. & Pollock, D.G. "Design of Wood Structures – ASD, 5th Edition," New York, NY: McGraw Hill; 1999.

5. Buell, T.W. & Saadatmanesh, H. "Strengthening Timber Bridge Beams Using Carbon Fiber," Journal of Structural Engineering, Volume 131, No. 1, 2005, pp. 173-187.

6. Bureau of Transportation Statistics. "Transportation Statistics Annual Report," Washington DC: Bureau of Transportation Statistics, U.S. Department of Transportation; October 2003.

7. Burgers, T.A. "Composite Repair of Full-Scale Timber Bridge Chord Members through the Process of Shear Spiking," M.S. Thesis, Department of Civil Engineering, Colorado State University, Fort Collins, CO; May 2005.

8. Burgers, T.A., Gutkowski, R.M., Radford, D.W. & Balogh, J. "Composite Repair of Full-Scale Timber Bridge Chord Members through the Process of Shear Spiking," Report No. 05-173, Mountain-Plains Consortium, North Dakota State University, Fargo, ND; December 2005.

9. Davalos, J.F., Qiao, P.Z., & Trimble, B.S. "Fiber-Reinforced Composite and Wood Bonded Interfaces: Part 1 – Durability and Shear Strength," Journal of Composites Technology & Research, Volume 22, No. 4, October 2000, pp. 224-231.

10. Davalos, J.F., Qiao, P.Z. & Trimble, B.S. "Fiber-Reinforced Composite and Wood Bonded Interfaces: Part 2. Fracture," Journal of Composites Technology & Research, Volume 22, No. 4, October 2000, pp. 232-240.

11. Davalos, J.F., Zipfel, M.G. & Qiao, P. "Feasibility Study of Prototype GFRP Reinforced Wood Railroad Crosstie," Journal of Composites for Construction, Volume 3, No. 2, May 1999, pp. 92-99.

12. Delmhorst Instrument Co. "R-2000 Owners Manual;" 1999.

13. Doyle K.R. "Laboratory Test and Analysis of Full-Scale Open Timber Trestle Railroad Bridge Chords," M.S. Thesis, Department of Civil Engineering, Colorado State University, Fort Collins, CO; 2000.

---

[1] AREA has since added "and Maintenance of Way" to its name and is now known as the American Railway Engineering and Maintenance of Way Association (AREMA).

14. Duwadi, S.R. & Ritter, M.A. “Timber Bridges in the United States,” Public Roads, Winter, 1997, pp. 32-40.

15. Federal Railroad Administration “FRA’s Interim Statement of Policy on the Safety of Railroad Bridges Report No. TR-1999-077,” Washington DC: Federal Railroad Administration; March 1999.

16. Forest Products Laboratory “Wood Handbook: Wood as an Engineering Material. General Technical Report FPL-GTR-113,” Madison, WI: U.S. Department of Agriculture, Forest Service, Forest Products Laboratory; 1999.

17. GangaRao, H.V.S., Sonti, S.S. & Supefesky, M.C. “Static Response of Wood Crossties Reinforced with Composite Fabrics,” International Society of the Advancement of Materials and Process Engineering Symposium and Exhibition, Volume 41, No. 2, 1996, pp. 1291-1303.

18. Gentile, C., Svecova, D., & Rizkalla, S.H. “Timber Beams Strengthened with GFRP Bars: Development and Applications,” Journal of Composites for Construction, Volume 6, No. 1, February 2002, pp. 11-20.

19. Gilfillan, J.R., Gilbert, S.G., & Patrick, G.R.H. “The Use of FRP Composites in Enhancing the Structural Behavior of Timber Beams,” Journal of Reinforced Plastics and Composites, Volume 22, 2003, pp. 1373-1388.

20. Gutkowski, R.M., Shigidi, A., Tran A.V., Uppal, S.A. & Otter, D.E. “Field Study of a Strengthened Timber Railroad Bridge,” Report R-956, Association of American Railroads, Transportation Technology Center, Inc., Pueblo, CO; July 2002.

21. Johns, K.C. & Lacroix, S. “Composite Reinforcement of Timber in Bending,” Canadian Journal of Civil Engineering, Volume 27, No. 5, 2000, pp. 899-906.

22. Lantos, G. “Reinforced and Post-Tensioned Glue-Laminated Beams under Development at TRADA Labs,” Civil Engineering and Public Works Review, London 49, 1964, pp. 690.

23. Muchmore, F.W. “Techniques to Bring New Life to Timber Bridges,” Journal of Structural Engineering, Volume 110, No. 8, August 1984, pp. 1832-1846.

24. Oomen, G. & Sweeney, R.A.P. “Application of Modern Technologies in Railway Bridge Infrastructure Management and Decision Making” Proceedings of Transportation Infrastructure – Environmental Challenges in Poland and Neighboring Countries, NATO ASI Series, Sub-Series 2, Volume 5, pp. 339-346. Berlin: Springer Verlag; 1996.

25. Peterson, J.L. “Wood Beams Prestressed with Bonded Tension Elements,” ASCE Journal of the Structural Division, Volume 91, No. 1, February 1965, pp. 103-119.

26. Radford, D.W., VanGoethem, D. & Peterson, M.L. “Composite Repair of Timber Structures,” Report No. 00-112, Mountain-Plains Consortium, North Dakota State University, Fargo, ND; June 2000.

27. Radford, D.W., Gutkowski, R.M., VanGoethem, D. & Peterson, M.L. “Composite Repair of Timber Bridges,” Proceedings 9th International Conference and Exhibition in Structural Faults and Repair, July 2001, ASCE, London, UK; 2001.

28. Radford, D.W., Gutkowski, R.M., VanGoethem, D. & Peterson, M.L. “Composite Repair of Timber Structures,” Construction and Building Materials, Elsevier Publications, October 2002, pp. 417-425.

29. Radford, D.W., Gutkowski, R.M., VanGoethem, D. & Peterson, M.L. “Pultruded Composite Shear Spike for Repair of Timber Members,” STREMAH 2003, Eighth International Conference on Structural Studies, Repairs and Maintenance of Heritage Architecture, Halkidiki, Greece, Essex Institute of Technology, Southampton, UK, 2003, pp. 737-750.

30. Robinson, G.C. “Field Testing of Open-Deck Timber Trestle Railroad Bridges,” Department of Civil Engineering, Colorado State University, Fort Collins, CO; 1998.

31. Robinson, G.C., Gutkowski, R.M., Peterson, M., Uppal, S.A., Oliva-Maal, D. & Otter, D.E. “Field Studies of Timber Railroad Bridges,” Report R-933, Association of American Railroads, Transportation Technology Center, Inc., Pueblo, CO; August 1998.

32. Schilling, TJ. T. “Composite Repair of Railroad Crossties through the Process of Shear Spiking,” M.S. Thesis, Department of Civil Engineering, Colorado State University, Fort Collins, CO; June 2004.

33. Schilling, TJ. T, Gutkowski, R.M. & Radford, D.W. “Composite Repair of Railroad Crossties through the Process of Shear Spiking,” Report No. 04-163, Mountain-Plains Consortium, North Dakota State University, Fargo, ND; June 2004.

34. Schilling, TJ. T, Gutkowski, R.M. & Radford, D.W. “Composite Repair of Railroad Crossties by Shear Spiking,” Proceedings of 11th International Conference and Exhibition in Structural Faults and Repair, June 2006, ASCE, Edinburgh, Scotland, UK; 2006.

35. Sitar, M. “Glulam Beam Repair and Strengthening,” Structural Engineer, Volume 7, No. 4, May 2006, pp. 32-36.

36. Sliker, A. “Reinforced Wood Laminated Beams,” Forest Products Journal, Volume 12, No. 2, February 1962, pp. 91-96.

37. Triantafillou, T.C. “Shear Reinforcement of Wood using FRP Materials,” Journal of Materials in Civil Engineering, Volume 9, No. 2, May 1997, pp. 65-69.

38. Uppal, A.S. & Otter, D.E. “Methodologies for Strengthening and Extending the Life of Timber Railroad Bridges,” Association of American Railroads, Transportation Technology Center, Inc., Report No. R-922; 1998.

39. Uppal, A.S., et al. “Field Study of a Strengthened Timber Railroad Bridge,” Association of American Railroads, Transportation Technology Center, Inc., Report No. R-956; July 2002.